IntechOpen

Pattern Recognition

Analysis and Applications

Edited by S. Ramakrishnan

PATTERN RECOGNITION - ANALYSIS AND APPLICATIONS

Edited by **S. Ramakrishnan**

Pattern Recognition - Analysis and Applications
http://dx.doi.org/10.5772/62619
Edited by S. Ramakrishnan

Contributors

Nadia Abd-Alsabour, Christopher Chukwuemeka Ohagwu, Kenneth K. Agwu, Pavel Yezhov, Alexander Kuzmenko, Jin-Tae Kim, Alexander Ostroukh, Diego Alexander Tibaduiza Burgos, Jaime Vitola, Francesc Pozo, Maribel Anaya, Joanna Isabelle Olszewska, Julie Thompson

Notice

First published in Croatia, 2016 by INTECH d.o.o.
eBook (PDF) Published by IN TECH d.o.o.
Place and year of publication of eBook (PDF): Rijeka, 2019.
IntechOpen is the global imprint of IN TECH d.o.o.
Printed in Croatia

Legal deposit, Croatia: National and University Library in Zagreb

Additional hard and PDF copies can be obtained from orders@intechopen.com

Pattern Recognition - Analysis and Applications
Edited by S. Ramakrishnan

p. cm.

Print ISBN 978-953-51-2803-8

Online ISBN 978-953-51-2804-5

eBook (PDF) ISBN 978-953-51-5790-8

Meet the editor

Dr. S. Ramakrishnan is a Professor and the Head of the Department of Information Technology, Dr. Mahalingam College of Engineering and Technology, Pollachi, India. Dr. Ramakrishnan is a reviewer of 25 international journals such as *IEEE Transactions on Image Processing*, *IET Journals* (Formally IEE), *ACM Computing Reviews*, Elsevier Science Journals, Springer Journals, and Wiley Journals. He is a guest editor of special issues in three international journals, including *Telecommunication Systems Journal of Springer*. He has published 116 papers in international, national journals and conference proceedings. Dr. S. Ramakrishnan has published a book on wireless sensor networks for CRC Press, USA, three books on speech processing for InTech Publisher, Croatia, and a book on computational techniques for Lambert Academic Publishing, Germany.

Contents

Preface

Pattern recognition continued to be one of the important research fields in computer science and electrical engineering. Lots of new applications are emerging and hence pattern analysis and synthesis become significant subfields in pattern recognition. This book is an edited volume and has six chapters arranged into two sections, namely, pattern recognition analysis and pattern recognition applications. These two sections have three chapters each.

Chapter 1 is on motif discovery in protein sequences. This chapter covers basics of motif representation nicely and provides methods for motif discovery using probabilistic models. This chapter also provides the details of the tools available for motif discovery.

Chapter 2 is on metaheuristics for classification problems. Authors of this chapter give the need for metaheuristics and how that can be used for classification problems. This chapter particularly focuses on hybridizing metaheuristics and suggests various methods for hybridization.

Chapter 3 is on synthesized phase objects in the optical pattern recognition. This chapter is highly comprehensive and has the required basics such as definitions and properties. Authors of this chapter provide a clear note on the required experimental setups and results with discussions. Methodologies used for the optical pattern recognition are also well explained.

Chapter 4 is on face recognition. Authors provide a nice overview for the face recognition systems. Authors critically study and address several challenges in the face recognition systems, namely, pose variations, the presence/absence of structuring elements/occlusions, facial expression changes, aging of the face, varying illumination conditions, image resolution, and modality.

Chapter 5 is on the classification of brain tissues using textures. Authors of this chapter critically study texture analysis and statistical methods and apply those for the classification of CT images using histogram-based features and neural networks. Experimental results and discussions are also represented neatly.

The last chapter is on structural damage detection using machine learning techniques. Authors of this chapter examine the role of pattern recognition techniques in structural health monitoring. They successfully apply PCA and k-NN for the purpose of damage detection and present the experimental results.

Overall this book is brief and comprehensive and will be a useful resource for the graduate students, researchers, and practicing engineers in the field of machine vision and computer science and engineering.

I would like to express my sincere thanks to all authors for their contribution and effort to compile this wonderful book and my earnest gratitude and appreciation to the InTech publisher, in particular Ms. Maja Bozicevic, Publishing Process Manager, who has drawn together the authors to publish this book. I would also like to express my heartfelt thanks to the management, secretary, director, and principal of my institute. Finally, I extend my dearest thanks to my family members and in particular to my sweet daughter Abirami.

Dr. S. Ramakrishnan
Professor and Head, Department of Information Technology
Dr. Mahalingam College of Engineering and Technology
Pollachi, India

Section 1

Pattern Recognition: Analysis

Chapter 1

Motif Discovery in Protein Sequences

Salma Aouled El Haj Mohamed ,
Mourad Elloumi and Julie D. Thompson

Additional information is available at the end of the chapter

http://dx.doi.org/10.5772/65441

Abstract

Biology has become a data-intensive research field. Coping with the flood of data from the new genome sequencing technologies is a major area of research. The exponential increase in the size of the datasets produced by "next-generation sequencing" (NGS) poses unique computational challenges. In this context, motif discovery tools are widely used to identify important patterns in the sequences produced. Biological sequence motifs are defined as short, usually fixed length, sequence patterns that may represent important structural or functional features in nucleic acid and protein sequences such as transcription binding sites, splice junctions, active sites, or interaction interfaces. They can occur in an exact or approximate form within a family or a subfamily of sequences. Motif discovery is therefore an important field in bioinformatics, and numerous methods have been developed for the identification of motifs shared by a set of functionally related sequences. This chapter will review the existing motif discovery methods for protein sequences and their ability to discover biologically important features as well as their limitations for the discovery of new motifs. Finally, we will propose new horizons for motif discovery in order to address the short comings of the existent methods.

Keywords: motif discovery, bioinformatics, biological sequences, protein sequences, bioinspired algorithms

1. Introduction

Biology has been transformed by the availability of numerous complete genome sequences for a wide variety of organisms, ranging from bacteria and viruses to model plants and animals to humans. Genome sequencing and analysis is constantly evolving and plays an increasingly

important part of biological and biomedical research. This has led to new challenges related to the development of the most efficient and effective ways to analyze data and to use them to generate new insights into the function of biological systems. The completion of the genome sequences is just a first step toward the beginning of efforts to decipher the meaning of the genetic "instruction book." Whole-genome sequencing is commonly associated with sequencing human genomes, where the genetic data represent a treasure trove for discovering how genes contribute to our health and well-being. However, the scalable, flexible nature of next-generation sequencing (NGS) technology makes it equally useful for sequencing any species, such as agriculturally important livestock, plants, or disease-related microbes.

The exponential increase in the size of the datasets produced by this new generation of instruments clearly poses unique computational challenges. A single run of a NGS machine can produce terabytes of data, and even after image processing, base calling, and assembly, there will be hundreds of gigabytes of uncompressed primary data that must be stored either in flat files or in a database. Efficient treatment of all this data will require new computational approaches in terms of data storage and management, but also new effective algorithms to analyze the data and extract useful knowledge.

The major challenge today is to understand how the genetic information encoded in the genome sequence is translated into the complex processes involved in the organism and the effects of environmental factors on these processes. Bioinformatics plays a crucial role in the systematic interpretation of genome information, associated with data from other high-throughput experimental techniques, such as structural genomics, proteomics, or transcriptomics.

A widely used tool in all these stages is the comparison (or alignment) of the new genetic sequences with existing sequences. During genome assembly, short read sequences are often aligned to a reference genome to form longer contigs. Identification of coding regions then involves alignment of known genes to the new genomic sequence. Finally, functional significance is most often assigned to the protein coding regions by searching public databases for similar sequences and by transferring the pertinent information from the known to the unknown protein. A wide variety of computational algorithms have been applied to the sequence comparison problem in diverse domains, notably in natural language processing. Nevertheless, the analysis of biological sequences involves more than abstract string parsing, for behind the string of bases or amino acids is the whole complexity of molecular and evolutionary biology.

One major problem is the identification of important features, such as regulatory sites in the genomes, or functional domains or active sites in proteins, that are conserved within a family of sequences, without prior alignment of the sequences. In this context, motif recognition and discovery tools are widely used. The retrieved motifs are often compiled in databases including DNA regulatory motifs in TRANSFAC [1], JASPAR [2], or RegulonDB [3], and protein motifs in PRINTS [4], PROSITE [5], or ELM [6]. These well-characterized motifs can be used as a starting point for the identification of known motifs in other sequences. This is otherwise known as the pattern recognition problem. The challenges associated with *de novo* pattern

discovery, or the detection of previously unknown motifs [7], is far more difficult due to the nature of the motifs.

Biological sequence motifs are defined as short, usually fixed length, sequence patterns that may represent important structural or functional features in nucleic acid and protein sequences such as transcription binding sites, splice junctions, active sites, or interaction interfaces. They occur in an exact or approximate form within a family or a subfamily of sequences. Motif discovery is therefore an important challenge in bioinformatics and numerous methods have been developed for the identification of motifs shared by a set of functionally related sequences.

Consequently, much effort has been applied to *de novo* motif discovery, for example, in DNA sequences, with a large number of specialized methods that were reviewed recently in [8]. One interesting aspect is the development of nature-inspired algorithms, for example, particle swarm optimization has been used to find gapped motifs in DNA sequences [9], while DNA motifs have been discovered using an artificial immune system (AIS) [10]. Unfortunately, far fewer tools have been dedicated to the *de novo* search for protein motifs. This is due to the combinatorial explosion created by the large alphabet size of protein sequences, as well as the degeneracy of the motifs, i.e., the large number of wildcard symbols within the motifs. Some tools, such as Teiresias [11], or the MEME suite [12], can discover motifs in both DNA and protein sequences. Other work has been dedicated to the discovery of specific types of protein motifs, such as patterns containing large irregular gaps with "eukaryotic linear motifs" with SLiMFinder [13] or phosphorylation sites [14]. Many studies have been conducted to compare these specific motif discovery tools, such as [15].

In most cases, *de novo* motif discovery algorithms take as input a set of related sequences and search for patterns that are unlikely to occur by chance and that might represent a biologically important sequence pattern. Since protein motifs are usually short and can be highly variable, a challenging problem for motif discovery algorithms is to distinguish functional motifs from random patterns that are overrepresented. One solution to this challenge is to first construct a global multiple alignment of the sequences and then search for motifs in the aligned sequences. This reduces the search space to the aligned regions of the sequences, but also severely limits the possibilities of finding new motifs.

Furthermore, existing motif discovery methods are able to find motifs that are conserved within a complete family, but most of them are still unable to find motifs that are conserved only within a subfamily of the sequences. These subfamily-specific motifs, which we will call "rare" motifs, are often conserved within groups of proteins that perform the same function (specificity groups) and vary between groups with different functions/specificities. These sites generally determine protein specificity either by binding specific substrates/inhibitors or through interaction with other protein.

In Section 2, we will provide a brief description of protein sequences and the motifs that characterize them. Then, in Section 3, the main approaches used for discovery of motifs in protein sequences will be presented. Section 3 also deals with motif recognition in protein sequences. In Section 4, the main approaches used for the more difficult problem of *de novo*

motif discovery will be presented. Finally, in Section 5, we will propose new horizons for motif discovery in order to address the short comings of the existent methods.

2. Protein sequences, active sites, and motifs

Some basic concepts in protein biology are necessary for understanding the rest of this chapter. For many readers, this will be a familiar territory and in this case, they may want to skip this section and go directly to Section 3.

The genetic information encoded in the genome sequence of any organism contains the blueprint for its potential development and activity. However, the translation of this information into cellular or organism-level behavior depends on the gene products, especially proteins. Proteins perform a wide variety of cellular functions, ranging from catalysis of reactions, nutrient transport, and signal transmission to structural and mechanical roles. A protein is composed of a single chain of amino acids (of which there are 20 different kinds), represented by their single letter codes. This "primary structure" or sequence is none other than a string of characters that we can read from left to right, i.e., from NH_2 part (*N*-terminal) to the COOH part (*C*-terminal).

Every protein molecule has a characteristic three-dimensional (3D) shape or conformation, known as its native state. The process by which a protein sequence assumes its 3D structure is known as folding. Protein folding can be considered as a hierarchical process, in which the primary sequence defines secondary structure, which in turn defines the tertiary structure. Individual protein molecules can then interact with other proteins to form complex quaternary structures. The precise 3D structure of a protein molecule is generally required for proper biological function since a specific conformation is needed that the cell factors can recognize and interact with.

During evolution, random mutagenesis events take place, which change the genomic sequences that encode proteins. There are several different types of mutation that can occur. A single amino acid can be substituted for another one. Insertions and deletions also occur, involving a single amino acid up to several hundred amino acids. Some of these evolutionary changes will adversely affect the function of a protein, e.g., mutations of active sites in an enzyme, or mutations that disrupt the 3D structure of the protein. If this happens to a protein that takes part in a crucial process for the cell, it will result in cell death. As a result, amino acids that are essential for a protein's function, or that are needed for the protein to fold correctly, are conserved over time. Occasionally, mutations occur that give rise to new functions. This is one of the ways that new traits and eventually species may come about during evolution.

By comparing related sequences and looking for those amino acids that remain the same in all of the members in the family, we can predict the sites that might be essential for function. Some examples of important functional sites include the following:

- Enzyme active sites: to catalyze a reaction, an enzyme will bind to one or more reactant molecules, known as its substrates. The active site consists of the enzyme's amino acids that

form temporary bonds with the substrate, known as the binding site, and the amino acids that catalyze the reaction of that substrate.

- Ligand-binding sites: a binding site is a region on a protein molecule where ligands (small molecules or ions) can form a chemical bond. Ligand binding often plays a structural or functional role, for example, in stabilization, catalysis, modulation of enzymatic activity, or signal transmission.
- Cleavage sites: the location on a protein molecule where peptide bonds are broken down by hydrolysis. For instance, in human digestion, proteins in food are broken down into smaller peptide chains by digestive enzymes. Many viruses also produce their proteins initially as a single polypeptide chain which is then cleaved into individual protein chains.
- Posttranslational modification sites: some amino acids in a protein can undergo chemical modification, produced in most cases by an enzyme after its synthesis or during its life in the cell. This change usually results in a change of the protein function, whether in terms of its action, half-life, or its cellular localization.
- Targeting sites: within a cell, the localization of a protein is essential for its proper functioning, but the production site of a protein is often different from the place of action. Protein targeting signals, such as nuclear or mitochondrial localization signals, can be encoded within the polypeptide chain to allow a protein to be directed to the correct location for its function.

An example of a simple functional site is the N-glycosylation site, which is a posttranslational modification where a carbohydrate is attached to a hydroxyl or other functional group of a protein molecule. The sequence motif representing this site can be indicated by N-X-S/T. The first amino acid is asparagine (N), the second amino acid can be any of the 20 amino acids (X), and the third amino acid is either serine (S) or threonine (T). This example introduces the first complication in protein motif discovery: the motifs can contain both exact and ambiguous elements. Asparagine is a necessary amino acid, since this is the site that will be glycosylated, and is represented by an exact element. The third position should be a hydroxyl-containing amino acid (serine or threonine), while the second position is a "wild card." Nevertheless, the N-glycosylation motif shown here is uninterrupted, and so it is relatively easy to recognize. The spacing between the elements in many other sequence motifs can vary considerably, but the presence of such motifs is generally detected from the structure rather than sequence and this kind of motif will not be discussed in detail here. Finally, it should be pointed out that, just because this motif appears in a protein sequence, it does not mean that the site is glycosylated. The functional implications of a motif will depend on the neighboring amino acids and the surrounding 3D context. Therefore, in practice, identifying functional motifs from a protein sequence is far from straightforward.

3. Motif recognition in protein sequences

The motif recognition problem takes as input a set of known patterns or features that in some way define a class of proteins. The goal is then to search in an unsupervised or supervised way for other instances of the same patterns. As mentioned in the Introduction, the known motifs in biological sequences are generally compiled databases that are publically available over the Internet. For example, the PRINTS database (www.bioinf.manchester.ac.uk/dbbrowser/PRINTS) contains "protein fingerprints," where a fingerprint is composed of a group of motifs that characterize a given set of protein sequences with the same molecular function. In contrast, the PROSITE (prosite.expasy.org) and ELM (elm.eu.org) databases contain single motifs that correspond to known functionally or structurally important amino acids, such as those involved in an active site or a ligand binding site. The motifs contained in these resources are generally manually curated and the entries in the databases include extensive documentation of the specific biological function associated with the sites.

3.1. Motif representation

Over the years, a variety of motif representation models have been developed to take into account the complexity of protein motifs. The models are attempts to construct generalizations based on known functional motifs, and are used to help characterize the functional sites and to facilitate their identification in unknown protein sequences. They can be divided into two main categories.

3.1.1. Deterministic models

Consensus sequences are the simplest model for representing protein motifs. They can be constructed easily by selecting the amino acid found most frequently at each position in the signal. The number of matches between a consensus and an unknown candidate sequence can be used to evaluate the significance of a potential functional site. However, consensus sequences are limited models, since they do not capture the variability of each position. To support some degree of ambiguity, regular expressions can be used. Regular expressions are typically composed of exact symbols, ambiguous symbols, fixed gaps, and/or flexible gaps [16]. For example, the IQ motif is an extremely basic unit of about 23 amino acids, whose conserved core can be represented by the regular expression:

[FILV]Qxxx[RK]Gxxx[RK]xx[FILVWY]

where x signifies any amino acid, and the square brackets indicate an alternative.

3.1.2. Probabilistic models

Although deterministic models provide useful ways to construct human-readable representations of motifs, their main drawback is that they lose some information. For instance, in the IQ motif discussed above, the first position is usually I and both [RK] are most often R.

Probabilistic models can be used to overcome such loss of information. The position-specific scoring matrix (PSSM) [17], also known as the probability weight matrix (PWM), is undoubtedly one of the most widely used probabilistic models. This model is represented by a matrix where each entry (i,a) is the probability of finding an amino acid a at the ith position in the sequence motif. For example, for a set of motifs:

- WSEW
- WSRW
- CSKW
- CSKW
- YSKY

The corresponding PSSM is shown in **Table 1**.

Position	1	2	3	4
C	0.4	0.0	0.0	0.0
E	0.0	0.0	0.2	0.0
K	0.0	0.0	0.6	0.0
R	0.0	0.0	0.2	0.0
S	0.0	1.0	0.0	0.0
W	0.4	0.0	0.0	0.8
Y	0.2	0.0	0.0	0.2

Table 1. Example of a position specific scoring matrix (PSSM).

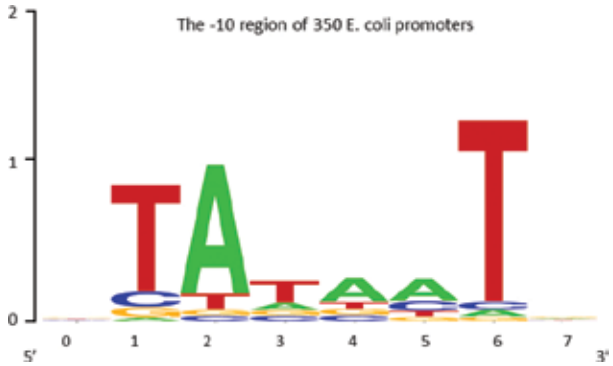

Figure 1. An example of a sequence logo for representing patterns in biological sequences. The logo represents the Pribnow box, a conserved region found upstream of the some genes in prokaryotic genomes.

Although in this example, PSSM containing entries having a value of 0, in general, pseudocounts are applied, especially when using a small dataset, in order to allow the calculation of probabilities for new motifs.

The information summarized in the PSSM can also be represented by a sequence logo [18], which is a graphical representation of the motif conservation as shown in **Figure 1**. A logo consists of a stack of letters at each position in the motif, where the relative sizes of the letters indicate their frequency in the sequences. The total height of the letters corresponds to the information content of the position, in bits.

Another widely used probabilistic model is the hidden Markov model (HMM), a statistical model that is generally applicable to time series or linear sequences. They were first introduced in bioinformatics for DNA sequences [19]. A HMM can be visualized as a finite state machine that moves through a series of states and produces some kind of output. The HMM generates a protein sequence by emitting amino acids as it progresses through a series of states. Each state has a table of amino acid emission probabilities, and transition probabilities for moving from state to state.

All of the representations mentioned so far inherently assume that positions within the motif are independent of each other. However, in some cases, this strong independence assumption may not be reasonable. Markov models of higher order, permuted Markov models, or Bayesian networks can be used to capture local dependencies by considering how each position depends on the other.

3.2. Motif detection

The models described in the previous section can be applied to the task of scanning a user-submitted sequence for matches to known motifs, thus providing evidence for the function of the protein and contributing to its classification in a given protein family. Ideally, a motif model would recognize all and only the members of the family. Unfortunately, this is seldom the case in practice.

In the case of deterministic models including consensus sequences and regular expressions, the models are often either too specific leading to a large number of false negative predictions, or too degenerate resulting in many false positives. The statistical power of such models can be estimated using standard measures, such as the positive and negative predictive values (PPV and NPV, respectively).

In the case of probability matrices or HMM-based methods, a log-odds score can be calculated that is a measure of how probable it is that a sequence is generated by a model rather than by a random null model, representing the universe of all sequences (also known as the "background"). The log-odds score of a motif is defined as:

$$score(s) = \log_z \frac{P_m(s)}{P_\varnothing(s)} \tag{1}$$

where P_m is the probability that the sequence was generated by the motif model m and P_ϕ is the probability that the sequence was generated by the null model. The logarithm is usually

base 2, and the score is given in bits. A log-odds score greater than zero indicates that the sequence fits the motif model better.

4. Motif discovery in protein sequences

4.1. Methods for motif discovery

Given a set of functionally related sequences, the main aim of motif discovery algorithms is to find new and *a priori* unknown motifs that are frequent, unexpected, or interesting according to some formal criteria. The methods used to discover such motifs follow the same general schema, as shown in **Figure 2**. They can be grouped into two main categories: alignment-based methods and methods that search for motifs in unaligned sequences.

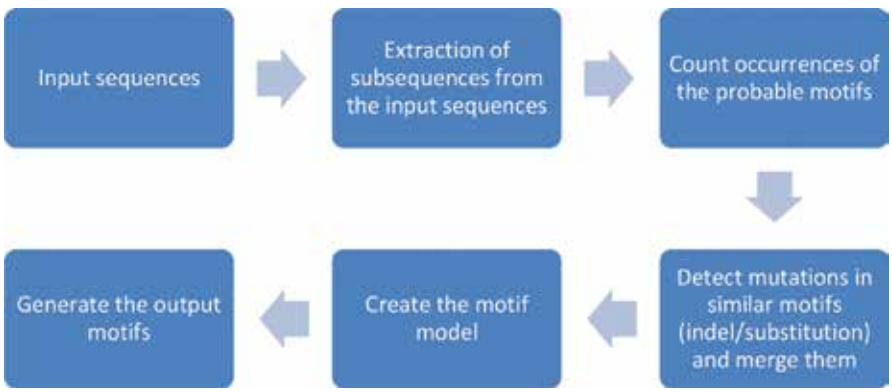

Figure 2. General motif discovery process.

4.1.1. Alignment-based methods

Alignment-based methods for motif discovery first construct a multiple sequence alignment of the set of sequences, where each sequence of amino acids is typically represented as a row within a matrix. Gaps are inserted between the amino acids so that identical or similar characters are aligned in successive columns. Once the multiple alignments are constructed, the patterns are extracted from the alignment by combining the substrings common to most of the sequences.

One of the first automatic methods for the identification of conserved positions in a multiple alignment was the AMAS program [20], using a set-based description of amino acid properties. Since then, a large number of different methods have been proposed. For example, Al2Co [21] calculates a conservation index at each position in a multiple sequence alignment using weighted amino acid frequencies at each position. The DIVAA method [22] is based on a statistical measure of the diversity at a given position. The diversity measures the proportion of the 20 possible amino acids that are observed.

The advantage of the alignment-based approach is that no upper limit has to be imposed on the length of the motifs. Moreover, these algorithms usually do not need as input a maximum threshold value for the motif distance from the sequences. In general, this approach works well if the sequences are sufficiently similar and the patterns occur in the same order in all of the sequences. Unfortunately, this is not usually the case and therefore most methods for motif discovery in protein sequences assume that the input sequences are unaligned.

4.1.2. Alignment-free methods

The vast majority of motif discovery methods in bioinformatics are alignment-free approaches that do not rely on the initial construction of a multiple sequence alignment. Instead, they generally search for patterns that are overrepresented in a given set of sequences. The simplest solution is to generate all possible motifs up to a maximum length l, and then to search separately for the approximate occurrences of each motif in the set of sequences. Once a list of candidate patterns is obtained, the ones with the highest significance scores are selected. This approach guarantees to find all motifs that satisfy the input constraints. Moreover, the sequences can be organized in suitable indexing structures, such as suffix trees, etc., so that the time needed by the algorithm to search for a single motif is linear in the overall length of the sequences.

This simplistic approach has an evident disadvantage: the number of candidate motifs, and therefore the time required by the algorithm, grows exponentially with the length of the sequences. Computing a significance score for each motif further increases the time required by the algorithm. A number of more efficient tools have been developed to address these issues and in the next chapter, we will discuss some of the more widely used ones.

4.2. Tools for motif discovery

In this section, we will present of the programs that are specifically designed to search for motifs in protein sequences that are biologically significant. The search for motifs in a set of unaligned sequences is a complex problem because many factors come into play, such as the precise start and end boundaries of the motif, the size variability (presence of gaps or not), or stronger or weaker motif conservation during evolution.

De novo motif discovery programs are generally based on one of the following three algorithms:

- Enumeration is a method that involves counting all substrings of a certain length (known as words or k-mers) and then seeking overrepresentations. Such exhaustive motif finding approaches are guaranteed to report all instances of motifs in a set of sequences. However, the exponential complexity of such searches means that the problem quickly becomes intractable for large alphabets.
- Deterministic optimization is based on the expectation-maximization (EM) algorithm that estimates the likelihood of a motif from existing data in two stages repeated iteratively. The first uses a set of parameters to reconstruct the hidden motif structure. The second uses this structure to reestimate the parameters. This method allows finding alternate sequences representing the motif and updating the motif model.

- Probabilistic optimization is an iterative method in which a random subsequence is extracted from each sequence to build an initial model. In each subsequent iteration, the *i*th sequence is removed and the model is recalculated. Then, a new motif is extracted from the *i*th sequence. This process is repeated until convergence.

Below, and in **Table 2**, we present the most used motif discovery programs and discuss their advantages and limitations.

Teiresias [11] is based on an enumeration algorithm. It operates in two phases: scanning and convolution. During the scanning phase, elementary motifs with sufficient support are identified. These elementary motifs constitute the building blocks for the convolution phase. They are combined into progressively larger motifs until all the existing maximal motifs are generated.

MEME [12] is an example of a deterministic optimization algorithm. It allows discovery of motifs in DNA or protein sequences based on expectation maximization (EM). MEME discovers at least three motifs, each of which may be present in some or all of the input sequences. MEME chooses the width and number of occurrences of each motif automatically in order to minimize the "E-value" of the motif, i.e., the probability of finding a similarly well-conserved pattern in random sequences. With default parameters, only motif widths between 6 and 50 are considered, but the user have the possibility to change this as well as several other parameters (options) of the motif discovery.

Pratt [23] is based on probabilistic optimization. It first searches the space of motifs, as constrained by the user, and compiles a list of the most significant sequences that matches at least the user-defined minimum number of sequences. If the user has not switched off the refinement, these motifs will be input to one of the motif refinement algorithms. The most significant motifs resulting from this are then output to a file.

qPMS [24] stands for quorum planted motif search. The program searches for motifs in either DNA or protein sequences. It uses the (l, d) motif search algorithm known as the planted motif search. qPMS takes as input a set of sequences and two values, l and d. It returns all sequences M of length l, which appear in at least q% of the sequences.

SLiMFinder [13] identifies novel short linear motifs (SLiMs) in a set of sequences. SLiMs are microdomains that have important functions in many diverse biological pathways. SLiM-mediated functions include posttranslational modification, subcellular localization, and ligand binding. SLiMs are generally less than 10 amino acids long, many of which will be "flexible" in terms of the conserved amino acid. SLiMFinder constructs such motifs by grouping dimers into longer patterns: motifs with fixed amino acid positions are identified and then grouped to include amino acid ambiguity and variable-length wildcards. Finally, motifs that are overrepresented in a set of unrelated proteins are identified.

Dilimot [25] proceeds as follows: in the first step, a user provided set of protein sequences is filtered to eliminate repetitive sequences as well as the regions least likely to contain linear motifs. In the second step, overrepresented motifs are identified in the nonfiltered sequences and ranked according to scores that take into account the background probability of the motif,

the number of sequences containing the motif, the size of the sequence set, and the degree to which the motif is conserved in other orthologous proteins.

Program	Description	Advantages	Disadvantages
Teiresias	Finds motifs that are frequent in a set of related sequences	Does not need background sequences; Very fast	Too many redundant motifs discovered
MEME	Finds motifs in related sequences using Gibbs sampling and expectation maximization	Does not need background sequences; Fast, Multi-thread version available; User friendly output	User defines the number of motifs to discover
Pratt	Discovers flexible motifs in related sequences	Does not need background sequences	Unable to discover effectively exact motifs
qPMS	Finds overrepresented motifs in a set of sequences based on Quorum Planted Motif Search	Fast; Low memory consumption	Limited to 20 protein sequences
SlimFinder	Finds overrepresented motifs in a set of unrelated sequences relative to background sequences	Well documented; Can use filters	Needs background sequences
MotifHound	Exhaustively finds motifs overrepresented in a set of unrelated sequences relative to background sequences	Exhaustive exploration of motifs; Can use filters Fast; Multi-thread version available	Needs background sequences
Dilimot	Finds overrepresented motifs in a set of unrelated sequences relative to a background sequences	Integrates several types of sequence information on motifs	Needs background sequences; Source code not available
FirePro	Correlates overrepresented motifs in a set of sequences with specific functions or behaviors	User friendly output	Needs background sequences

Table 2. Advantages and limitations of the most used motif discovery programs.

MotifHound [26] is suitable for the discovery of small and degenerate linear motifs. The method needs two input datasets: a background set of protein sequences and a subset of this background set that represents the query sequences. MotifHound first enumerates all possible motifs present in the query sequences, and then calculates the frequency of each motif in both the query and the background sets.

FIRE-pro [27] stands for finding informative regulatory elements in proteins. Its main goal is to discover protein motifs that correlate with the biological behavior of the corresponding proteins. FIRE-pro calculates a mutual information measure between frequent k-mer motifs and a "protein behavior profile" containing experimental data about the function of the proteins.

Most of these programs need prior knowledge about either the input sequences or the motif structure. Furthermore, they are generally designed to discover frequent motifs that occur in all or most of the sequences. The subfamily-specific motifs, which differentiate a specific subset of sequences, pose a greater challenge due to the statistical nature of these programs or the default choice of parameters used. Nevertheless, these "rare" motifs are often characteristic of important biological functions or context-specific modifications, including substrate binding sites, protein-protein interactions, or posttranslational modification sites.

In the final section of this chapter, we will discuss the use of "intelligent algorithms" that should be more reliable for the discovery of significant rare motifs in addition to the conserved and known ones.

5. Intelligent algorithms for protein motif discovery

Intelligent algorithms include optimization and nature inspired algorithms. Among these, artificial immune systems are especially adapted to pattern discovery, and have been used recently for motif discovery in DNA sequences. The high complexity and dimensionality of the problems in bioinformatics are an interesting challenge for testing and validating new computational intelligence techniques. Similarly, the application of AIS to bioinformatics may bring important contributions to the biological sciences, providing an alternative form of analyzing and interpreting the huge volume of data from molecular biology and genomics [28].

Artificial immune systems are a class of computationally intelligent systems inspired by the principles and processes of the vertebrate immune system. The algorithms typically apply the structure and function of the immune system to solving hard computational problems. Since their introduction in the 1990s, a number of common techniques have been developed, including:

- Clonal selection algorithms model how antibodies of the immune system adaptively learn the features of the intruding antigen and defend the body from it. The algorithms are most commonly applied to optimization and pattern recognition domains.
- Negative selection refers to the identification and deletion of self-reacting cells, i.e., cells that may attack self-tissues. The algorithms are typically used for classification and pattern recognition problems, especially in the anomaly detection domain.
- Immune network algorithms focus on the network graph structures involved where antibodies represent the nodes and the training algorithm involves growing or pruning edges between the nodes based on affinity. The algorithms have been used to solve clustering, data visualization, control, and optimization problems.
- Dendritic cell algorithms are inspired by the danger theory algorithm of the mammalian immune system, and particularly the role and function of dendritic cells, from the molecular networks present within the cell to the behavior exhibited by a population of cells as a whole.

Although a number of these different AIS can be used for pattern recognition, the clonal selection algorithm seems to be particularly well suited for protein motif discovery in large sets of sequences. In particular, the capabilities for self-organization of huge numbers of immune cells mean that no prior information is needed. In addition, the system does not require outside intervention and so it can automatically classify pathogens (motifs) and it can react to pathogens that the body has never seen before. Another advantage of AIS is the fact that there are varying types of elements that protect the body from invaders, and there are different lines of defense, such as innate and adaptive immunity. These features can be abstracted to model the diverse types of motifs found in protein molecules (see Section 1). These different mechanisms are organized in multiple layers that act cooperatively to provide high noise tolerance and high overall security.

The use of such intelligent algorithmic approaches should improve the whole motif discovery process: from the selection of suitable sets of sequences, via data cleaning and preprocessing, motif identification and evaluation, to the final presentation and visualization of the results. Nevertheless, a number of issues remain to be addressed before such systems can be applied to the very large datasets produced by NGS technologies. In particular, the substantial time and memory requirements of AIS are a limiting factor, although these can be significantly reduced thanks to the inherently parallel nature of the algorithms.

Acknowledgements

We would like to thank the members of the BICS and BISTRO Bioinformatics Platforms in Strasbourg for their support. This work was supported by Institute funds from the CNRS, the Université de Strasbourg and the Faculté de Médecine de Strasbourg.

Author details

Salma Aouled El Haj Mohamed[1,2,3], Mourad Elloumi[2] and Julie D. Thompson[3*]

*Address all correspondence to: thompson@unistra.fr

1 Faculty of Science, Doctoral School of Mathematics, Computer Science and Material Science and Technology, University of Tunis El Manar, Tunis, Tunisia

2 Laboratory of Technologies of Information and Communication and Electrical Engineering (LaTICE), University of Tunis, Tunis, Tunisia

3 Department of Computer Science, ICube, UMR 7357, University of Strasbourg, CNRS, Strasbourg Federation of Translational Medicine (FMTS), Strasbourg, France

References

[1] Matys V, Kel-Margoulis OV, Fricke E, Liebich I, Land S, Barre-Dirrie A, et al. TRANSFAC and its module TRANSCompel: transcriptional gene regulation in eukaryotes. Nucleic Acids Res. 2006 34:D108–D110.

[2] Mathelier A, Fornes O, Arenillas DJ, Chen CY, Denay G, Lee J, Shi W, Shyr C, Tan G, Worsley-Hunt R, Zhang AW, Parcy F, Lenhard B, Sandelin A, Wasserman WW. JASPAR 2016: a major expansion and update of the open-access database of transcription factor binding profiles. Nucleic Acids Res. 2016 44:D110-–D115.

[3] Gama-Castro S, Salgado H, Santos-Zavaleta A, Ledezma-Tejeida D, Muñiz-Rascado L, García-Sotelo JS, Alquicira-Hernández K, Martínez-Flores I, Pannier L, Castro-Mondragón JA, Medina-Rivera A, Solano-Lira H, Bonavides-Martínez C, Pérez-Rueda E, Alquicira-Hernández S, Porrón-Sotelo L, López-Fuentes A, Hernández-Koutoucheva A, Moral-Chávez VD, Rinaldi F, Collado-Vides J. RegulonDB version 9.0: high-level integration of gene regulation, coexpression, motif clustering and beyond. Nucleic Acids Res. 2016 44:D133-143.

[4] Attwood TK, Coletta A, Muirhead G, Pavlopoulou A, Philippou PB, Popov I, Romá-Mateo C, Theodosiou A, Mitchell AL. The PRINTS database: a fine-grained protein sequence annotation and analysis resource--its status in 2012. Database J Biol Databases Curation. 2012 bas019.

[5] Sigrist CJ, De Castro E, Cerutti L, Cuche BA, Hulo N, Bridge A, Bougueleret L, Xenarios I. New and continuing developments at PROSITE. Nucleic Acids Res. 2013 41:D344–D347.

[6] Dinkel H, Van Roey K, Michael S, Kumar M, Uyar B, Altenberg B, Milchevskaya V, Schneider M, Kühn H, Behrendt A, Dahl SL, Damerell V, Diebel S, Kalman S, Klein S, Knudsen AC, Mäder C, Merrill S, Staudt A, Thiel V, Welti L, Davey NE, Diella F, Gibson TJ. ELM 2016-data update and new functionality of the eukaryotic linear motif resource. Nucleic Acids Res. 2016 44:D294–D300.

[7] Tompa P, Davey NE, Gibson TJ, Babu MM. A million peptide motifs for the molecular biologist. Mol Cell. 2014 55:161–169.

[8] Boeva V. Analysis of genomic sequence motifs for deciphering transcription factor binding and transcriptional regulation in eukaryotic cells. Front Genet. 2016 7:24.

[9] Lei C, Ruan J. A particle swarm optimization-based algorithm for finding gapped motifs. BioData Mining. 2010 3:9–10.

[10] Seeja KR. AISMOTIF- An artificial immune system for DNA motif discovery. Int J Comput Sci. Issues. 2011 8:143–149.

[11] Rigoutsos I, Floratos A. Combinatorial pattern discovery in biological sequences: the TEIRESIAS algorithm. Bioinformatics. 1998 14:55–67.

[12] Bailey TL, Bodén M, Whitington T, Machanick P. The value of position-specific priors in motif discovery using MEME. BMC Bioinformat. 2010 11:179.

[13] Edwards RJ, Davey NE, Shields D. SLiMFinder: A probabilistic method for identifying over-represented, convergently evolved, short linear motifs in proteins. PLoS One. 2007 2:e967.

[14] Frades I, Resjö S, Andreasson E. Comparison of phosphorylation patterns across eukaryotes by discriminative N-gram analysis. BMC Bioinformat. 2015 16:239.

[15] Bhowmick P, Guharoy M, Tompa P. Bioinformatics approaches for predicting disordered protein motifs. Adv Exp Med Biol. 2015; 870:291–318.

[16] Brazma A, Jonassen I, Eidhammer I, Gilbert D. Approaches to the automatic discovery of patterns in biosequences. J Comp Biol. 1998 5:279–305.

[17] Henikoff S, Henikoff JG. Position-based sequence weights. J Mol Biol. 1994 243:574–578.

[18] Schneider TD, Stephens RM. Sequence logos: a new way to display consensus sequences. Nucleic Acids Res. 1990; 18:6097–6100.

[19] Churchill GA. Stochastic models for heterogeneous DNA sequences. Bull Math Biol. 1998; 51:79–94.

[20] Livingstone CD, Barton GJ. Protein sequence alignments: a strategy for the hierarchical analysis of residue conservation. Comput Appl Biosci. 1993; 9:745–756.

[21] Pei J, Grishin NV. AL2CO: calculation of positional conservation in a protein sequence alignment. Bioinformatics. 2001; 17:700–712.

[22] Rodi DJ, Mandava S, Makowski L. DIVAA: analysis of amino acid diversity in multiple aligned protein sequences. Bioinformatics. 2004; 20:3481–3489.

[23] Jonassen I, Collins JF, Higgins DG. Finding flexible patterns in unaligned protein sequences. Protein Sci. 1995; 4:1587–1595.

[24] Dinh H, Rajasekaran S, Davila J. qPMS7: a fast algorithm for finding (l,d) motifs in DNA and protein sequences. PLoS One. 2012; 7:e41425.

[25] Neduva V, Russell RB. DILIMOT: discovery of linear motifs in proteins. Nucleic Acids Res. 2006; 34:W350–W355.

[26] Lieber DS, Elemento O, Tavazoie S. Large-scale discovery and characterization of protein regulatory motifs in eukaryotes. PLoS One. 2010; 5:e14444.

[27] Kelil A, Dubreuil B, Levy ED, Michnick SW. Fast and accurate discovery of degenerate linear motifs in protein sequences. PLoS One. 2014; 9:e106081.

[28] Al-Enezi A, Abbod MF, Alsharhan Al-Enezi S. Artificial immune systems-models, algorithms and applications. IJRRAS. 2010; 3:118–131.

Chapter 2

Hybrid Metaheuristics for Classification Problems

Nadia Abd-Alsabour

Additional information is available at the end of the chapter

http://dx.doi.org/10.5772/65253

Abstract

High accuracy and short amount of time are required for the solutions of many classification problems such as real-world classification problems. Due to the practical importance of many classification problems (such as crime detection), many algorithms have been developed to tackle them. For years, metaheuristics (MHs) have been successfully used for solving classification problems. Recently, hybrid metaheuristics have been successfully used for many real-world optimization problems such as flight scheduling and load balancing in telecommunication networks. This chapter investigates the use of this new interdisciplinary field for classification problems. Moreover, it demonstrates the forms of metaheuristics hybridization as well as designing a new hybrid metaheuristic.

Keywords: metaheuristics, hybrid metaheuristics, classification problems

1. Introduction

Before starting this chapter, let us know the trip that led to the appearance of hybrid metaheuristics. Traditionally, rigorous approaches (that are based on hypotheses, characterizations, deductions, and experiments) were used for solving many optimization problems.

However, in order to find possible good solutions for new complex optimization problems, researchers went toward the use of heuristics. Heuristics are rules of thumb, trails and error, common sense, etc. Many of these heuristics strategies are often independent of the undertaken optimization problems and share common aspects. This introduced the term metaheuristics which refers to general techniques that are not specific to a particular problem [1]. Metaheuristics are approximate algorithms, and each of them has its own historical background [2–4]. A metaheuristic is a set of algorithmic concepts used for defining heuristic methods that can

be applied to a variety of optimization problems with relatively few modifications in order to adapt them to particular optimization problems [5, 6].

Metaheuristics have successfully found high-quality solutions for a wide spectrum of NP hard optimization problems [1], that is, they are hard to be solved. This means the needed time to solve an instance of these optimization problems grows exponentially with the instance size in the worst case. These optimization problems are so complex as there is no known algorithm that can solve them in polynomial time. They still have to be solved in a huge number of practical settings. Therefore, a large number of optimization algorithms were proposed to tackle them [5, 6].

Of great importance for the success of designing a new metaheuristic is considering that this metaheuristic will have to explore the search space effectively and efficiently. The search process should be intelligent in order to intensively explore areas of the search space that have high-quality solutions and to move to unexplored areas. This is called intensification and diversification, respectively. Intensification is the exploitation of the gathered information by the metaheuristic at a given time, while diversification is the exploration of the areas imperfectly taken into account. The use of these two important characteristics of a metaheuristic can lead to getting high-quality solutions. Crucial for the success of a metaheuristic is a well-adjusted balance between these two features. This is to on one side identify quickly search areas with high-quality solutions and on the other side to avoid spending too much time in areas consisting of poor-quality solutions or have been well explored [1, 7–11].

There are many classifications for metaheuristics as follows:

- Nature-inspired metaheuristics [such as ant colony optimization (ACO) algorithms, genetic algorithms (GAs), particle swarm optimization (PSO), and simulated annealing (SA)] vs. nonnature-inspired metaheuristics [such as iterated local search (ILS), and tabu search (TS)]. This is based on the origins of a metaheuristic.

- Memory-based metaheuristics vs. memory-less metaheuristics. This is based on the use of the search history, that is, whether they use memory or not. The use of memory is considered one of the crucial elements of a powerful metaheuristic.

- Population-based metaheuristics vs. single-point metaheuristics. This is based on how many used solutions at any given time by a metaheuristic. Population metaheuristics manipulate a set of solutions (at each iteration) from which the population of the next iteration is produced. Examples are evolutionary algorithms and scatter search, and construction-oriented techniques such as ant colony optimization and the greedy randomized adaptive search procedure. The metaheuristics that deal with only one solution at any given time are called trajectory metaheuristics where the search process describes a trajectory in the search space [1, 2, 4] as shown in **Figure 1** [12].

When they first appeared, pure metaheuristics quickly became state-of-the-art algorithms for many optimization problems as they found high-quality solutions for these optimization problems. This was reported in many specific conferences and workshops. This success had motivated researches toward finding answers to questions such as:

http://dx.doi.org/10.5772/65253

- Why a given metaheuristic is successful?
- Which characteristics of a problem instance should be exploited?
- Which metaheuristic is best for a given optimization problem? [1, 2]

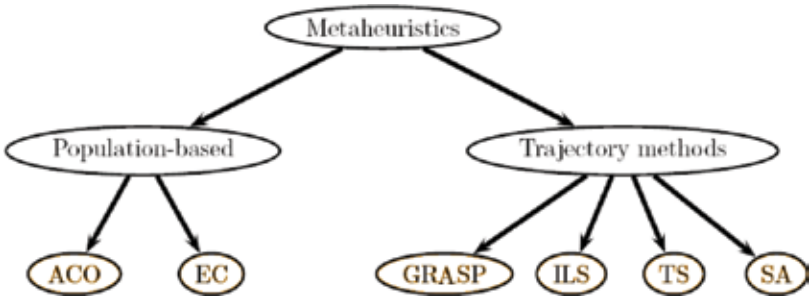

Figure 1. Metaheuristics classification [12].

Despite this success, it became recently evident that the focus on pure metaheuristics is restrictive when tackling particular optimization problems such as real-world and large-scale optimization problems [2]. A skilled combination of a metaheuristic with components from other metaheuristics or with other optimization algorithms such as operations research techniques (mathematical programming), artificial intelligence techniques (constraint programming), or complete algorithms (branch and bound) can lead to getting much better solutions for these optimization problems. This interdisciplinary field is called hybrid metaheuristics which goes beyond the scope of a pure metaheuristic [1]. Over the years, many algorithms that do not purely follow the paradigm of a pure metaheuristic were developed. They combine various algorithmic components originating from different optimization algorithms [2]. This is explained in Section 3.

The rest of this chapter is organized as follows. The following section introduced classification problems. Section 3 explains the main forms of hybridizing metaheuristics. Section 4 demonstrates designing a hybrid metaheuristic. The fifth section demonstrates hybrid metaheuristics for classification problems. The discussion is given in Section 6. The last section concludes this chapter and highlights future work in this area.

2. Classification problems

Classification involves training and testing data which consist of data instances (objects). Each instance in the training set contains one class label (called target, dependent, response, or features) and other features (called attributes, inputs, predictors, or independent features) [13–15]. Classification consists of examining the features of a new object and then assigning it to one of the predefined set of classes. The objects to be classified are generally represented by records in a dataset. The classification task is to build a model that will be applied to unclas-

sified data to classify it, that is, predicting the target values of instances (that are given only the input features) in the testing set [15, 16]. The classification task (determining which of the fixed set of classes an example belongs to) is illustrated in **Figure 2**.

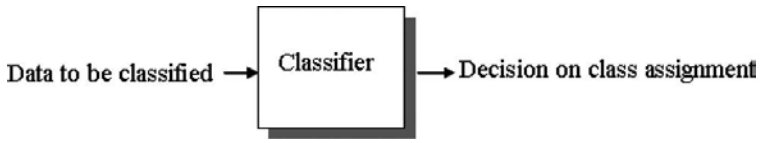

Figure 2. The classification task.

Examples of classification problems are:

- classifying credit applications such as low, medium, or high risky,
- determining whether a customer with a given profile will buy a new computer,
- predicting which of three specific treatments a breast cancer patient should receive,
- determining whether a will was written by the real person or somebody else,
- diagnosing whether a particular illness is present or not,
- choosing particular contents to be displayed on a web page,
- determining which phone numbers correspond to fax machines,
- placing a new student into a particular track based on special needs,
- identifying whether a behavior indicates a possible terrorist threat, and
- spotting fraudulent insurance claims.

In these examples, the classifier is built to predict categorical labels such as "low risky," "medium risky," or "high risky" for the first example; "yes" or "no" for the second example; "treatment A," "treatment B," or "treatment C" for the third example, etc. [16–18].

The accuracy of a classifier refers to how well it can predict the value of the predictor feature for a previous unseen data and how well it captured the dependencies among the input features. Classifier accuracy is the main measure for classification and is widely used. The classifier accuracy goes up when comparing between different classifiers [18–20].

The classifier is considered the basic component of any classification system, and its task is to partition the feature space into class-labeled decision regions (one for each category). Classifiers' performance is sensitive to the choice of the features that are used for constructing those classifiers. This choice affects the accuracy of these classifiers, the time needed for learning, and the number of examples needed for learning. Feature selection (FS) can be seen as an optimization problem that involves searching the space of possible solutions (feature subsets) to identify the optimal one. Many metaheuristics (such as ant colony optimization algorithms, particle swarm optimization, genetic algorithms, simulated annealing, and tabu search) have been used for solving the feature selection problem [20, 21].

http://dx.doi.org/10.5772/65253

Feature selection (deleting a column from a dataset) is one of the main aspects of dimension reduction besides instance reduction (deleting a row from a dataset). This is illustrated in **Figure 3** [18]. Both of these should keep the characteristics of the original input data after excluding some of it.

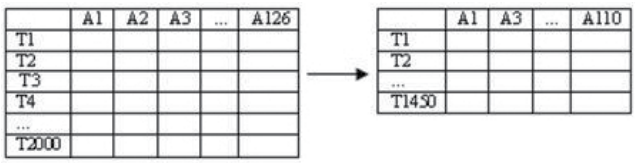

Figure 3. Data reduction [18].

Figure 4 [22] illustrates the revised classification with the use of dimension reduction phase as an intermediate step. In **Figure 4**, dimension reduction is performed first to the given data, and then, the prediction methods are applied to the reduced data.

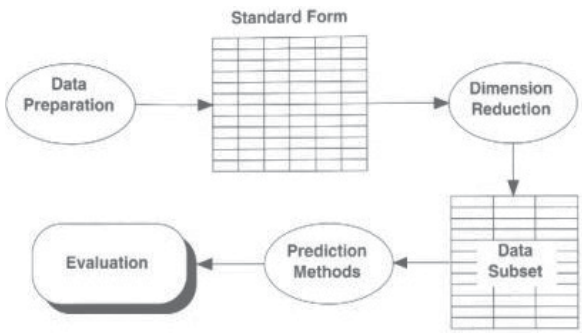

Figure 4. The role of dimension reduction [22].

3. Hybridization of metaheuristics

Although combining different algorithms together dates back to 1980s, in recent years only hybrid metaheuristics have been commonly used. Then, the advantage of combining different algorithms together has been widely recognized [1, 4]. Forms of hybridization can be classified into two categories (as in **Figure 5**): (1) combining components from a metaheuristic into another metaheuristic (examples are: using trajectory methods into population algorithms or using a specific local search method into a more general trajectory algorithm such as iterated local search) and (2) combining metaheuristics with other techniques such as artificial intelligence and operations research (examples are: combining metaheuristics with constraint programming (CP), integer programming (IP), tree-based search methods, data mining techniques, etc.) [1]. The following two subsections explain these types.

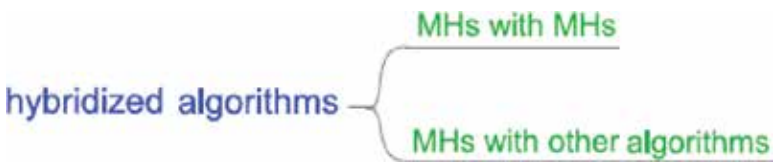

Figure 5. Forms of hybridization [4].

3.1. Hybridizing metaheuristics with metaheuristics

This category represents the beginning of hybridizing metaheuristics. Later, it got widely used especially integrating nature-inspired metaheuristics with local search methods. This is well illustrated in the most common type of this category which is in ant colony optimization algorithms and evolutionary algorithms that often use local search methods in order to refine the generated solutions during the search process. The reason for that is these nature-inspired metaheuristics explore well the search space and identify the regions having high-quality solutions (since they first capture a global picture of the search space and then they successively focus the search toward the promising regions). However, these nature-inspired metaheuristics are not effective in exploiting the accumulated search experiences that can be achieved by adding local search methods into them. Therefore, the resulting hybrid metaheuristic will work as follows: the nature-inspired metaheuristic will identify the promising search areas from which the local search method can then determine quickly the best solutions. Based on the above–mentioned fact, the resulting hybrid metaheuristic combining the strengths of both metaheuristics is often very successful. Apart from this hybridization, there are other hybrids. We mentioned it only here as it is considered the standard way of hybridization [1, 2].

3.2. Hybridizing metaheuristics with other algorithms

There are many possible ways of integration between metaheuristics and other algorithms. For example, metaheuristics and tree search methods can be interleaved or sequentially applied. This can be achieved by using a tree search method for generating a partial solution that a metaheuristic can then complete. Alternatively, a metaheuristic improves a solution generated by a tree search method. Another example is that constraint programming techniques can be used to reduce the search space (or the neighborhoods) that will be explored by a local search method [1, 4].

It should be noted that all of the hybrid metaheuristics mentioned above are integrative combinations in which there is some kind of master algorithm including one or more subordinate components (either embedded or called). Another way of combinations is called either collaborative or cooperative combinations in which the search is performed by different algorithms that exchange information about states, models, entire subproblems, solutions, or search space characteristics. The cooperative search algorithms consist of parallel execution of search algorithms that can be different or instances of the same algorithm working on different models or running with different parameter settings. Therefore, the control strategy in hybrid

metaheuristics can be integrative or collaborative, and the order of executing the combined parts can be sequential, parallel, or interleaved [1, 4, 12]. These are shown in **Figures 6** and **7**.

Figure 6. The control strategy in hybrid metaheuristics [4].

Figure 7. The order of executing the combined algorithms in hybrid metaheuristics [4].

4. Designing a hybrid metaheuristic

The main motivation behind combining various algorithmic ideas from different metaheuristics is to get better performing system that exploits and includes advantages of the combined algorithms [3, 4]. These advantages should be complementary to each other so that the resulting hybrid metaheuristic can benefit from them [2, 3, 23]. The key to achieving high performance in the resulting hybrid metaheuristic (especially when tackling hard optimization problem) is to choose suitable combinations of complementary algorithmic concepts. Therefore, this task of developing a highly effective hybrid metaheuristic is complicated and not easy [3]. The reasons for that are as follows:

1. It requires creative thinking and the exploration of new research directions.
2. Designing and implementing a hybrid metaheuristic involves wide knowledge about algorithms, data structure, programming, and statistics [3].
3. It requires expertise from different optimization areas [2].
4. It should include exploration and intensification capabilities.

According to Blum et al. [2], before starting to develop a hybrid metaheuristic, we should consider whether it is the appropriate choice for the given optimization problem. This can be achieved by answering the following questions:

- What is the optimization objective? Do we need a reasonable good solution? And whether this solution is needed very quickly or not? Or we can sacrifice the computation time in

order to get a very good solution? (these questions in general guide us toward using metaheuristics or complete methods) In this case, when very good solution is needed and it cannot be obtained by the existing complete algorithms in reasonable time, then we need to know the answer of the next question in order to decide on developing a hybrid metaheuristic.

- Is there any existing metaheuristic that can get the required solution for the given optimization problem? If no, can we enhance any of the existing metaheuristics to better suit this optimization problem? If no, then the decision is to develop a hybrid metaheuristic and we will need to know the answer of the following questions.
- Which hybrid metaheuristic will work well for this optimization problem? Unfortunately, till now, there is no answer to this question as it is difficult to set guidelines for developing a well-performing hybrid metaheuristic, but the following can help:
  - Searching the literature carefully for the most successful optimization algorithms for the given optimization problem or for similar optimization problems, and
  - Studying different ways of combining the most promising characteristics of the selected optimization algorithms to be combined [2, 3].
- Identifying special characteristics of the given optimization problem and finding effective ways in order to exploit them [4].

Besides, in order to set guidelines for developing a new hybrid metaheuristic, it is crucial to improve the used research methodology that consists of combining different algorithmic components without identifying the contributions of these components to the performance of the resulting hybrid metaheuristic. The used methodology should consist of theoretical models for the characteristics of the hybrid metaheuristics. It can be experimental such as those used in natural sciences. Moreover, testing and statistical assessment of the obtained results should be included as well [2].

5. Hybrid metaheuristics for classification problems

The first category of using hybrid metaheuristics for classification problems concerns with using a metaheuristic for the feature selection problem besides the used classifier. This is because selecting the most relevant set of input features to use for building the used classifier plays an important role in classification. The most common metaheuristics for the feature selection problem are genetic algorithms, ant colony optimization algorithms, and particle swarm optimization algorithms [24] which are hybridized with the used classifier in each application. This is explained below.

The feature selection problem is used in many applications from choosing the most important social-economic parameters in order to identify who can return a bank loan to dealing with a chemical process and selecting the best set of ingredients. It is used to simplify the datasets by eliminating irrelevant and redundant features without reducing the classification accuracy.

http://dx.doi.org/10.5772/65253

Examples of these applications are: face recognition, speaker recognition, face detection, bioinformatics, web page classification, and text categorization [24, 25].

The idea of using genetic algorithms for solving optimization problems is that they start with a population of individuals each of which represents a solution to the given optimization problem. Initially, the population includes all randomly generated solutions (the first generation of the population). Then, the various genetic operators are applied over the population to produce a new population. Within a population, the goodness (measured by a fitness function) of a solution varies from individual to individual [26].

Genetic algorithms are one of the most common approaches for the feature selection problem. The usual usage is to use them for first selecting the most relevant features (from the given dataset) that will be used for building the used classifier. Examples are the work of Yang and Honavar [27] and Tan et al. [28].

There are other directions for using genetic algorithms for the feature selection problem, for instance, hybridizing the used genetic algorithm with another metaheuristic in order to select the most appropriate feature subset before building the given predictor (such as Oh et al. [29] who embedded local search into the used genetic algorithm). Another example is the work of Salcedo-Sanz et al. [30] who used extra genetic operator in order to fix (in each iteration) the number of features to be chosen out of the available ones.

Similar to the way of using genetic algorithms for the feature selection problem is the use of ant colony optimization algorithms that have been widely used for this optimization problem. Examples are the work of Yang and Honavar [27] and the work of Abd-Alsabour and Randall [31].

There are other ways for using ant colony optimization algorithms for the feature selection problem. An example is the work of Vieira et al. [32] who used two cooperative artificial ant colonies: one for determining the number of features to be selected and the second one for selecting the features based on the cardinality given by the first colony. Another direction is to use ensemble (more than one classifier is built and then is combined to produce a better classification—this is called ensemble techniques [33]) of classifiers to perform the classification besides the used metaheuristic for the feature selection problem.

Another metaheuristic that has also been used for the feature selection problem is particle swarm optimization. Researchers developed variants of PSO in order to be suitable for the feature selection problem such as the work of Chuang et al. [34] who proposed a variant of PSO called complementary PSO (CPSO) with the use of k-nearest neighbor classifier. Another example is Zahran and Kanaan [35] who implemented a binary PSO for feature selection. Also, Jacob and Vishwanath [36] proposed multi-objective PSO that outperformed a multi-objective GA in the same authors' experiments. Moreover, Yan et al. [37] proposed a new discrete PSO algorithm with a multiplicative likeliness enhancement rule for unordered feature selection. Also, Sivakumar and Chandrasekar [38] developed a modified continuous PSO for the feature selection problem with k-nearest neighbor classifier that served as a fitness function for the PSO.

There are other ways for using particle swarm optimization algorithms for the feature selection problem. An example is the work of Wahono and Suryana [39] who used a combination of PSO and a bagging of classifiers (bagging is an ensemble technique where many classifiers are built and the final classification decision is made based on voting of the committee of the combined classifiers. It is used in order to improve the classification accuracy [33]). Another example is the work of Nazir et al. [40] who combined a PSO and a GA to perform together the feature selection.

The classification task involves other subtasks besides the feature selection problem, and many metaheuristics have been used for solving these subtasks, for example, the use of ant colony optimization for designing a classifier ensemble such as the work of Palanisamy and Kanmani [41] who used the main concepts of the proposed ant algorithm in Abd-Alsabour and Randall [31] for designing an ensample of classifiers. Another example is the use of particle swarm optimization algorithms for producing good classification rules such as Kumar [42] who combined a PSO with a GA to produce them and Holden and Freitas [43] who later proposed several modifications to their proposed work in Holden and Freitas [44]. Another example is the work of Revathil and Malathi [45] who proposed a novel simplified swarm optimization algorithm as a rule-based classifier.

6. Discussion

The previous section closely explored the different ways to use hybrid metaheuristics for classification problems. In the light of that, we can come up with the following comments:

1. For solving many applications, using hybrid metaheuristics was crucial to get high-quality solutions especially for real-world applications (such as personnel and machine scheduling, educational timetabling, routing, cutting and packing, and protein alignment). An example for real-world classification problems is the work of Tantar et al. [46], who developed a hybrid metaheuristic (GA and SA) for predicting the protein structure. Examples for other real-world optimization problems are the work of Atkin et al. [47], who proposed a hybrid metaheuristic for runway scheduling at London Heathrow airport and the work of Xu and Qu [48], who used a hybrid metaheuristic to solve routing problems.

2. However, there are other situations where the hybridization was not important for the prediction accuracy. An example is the use of extra metaheuristic (besides the two algorithms used: one for performing feature selection and the classifier) to determine the number of the features to be selected. Similar to this is the use of two instances of a metaheuristic: one to determine the number of the features to be selected and the second one to perform the feature selection. These two scenarios can lead to worse results besides the extra computation cost. The authors should have been avoided using extra metaheuristic or an instance of the used metaheuristic. The reason for that is revealed from the work of Abd-Alsabour et al. [49] who proved that fixing the length of the selected feature subsets can lead to getting worse classification accuracy than not fixing the length of the selected

feature subsets (besides its extra computation). We should avoid selecting too few or too many features than necessary. This is because selecting insufficient features leads to degrading the information content to keep the concept of data. On the other side, if too many features are selected, the classification accuracy will decrease because of the interference of irrelevant features. Subset problems such as the feature selection problem do not have fixed length [49]. Another example is the use of more than one classifier (ensemble methods) rather than using one only. This is because of the extra computational cost, especially that there were already previous similar applications that had been successfully solved using only one classifier (besides the used metaheuristic for getting the best feature subset). This has been evidenced by many authors when they compared their work with the pervious ones and showed that their results were not better than the others. One more example is the use of two metaheuristics for performing the feature selection, while it was already solved using only one metaheuristic. These examples emphasize the fact that sufficient literature search before first hybridizing or adding extra computational steps can avoid extra computation, useless hybridization, or even moving toward a misleading research direction as illustrated in Section 4.

Therefore, choosing the suitable hybrid metaheuristic can achieve the top performance for many optimization problems, but this does not imply that more complex algorithms are always the best choice. This is because of the following disadvantages of the increased complexity:

- The software becomes more difficult to tune and maintain.
- Adaptations in problem specifications are frequently hard to adhere.

Therefore, an important design aim is to keep the proposed algorithm as simple as possible and include extensions only if they will really benefit [4].

Despite the difficulties in developing a new hybrid metaheuristic, it is nontrivial to generalize it, that is, a particular hybrid metaheuristic that works well for a particular optimization problem might not work well for another problem. This means that research on hybrid metaheuristics has gone toward being problem-specific rather than algorithm-oriented as was when promoting a new metaheuristic [1, 2].

7. Conclusions and future work

This chapter addressed the use of hybrid metaheuristics for classification problems. Besides, it demonstrated hybridizing metaheuristics and designing them as well. Moreover, the most common used hybrid metaheuristics for classification problems from literature were presented.

As a research direction, more applications of hybrid metaheuristics for different optimization problems in general and more particularly for real-word classification problems will be considered. Another research direction is to move more toward setting specific methodologies and general guidelines for developing a new hybrid metaheuristic. Moreover, comparisons between hybrid metaheuristics for similar classification problems should be conducted.

Author details

Nadia Abd-Alsabour

Address all correspondence to: nadia.abdalsabour@cu.edu.eg

Cairo University, Cairo, Egypt

References

[1] Blum C, and Roli A. Hybrid Metaheuristics: An Introduction. In: Blum C, Aguilera M, Roli A, and Sampels M, editors. Hybrid Metaheuristics – An Emerging Approach to Optimization. Studies in Computational Intelligence. Springer-Verlag Berlin Heidelberg, Springer; 2008. 114, p.1–30.

[2] Blum C, Puchinger J, Raidl G, and Roli A. Hybrid metaheuristics in combinatorial optimization: A survey. Applied Soft Computing. 2011; 11: 4135–4151.

[3] Blum C, Puchinger J, Raidl G, Roli A. A brief survey on hybrid metaheuristics. In: Filipic B, Silc J, editors. Proceedings of BIOMA 2010 – 4th International Conference on Bio-Inspired Optimization Methods and their Applications, Jozef Stefan Institute, Ljubljana, Slovenia, 2010, pp. 3–18.

[4] Raidl G. Decomposition based hybrid metaheuristics. European Journal of Operational Research. 2015; 244: 66–76

[5] Dorigo M, and Stutzle T. Ant Colony Optimization. MIT Press, Cambridge, MA; 2004.

[6] Blum C. Ant colony optimization: Introduction and recent trends. Physics of Life Reviews. 2005; 2: 353–373.

[7] Blum C, and Roli A. Metaheuristics in combinatorial optimization: Overview and conceptual comparison. ACM Computing Surveys. 2003; 35 (3): 268–308.

[8] Méndez P. Development of a hybrid metaheuristic for the efficient solution of strategic supply chain management problems: Application to the energy sector. M.Sc. Thesis. Polytechnic University of Catalonia, Catalonia, Spain, 2011

[9] Blum C. ACO Applied to Group Shop Scheduling: A Case Study on Intensification and Diversification. In: Dorigo M, et al., editors. Lecture Notes in Computer Science; 2463: p. 14–27, Springer. 2002.

[10] Randall M, and Tonkes A. Intensification and diversification strategies in ant colony search. Technical Report TR00-02, School of information technology, Bond University, Australia. 2002

[11] Abd-Alsabour N, and Moneim A. Diversification with an ant colony system for the feature selection problem. In Proceeding of 2nd International Conference on Management and Artificial Intelligence. IPEDR; 35: 35–39. IACSIT Press. 2012.

[12] Blum C. Hybrid metaheuristics. BIOMA 2010. Ljubljana, Slovenia.

[13] Hand D, Mannila H, and Smyth P. Principles of Data Mining. Massachusetts Institute of Technology, Cambridge, MA; 2001.

[14] Hastie T, Tibshirani R, and Friedman J. The Elements of Statistical Learning – Data Mining, Inference, and Prediction. Springer Verlag, Springer; 2009.

[15] Xie Y. An introduction to support vector machine. Available from: http://yihoi.name/cv/images/svm_Report_yihui.pdf. 2007. [Accessed: 2016-06-25]

[16] Berry M, and Linoff G. Data Mining Techniques for Marketing, Sales, and Customer Relationship Management. 2nd ed. Wiley, New York; 2004.

[17] Larose D. Discovering Knowledge in Data. John Wiley & Sons; Hoboken, New Jersey; 2005.

[18] Han J, and Kamber M. Data Mining Concepts and Techniques. 1st ed. Morgan Kaufmann Publishers, San Francisco; 2001.

[19] Skillicorn D. Understanding Datasets: Data mining with Matrix Decomposition. Chapman & Hall/CRC, London; 2007.

[20] Yang J, and Honavar V. Feature subset selection using a genetic algorithm. IEEE Intelligent Systems. 1998; 13(2): 44–49.

[21] Duda R.O., and Hart P.E. Pattern Classification and Scene Analysis. 1st ed. John Wiley & Sons, New York; 1973.

[22] Weiss S, and Indurkhya N. Predictive Data Mining, a Practical Guide. Morgan Kaufmann Publishers, San Francisco; 1998.

[23] Al-Duolia F, Rabadia G. Data mining based hybridization of meta-RaPS. Procedia Computer Science. 2014; 36: 301–307

[24] Rokach L, and Maimon O. Data Mining with Decision Trees. World Scientific Publishing, New Jersey; 2008.

[25] Abd-Alsabour N. A review on evolutionary feature selection. 2014 UKSim-AMSS 8th European Modeling Symposium. Italy. 2014. p. 20–26

[26] Shukla A, Tiwari R, and Kala R. Real Life Applications of Soft Computing. CRC Press, Boca Raton; 2010.

[27] Yang J, and Honavar V. Feature subset selection using a genetic algorithm. IEEE Intelligent Systems. 1998; 13(2): 44–49.

[28] Tan K C, Teoh E J, Yu Q, and Goh K.C. A hybrid evolutionary algorithm for attribute selection in data mining. Expert Systems with Applications. 2009; 36: 8616–8630

[29] Oh I, Lee J, and Moon B. Hybrid GAs for feature selection, IEEE Transactions on Pattern Analysis and Machine Intelligence. 2004; 26(11): 1424–1437.

[30] Salcedo-Sanz S, Camps-Valls G, and Pérez-Cruz F. Enhancing genetic feature selection through restricted search and Walsh analysis. IEEE Transactions on Systems, Man, and Cybernetics. Part C. 2004. 34(4):398–406.

[31] Abd-Alsabour N, and Randall M. Feature selection for classification using an ant colony system. In Proceedings of the 6th IEEE International Conference on e–Science Workshops. IEEE Press, 2010; p. 86–91.

[32] Vieira S M, Sousa J MC, and Runkler T A. Two cooperative ant colonies for feature selection using fuzzy models. Expert Systems with Applications; 2010. 37:2714–2723.

[33] Lui B. Web Data Mining. Springer; 2010.

[34] Chuang L, Jhang H, and Yang C. Feature selection using complementary PSO for DNA micro-array data. In Proceedings of the International Multi-Conference of Engineers and Computer Scientists, Hong Kong; 2013; 1. p. 291–294.

[35] Zahran B M, and Kanaan G. Text feature selection using particle swarm optimization algorithm. World Applied Sciences Journal. 2009; 7: pp. 69–74.

[36] Jacob M, and Vishwanath N. Multi-objective evolutionary PSO algorithm for matching surgically altered face images. International Journal of Emerging Trends in Engineering and Development. 2014; 2(4): 640–648.

[37] Yan Y, Kamath G, and Osadciw L. Feature selection optimized by discrete particle swarm optimization for face recognition. In Proceedings of Optics and Photonics in Global Homeland Security and Biometric Technology for Human Identification. SPIE. 2009; 7306.

[38] Sivakumar S, and Chandrasekar C. Modified PSO based feature selection for classification of lung CT images. International Journal of Computer Science and Information Technologies. 2014; 5(2): 2095–2098.

[39] Wahono R, and Suryana N. Combining PSO based feature selection and bagging technique for software defect prediction. International Journal of Software Engineering and Its Applications. 2013; 7(5):153–166.

[40] Nazir M, Majid-Mirza A, and Ali-Khan S. PSO-GA based optimized feature selection using facial and clothing information for gender classification. Journal of Applied Research and Technology. 2014; 12:145–152.

[41] Palanisamy S, and Kanmani S. Artificial Bee Colony Approach for Optimizing Feature Selection. International Journal of Computer Science Issues. 2012; 9(3):432–438.

[42] Kumar K. Intrusion Detection system for malicious traffic by using PSO-GA algorithm. IJCSET. 2013; 3(6):236–238.

[43] Holden N, and Freitas A A. A hybrid particle swarm/ant colony algorithm for the classification of hierarchical biological data. In Proceedings of 2005 IEEE Swarm Intelligence Symposium (SIS-05). 2005; p. 100–107.

[44] Holden N, and Freitas A A. A hybrid PSO/ACO algorithm for classification. GECCO'07, July 7–11, 2007, London, United Kingdom.

[45] Revathi1 S, and Malathi A. Network intrusion detection using hybrid simplified swarm optimization technique. International Journal of P2P Network Trends and Technology. 2013; 3(8): 375–379.

[46] Tantar A, Melab N, Talbi E. A grid-based genetic algorithm combined with an adaptive simulated annealing for protein structure prediction. Soft Computing. 2008; 12:1185–1198

[47] Atkin J, Burke E, Greenwood J, Reeson D. Hybrid metaheuristics to aid runway scheduling at London Heathrow Airport. Transportation Science. 2007; 41(1):90–106.

[48] Xu Y, Qu R. Solving Multi-objective multicast routing problems by evolutionary multi-objective simulated annealing algorithms with variable neighborhoods. Journal of the Operational Research Society. 2011; 62:313–325.

[49] Abd-Alsabour N, Randall M, and Lewis A. Investigating the effect of fixing the subset length using ant colony optimization algorithms for feature subset selection problems. In Proceedings of the 13th International Conference on Parallel and Distributed Computing: Applications and Technologies. Beijing, China. December 2012. IEEE Press. p. 733–738.

Chapter 3

Method of Synthesized Phase Objects in the Optical Pattern Recognition Problem

Pavel V. Yezhov, Alexander P. Ostroukh,
Jin-Tae Kim and Alexander V. Kuzmenko

Additional information is available at the end of the chapter

http://dx.doi.org/10.5772/65370

Abstract

To solve the pattern recognition problem, a method of synthesized phase objects (SPO-method) is suggested. The essence of the suggested method is that synthesized phase objects are used instead of real amplitude objects. The former is object-dependent phase distributions calculated using the iterative Fourier transform algorithm. The method is experimentally studied with an optical-digital Vanderlugt and joint Fourier transform 4F-correlators. The development of the SPO-method for the rotation invariant pattern recognition is considered as well. We present the comparative analysis of recognition results with the use of the conventional and proposed methods, estimate the sensitivity of the latter to distortions of the structure of objects, and determine the applicability limits. It is demonstrated that the SPO-method allows one: (a) to simplify the procedure of choice of recognition signs (criteria); (b) to obtain one-type δ-like recognition signals irrespective of the type of objects; and (c) to improve the signal-to-noise ratio for correlation signals by 20–30 dB on the average. To introduce recognition objects in a correlator, we use SLM LC-R 2500 and SLM HEO 1080 Pluto devices.

Keywords: pattern recognition, method of synthesized phase objects, iterative Fourier transform algorithm, rotation invariant pattern recognition, optical-digital recognition systems, spatial light modulators

1. Introduction

The studies in the fields of Fourier optics, holography, and digital and correlation optics aimed at the solution of the pattern recognition problem remain topical for a long time. This is related to the fact that the recognition problem is object-dependent, i.e., the change in the conditions

of recognition or in the type of an object requires, as a rule, the optimization of available methods of solution or the development of new ones [1, 2]. Among the known methods, it is worth to note the following ones: the digital synthesis of Fourier filters [3–6], method of discriminant curve [7, 8], method of stabilizing functional [9], method of projections onto convex sets [10], etc. We emphasize that the mentioned and other available methods lead to a significant number of dedicated solutions, for which the choice of characteristic signs of the object and the subsequent analysis of correlation signals are separate problems. Therefore, topical is the search for the more general solutions of the pattern recognition problem by means of the matched filtering [11] or the joint correlation [12], which are directed to a simplification of the analysis of input data and the main signs of recognition, determination of their connection with the parameters of correlation signals, etc.

Here, we develop a new approach to the solution of the recognition problem. The newness of the proposed approach consists in that we recognize not the object itself, but a certain object-dependent synthesized phase object (SP-object). The latter (its distribution of phases) is calculated with the help of the known iterative Fourier transform (IFT) algorithm [13]. In this case, the problem of recognition of amplitude objects, which belong to arbitrary classes, is reduced to the problem of recognition of phase objects of only one type [14–16].

We also present a development of the SPO-method for the rotation invariant pattern recognition [17]. For the conventional method and the SPO-method, the comparison of the parameters of correlation signals for a number of amplitude objects is executed at the realization of their rotation in an optical-digital joint Fourier transform (JT) correlator. It is shown that not only the invariance relative to a rotation at a realization of the joint correlation for SP-objects but also the main advantage of the SPO-method over the reference one such as the unified δ-like recognition signal with the largest possible signal-to-noise ratio (SNR) independent of the type of an object is attained.

The work is organized as follows: in Section 2, a new approach to the pattern recognition on the basis of SP-objects is presented. The basic results of computational and optical experiments are given. The behavior of cross-correlation signals is studied under the addition of a controlled amount of noises to the structure of objects. In Section 3, a development of the SPO-method for the rotation invariant pattern recognition with an optical-digital JT-correlator is presented.

2. SPO-method: definition, substantiation

We now define an approach, where not the object itself is recognized, but some object-dependent SP-object which is calculated with the help of the known IFT algorithm [13]. In this case, as mentioned above, the problem of recognition of amplitude objects of various classes can be reduced to the problem of recognition of phase objects that belong to the same class. Below, we present the experimental results of recognition of amplitude objects with the use of the conventional and proposed methods, estimate the sensitivity of the latter to changes in the structure of objects, and determine the boundaries of its application. Let us consider the operation of the algorithm (**Figure 1**). For the calculation of SP-objects, we apply IFT algorithm

http://dx.doi.org/10.5772/65370

in its kinoform version [18]. In the process of iterations, the phase structure of a kinoform $\psi(u, v)$ is formed in the spectral plane. Simultaneously, one more phase structure, namely $\varphi(x, y)$, appears in the object plane. The function $\phi(x, y) = exp(i\varphi(x, y))$ plays the role of a diffusive scatterer, which is optimized for the object $f(x, y)$ and is necessary for the leveling of the field amplitude in the Fourier plane, i.e., in the plane of a kinoform. However, in the context of the correlation methods of recognition, the phase structures $\varphi(x, y)$ with random distribution of the phase can also be of independent interest not related to the problem of calculation of the kinoform. The matter is as follows. Since the form of $\varphi(x, y)$ for the given number of iterations and the given initial diffuser $\varphi_0(x, y)$ is determined uniquely by the form of the function $f(x, y)$, it is logical to put two questions:

1. While solving the problem of recognition of the object $f(x, y)$, is it possible to replace it by the corresponding SP-object in the form of $\phi(x, y) = exp(i\varphi(x, y))$?
2. Will the solution of the problem with such replacement of the object be more efficient than that within the known methods?

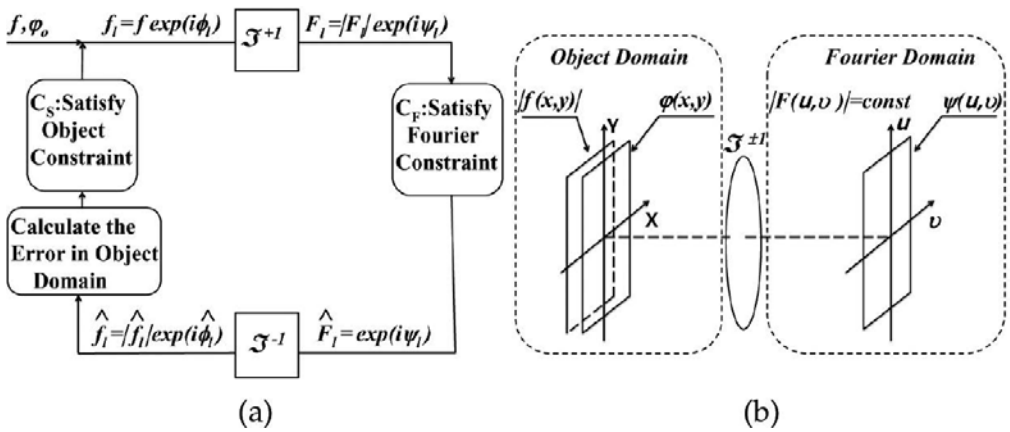

Figure 1. IFT algorithm (a), illustrative scheme of the IFT algorithm (b).

The computer-based and optical experiments executed by us give a positive answer to both questions. The method of recognition, where the SP-object $\phi(x, y)$ is recognized instead of a real amplitude object $f(x, y)$, is called the method of synthesized phase objects. We now consider the advantages and limitations of this method in more details. To study its basic characteristics in model and optical experiments, we need to determine a collection of recognition objects, to calculate an SP-object for each of them, and to carry out the recognition.

In view of the circumstance that the iteration method of synthesis of the functions $\varphi(x, y)$ for $f(x, y)$ gives no possibility to get a solution in the analytic form, we study the SPO-method for a finite collection of recognition objects. In order to most completely show the potentialities of the method, we choose objects with essentially different types of Fourier spectra.

For the comparison of the conventional and SPO methods, we need to compare their sensitivities to changes in the structure of objects under recognition. As a parameter for the estimation of the sensitivity, we chose the controlled changes that are introduced in the structure of recognition objects. These changes are carried out by means of the pairwise rearrangements of points of the object taken in an arbitrary order. The number of such rearrangements k varied in the limits from zero to several hundreds.

2.1. SP-objects and their basic properties: model experiments

For model experiments, we chose ten amplitude objects of the binary type 300 × 300 points in size. In **Figure 2**, the reference objects f_n (n = 1, 2, 3, 4) are presented.

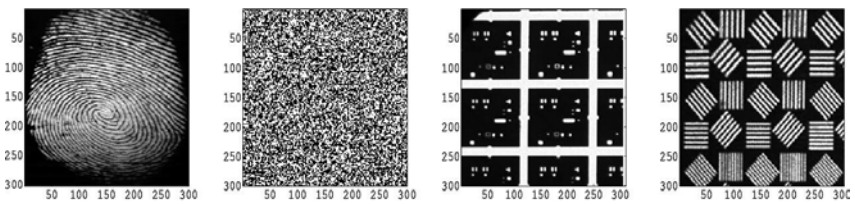

Figure 2. Objects: (a) f_1, (b) f_2, (c) f_3, (d) f_4.

For all of them, we calculated the autocorrelation functions $f_n \otimes f_n$. The SP-objects ϕ_n were calculated by the iteration scheme (**Figure 1a**) with the initial distribution of phases $\varphi_0 = const$. In order to find the degree of connection of ϕ_n with f_n, which determines the degree of suitability of the use of ϕ_n instead of f_n, we obtained ϕ_n for different numbers of iterations N, by gradually increasing N. At a fixed N, we calculated the correlation functions $\phi_{n,N} \otimes \phi_{n,N}$ for the entire totality of $\{\phi_{n,N}\}$. In **Figure 3**, we present object f_4 (1(a)), central fragment of its Fourier spectrum (2(a)), and autocorrelation signal (3(a)). On the right, we show, respectively, a fragment of the phase distribution $\varphi_{4,1}$ of the SP-object (1(b)), shape of its spectrum (2(b)), and a fragment of the autocorrelation signal (3(b)). Analogous results were also obtained for objects $f_1 - f_3$. The presented result is typical and demonstrates the main advantages of SP-objects such as the uniform distribution of the amplitude in the spectral plane and the δ-like autocorrelation signal, which are practically independent of the shapes of Fourier spectra and the type of the autocorrelation signals of real objects, for which they were calculated.

As a result of model experiments, for each f_n, we determined the criterion of choice of ϕ_n from the set $\{\phi_{n,N}\}$ at varying N. The obtained results are demonstrated by the example of object f_4 (**Figure 4a**). Curve (A) shows the behavior of the variance σ^2 of the amplitude of the retrieved image of object f_4 at the calculation of its SP-object relative to the amplitude of the reference object, and curve (B) presents the change in the maximum value of modulus of the Fourier spectrum amplitude of the $\phi_{4,N}$, as N increases. In **Figure 4**(**b–d**), we observe the redistribution of phases of the SP-object in the interval $[0 - 2\pi]$ for various numbers of iterations.

http://dx.doi.org/10.5772/65370

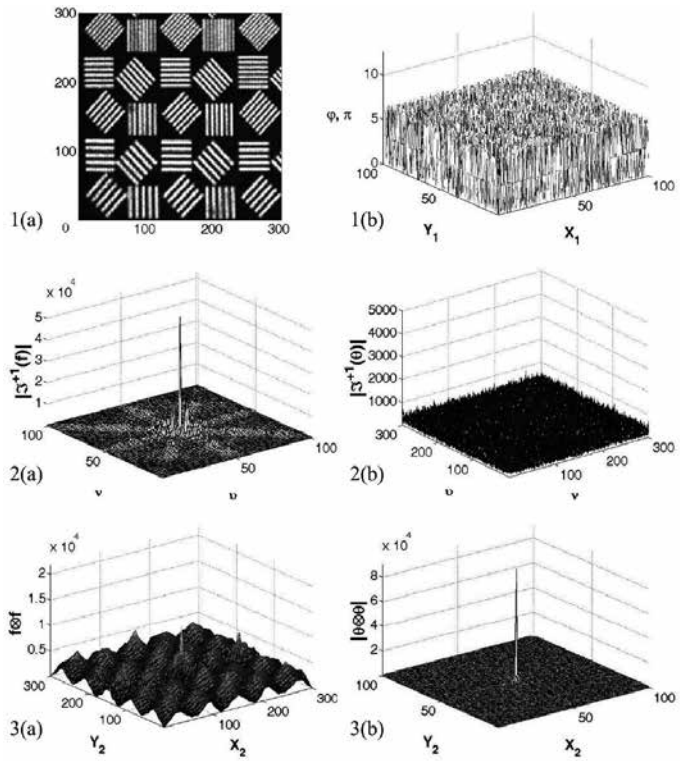

Figure 3. Left (a): distributions for the real object f_4; right (b): for the SP-object $\phi_4 = \exp(i\varphi_4)$: (1) object; (2) Fourier spectrum amplitude modulus; (3) autocorrelation signal.

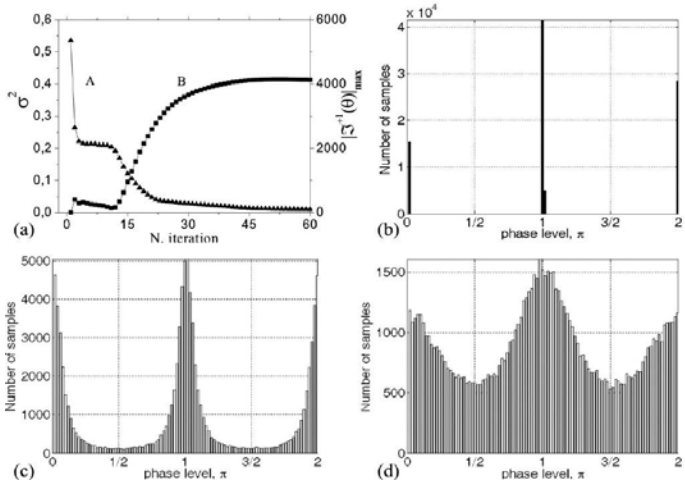

Figure 4. (a) Dependence of σ^2 (A) and $|\Im^{-1}(\phi)|_{max}$ (B) on the number of iterations N; histograms for: (b) $\varphi_{4,1}$; (c) $\varphi_{4,13}$; (d) $\varphi_{4,45}$ calculated for 1st, 13th, and 45th iterations.

On the basis of the results of numerical experiments with the whole collection of objects (**Figures 3** and **4**, **Table 1**), we can conclude the following:

- The binary distribution (0 or π) of a phase in the plane of an SP-object obtained on the first iteration is transformed into a continuous one in the interval [0 – 2π], as the iteration number increases.
- The distribution of phases in the plane of an SP-object is random.
- The modulus of the amplitude of the Fourier spectrum of an SP-object has a uniform distribution in all cases.

Number of an object no.	Objects		SP-objects	
	Frequency[a] $2\xi_{max}$, rel. un.	<SNR>[b], dB	Frequency $2\xi_{max}$, rel. un.	<SNR>, dB
1	0.30	5.2	0.50	26.2
2	0.25	16.3	0.50	26.2
3	0.20	7.7	0.50	26.2
4	0.37	6.8	0.50	26.2

[a]$2\xi_{max}$, effective band of frequencies.
[b]<SNR>, ratio of the peak value of amplitude of a correlation signal to the mean noise amplitude.

Table 1. Results of recognition of objects and SP-objects in model experiments.

The autocorrelation functions of SP-objects have the δ-like shape and ensure:

1. Maximally possible value of SNR characteristic as for the binary phase masks with a random distribution of elements [19].
2. Possibility to apply a simple threshold criterion to the analysis of the results of recognition.

This is true for both $\varphi_0 = const$ as well as for arbitrary φ_0. We have also established that the SP-objects calculated on the first and all subsequent N-iterations satisfy the following conditions:

1. If there is no correlation between the objects f_n and f_m ($f_n \otimes f_m = 0$), then the correlation is also absent for SP-objects ($\phi_{n,N} \otimes \phi_{m,N} = 0$).
2. If the signal of cross-correlation between the objects f_n and f_m exists ($f_n \otimes f_m \neq 0$), then it exists also for the SP-objects ($\phi_{n,N} \otimes \phi_{m,N} \neq 0$).

The first item indicates that the SP-objects obtained for the uncorrelated real objects are statistically independent of one another. The second shows the possibility to obtain a bijective interrelation between cross-correlation curves for the real and SP-objects.

Thus, we have established that, for SP-objects, the highest degree of uniformity of the amplitudes of their Fourier spectra is ensured already after the first iteration, conditions (1, 2) are satisfied, and the properties of real objects $f(x, y)$ (their significant signs) are integrally represented in the distribution of phase elements in the coordinate plane. Any changes in the

http://dx.doi.org/10.5772/65370

structure of $f(x, y)$ affect directly the distributions of the phase in a plane of the SP-object. This allows one to quantitatively evaluate the indicated variation in the object by a change in the level of a cross-correlation signal from SP-objects calculated for the reference and modified objects, respectively. The following step is the evaluation of the practical value of the proposed method. With this purpose, we will analyze the results of the recognition by the conventional method and the SPO-method executed in a Vanderlugt (VL) correlator.

2.2. Comparison of the SPO and conventional methods of recognition: optical experiment

We studied the matched filtering of amplitude objects. In **Figure 5**, we present scheme (a) and photo (b) of an optical-digital VL-correlator. In order to introduce the images in the object plane of the correlator, we applied spatial light modulator (SLM) LC-R2500. SLM is operated in the mode of phase modulation of the wave front. The amplitude objects were transformed in phase ones [20] and supplied to SLM as standard graphic files with regard to the characteristic curve of SLM. Let us consider the operation of the correlator in the mode of recording of matched filters and the mode of matched filtering.

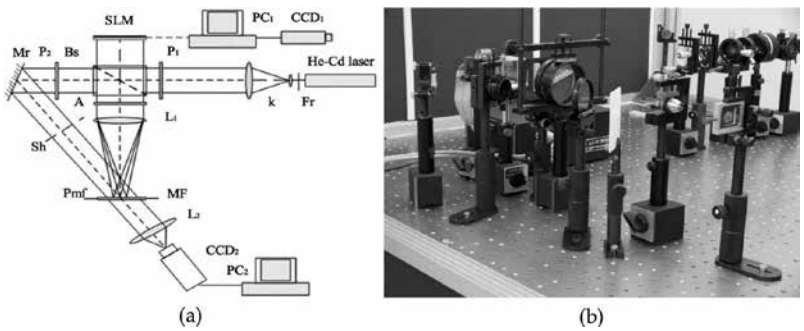

Figure 5. Optical-digital VL-correlator: (a) scheme; (b) photo: CCD_1, PC_1, laser, *Fr*, *k*, P_1, *Bs*, *SLM*, P_2, *Mr*, *Sh*, *A*, L_1, *MF*, P_{mf}, L_2, CCD_2, PC_2 are, respectively, a camera and a computer in the object plane, He-Cd laser (441.6 nm), Fresnel rhomb; collimator, polarizer, splitting cube, spatial light modulator LC-R2500, polarizer, mirror, gate, analyzer, Fourier lens, matched holographic filter, Fourier plane, lens, CCD camera COHU-4800, controlling computer.

Recording of a matched filter. The beam of a He-Cd laser is split into the reference and object beams, by passing through collimator *k* and splitter *Bs*. Fresnel rhomb *Fr* and analyzer *A* set the necessary polarization of the object beam, by ensuring the phase mode of operation of SLM. Polarizer P_1 and gate *Sh* are not used, and polarizer P_2 controls a level of the intensity of the reference beam. With the help of CCD_1 and computer PC_1, the graphic file with the image of the reference object in the grayscale format (1–255) is supplied onto SLM with regard to the characteristic curve of the device. The object beam and the collimated reference beam form a matched filter on a photopolymeric composition [15] in the Fourier plane P_{mf} of the correlator. We optimized the conditions of recording of matched filters in order to get the maximum diffraction efficiency at a minimum level of intrinsic noises and at a maximum SNR.

Matched filtering. The operation of the correlator in the mode of matched filtering consists in the following. At closed gate *Sh*, the collimated laser beam with the necessary direction of

polarization is reflected from the mirror of SLM, to which the image of a recognition object is supplied. After the Fourier transformation executed by lens L_1, the beam enters plane P_{mf}, where a matched filter *MF* for the reference object is placed. Then, camera CCD_2 in the correlation plane registers the signal of mutual correlation, which is obtained as a result of the inverse Fourier transformation of the product of the Fourier transforms of the input and reference images of objects executed by lens L_2.

Define the procedure of recognition by the SPO-method:

- For the reference object f_{ref}, the SP-object ϕ_{ref} is calculated with the help of the IFT algorithm. Into the object plane of the correlator, ϕ_{ref} is introduced instead of f_{ref}, and the recording of the matched filter is realized. For the comparison object f_{in}, the SP-object ϕ_{in} is calculated in the same way.
- Into the object plane of the correlator, ϕ_{in} is introduced instead of f_{in}, and the matched filtering is realized. In the correlation plane, the signal of mutual correlation $I_{corr} = |\phi_{ref} \otimes \phi_{in}|$ is registered.

To obtain the cross-correlation dependences, the same collection of objects $f_1 - f_4$ (**Figure 2**), as in computer experiments, was used. For each of the recognition objects, we calculated the series of $f_n(k)$, $k \in [1 - 800]$ objects obtained by means of the introduction of changes into their structure. As indicated above, the changes are the pairwise permutation of points (pixels) of the object taken in an arbitrary order, k being the number of such rearrangements. In **Figure 6**, we present the view of a fragment of the object f_1 for various numbers of rearrangements.

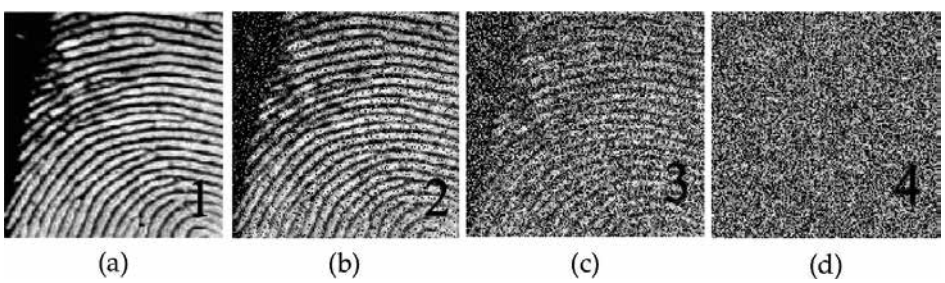

Figure 6. Fragments of object f_1 for: (a) $k = 0$; (b) $k = 200$; (c) $k = 400$; (d) $k = 800$.

For all objects f_n and series $f_n(k)$, we calculated the corresponding $\phi_{n,1}$ and series $\phi_{n,1}(k)$. Then, we recorded matched filters and carried out the recognition by the conventional and SPO methods. The cross-correlation signals were registered by camera CCD_2, and their SNRs were calculated. We obtained the dependences of the intensities of correlation signals I_{corr} on the level of changes in the structure of compared objects. We also estimated the degree of homogeneity of the intensities of the Fourier spectra of objects and SP-objects. The registration of the corresponding spectra was executed by camera CCD_2 mounted in the plane P_{mf} of the correlator (**Figure 5a**). In **Figure 7**, we show the typical results by the example of object f_1.

http://dx.doi.org/10.5772/65370

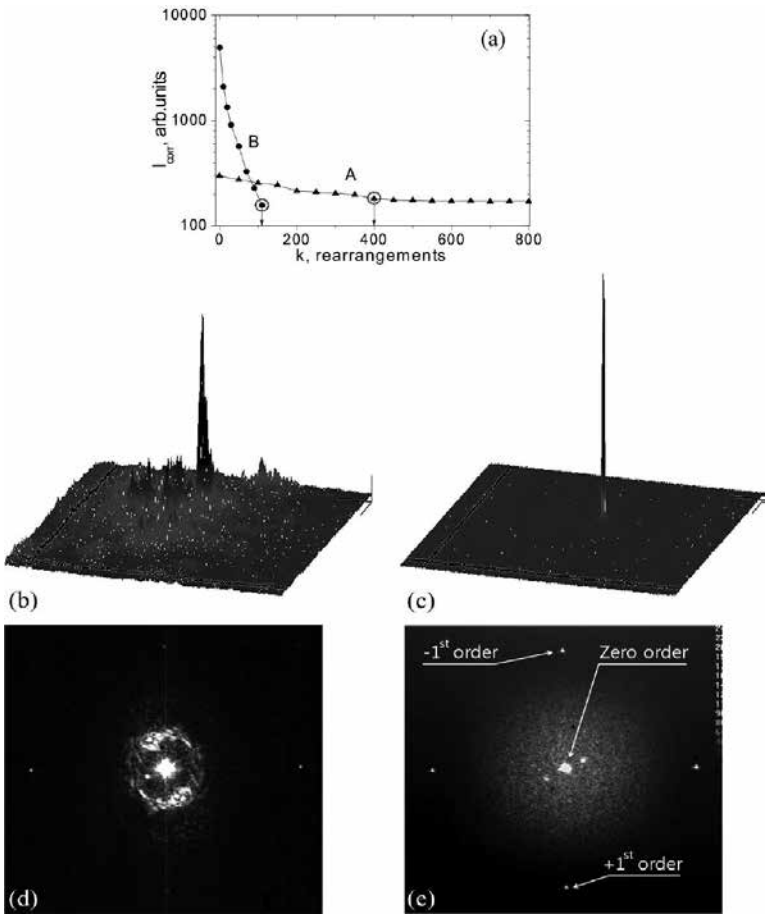

Figure 7. Experimental results for object f_1 (left) and the SP-object $\phi_{1,1}$ (right): (a) dependence of the intensity of a cross-correlation signal on k; (b and c) form of correlation signals at points A, B, respectively; (d and e) the shapes of Fourier spectra.

In **Figure 7a**, curves (A, B), we show changes in the correlation signal I_{corr} for f_1 and $\varphi_{1,1}$, respectively, as the parameter k increases. The autocorrelation signals for $f_1(x, y)$ with SNR of 2.1 dB and $\phi_{1,1}(x, y)$ with SNR of 24.8 dB are shown in **Figure 7b** and **c**, respectively. Fourier spectra of the object and the SP-object are presented in **Figure 7d** and **e**. In the photo of the SP-object Fourier spectrum, we indicate the zero and ± 1 orders of SLM. In the Fourier spectrum of object f_1, the zero order of SLM distorts the real view of the object Fourier spectrum in the zero frequency region. The character of cross-correlation dependences (A, B) (**Figure 7a**) is conserved for the whole collection of objects, which allows us to conclude that the SPO-method has a higher sensitivity to changes in the structure of an object. This can play both positive and negative roles, depending on the character of the recognition problem. On the basis of the results of matched filtering obtained for the whole collection of objects $f_1 - f_{10}$, we can conclude that the characteristic peculiarities and distinctions of the compared methods observed in model experiments are conserved also in optical experiments.

We have established that, in the applied scheme of a VL-correlator (it is true for the schemes with SLM) in the process of recording of matched filters, a part of light that does not diffract on SLM falls in the domain of zero frequencies of the Fourier spectrum of the object. These intense peaks are well noticeable in **Figure 7d** and **e**. The presence of such peaks is the reason for the appearance of a superfluous component in the recognition signals, which masks the real course of a curve in the domain of strong changes in the structure of an object. For example, it is seen in **Figure 7a** (curve A) that, for $k > 400$ where the structure of the object changes quite strongly, the intensity of the correlation signal is practically constant. This effect is observed for both the conventional and SPO methods.

Off-axis matched filtering. We have realized a means to remove a drawback of a VL-correlator with SLM related to the presence of a masking peak of the intensity on zero frequencies, by introducing a phase grating into the structures of input and reference objects. This allows us to spatially separate the Fourier spectra of objects and the zero-order SLM. For functions of the type $\phi(x, y) = exp(i\varphi(x, y))$ that are introduced in the objective plane of a correlator with the help of SLM, such grating is formed by means of the adding of a linear phase $2\pi(xu_0 + y\vartheta_0)$ to the phase $\varphi(x, y)$. The spatial separation of the recognition signal and noise components in the correlation plane by the covering of a synthesized filter in the Fourier plane by a phase grating was demonstrated in [16], but the increase in SNR of the recognition signal by means of the covering of the recognition objects in the objective plane of a VL-correlator by a phase grating is made for the first time by us.

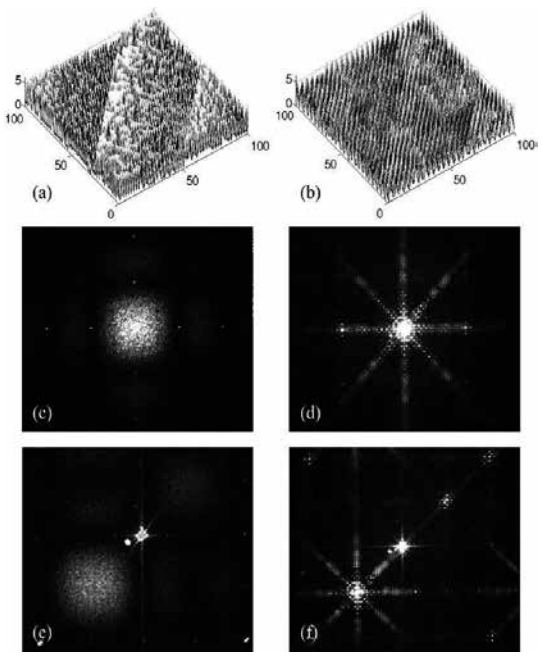

Figure 8. (a and b) Fragment of the phase encoded objects [20] f_2, f_4 with added gratings; (c and d) on-axis Fourier spectra; (e and f) off-axis Fourier spectra.

http://dx.doi.org/10.5772/65370

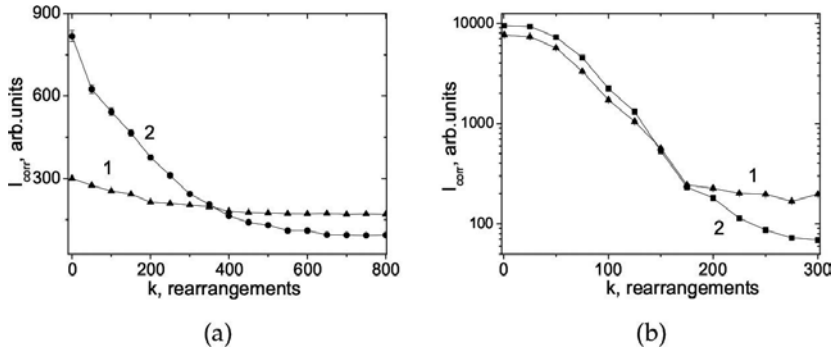

Figure 9. Intensities of cross-correlation signals versus the parameter k for object f_1 (a) and SP-object $\phi_{1,1}$ (b) for the on-axis (1) and off-axis (2) matched filtering.

Number of an object no.	Objects SNR[a], dB		SP-objects SNR, dB	
	On-axis	Off-axis	On-axis	Off-axis
1	2.1	9.32	24.8	29.0
2	10.4	18.1	29.1	39.5
3	9.2	19.7	30.0	39.8
4	10.5	20.7	33.9	39.6

[a]SNR, correlation peak intensity relative to the maximal intensity of the correlation noise.

Table 2. Results of matched filtering of objects and SP-objects.

The axis, relative to which the spectrum is shifted, passes through the centers of the objective and Fourier planes. We consider the recording of a filter for the reference object with the added phase grating and the subsequent matched filtering of recognition objects with the added phase grating as an off-axis matched filtering relative to the indicated axis (**Figure 8**). As distinct from the on-axis matched filtering, the implementation of such filtering within the conventional and SPO methods for all objects f_n and series $f_n(k)$, as well as for $\phi_{n,1}$ and series $\phi_{n,1}(k)$, gives the proper behavior of cross-correlation curves for the whole range of variation in the parameter k, including $k > 400$. In **Figure 9a** and **b**, we present the correlation curves for the on-axis (1) and off-axis (2) matched filtering for the object f_1 and SP-object $\phi_{1,1}$, respectively. It is seen that curves (2) are more suitable for the proper comparison of the sensitivities of methods in a wide range of k. Hence, the results of model and optical experiments aimed at the study of the SPO-method of recognition of amplitude objects show that the method gives the following possibilities: to simplify the procedure of choice of the criteria (signs) of recognition; to obtain the one-type δ-like signals irrespective of the class, to which the recognition object belongs; and to increase the signal/noise ratio for correlation signals by 2–3 orders. The off-axis matched filtering realized in the experiment increases additionally SNR of correlation signals by one order (**Figures 8** and **9**, **Table 2**).

3. SPO-method for pattern recognition with rotation invariance

As is known, one of the basic problems hampering the application of optical methods of recognition in practice is a fast degradation of the correlation signal under a variation in the scale of the object and its rotation around the coordinate origin. This problem is solved by means of the use of the integral Fourier-Mellin transformation instead of the pure Fourier transformation for the recognition. For the first time, the possibility of a realization of the Fourier-Mellin transformation in a hybrid electron-optical or optical-digital Fourier system was indicated by Kuzmenko [21]. Casasent used successfully this idea for the recognition of objects, which is invariant to the scaling, rotation, and shift, in a hybrid optical-digital 4F-system [22, 23]. In the subsequent years, a lot of works [24–35] were devoted to the invariant methods of recognition. In what follows, we will demonstrate a possibility to use the SPO-method for the pattern recognition with rotation invariance.

3.1. Computational experiment

Consider the rotation invariant recognition of objects realized by the conventional method and the SPO-method. Of interest is the comparison of the cross-correlation curves obtained with the help of both methods to recognition objects for various angles of its rotation.

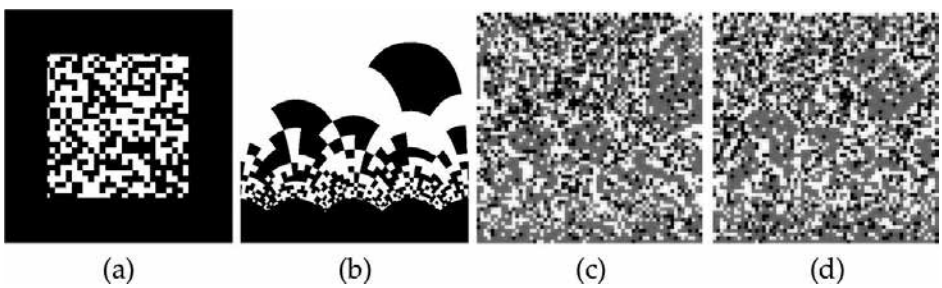

Figure 10. Reference objects: $f_1(x, y)$ (a); $g_1(exp(\rho), \theta)$ (b); $\phi_1(x, y)$ (c); $\chi_1(exp(\rho), \theta)$ (d).

As the reference objects for numerical experiments, we took a set of objects of the amplitude and half-tone types $f_i(x, y)$, $i = 1, 2, \ldots, 10$. For each of them, we define the sets of comparison objects $f_{i,\alpha_j}(x, y)$, $j = 1, 2, \ldots, 41$, which are obtained by the rotation of corresponding reference objects around the optical axis by an angle α with the step $\Delta\alpha = 0.5°$ in the limits [0°–20°]. In addition, for all reference objects and comparison objects, we define the sets $g_{i,}$ $(exp(\rho), \theta)$, $i = 1, 2, \ldots, 10$, of reference objects and $g_{i,\alpha_j}(exp(\rho), \theta)$, $j = 1, 2, \ldots, 41$, of comparison objects after a logarithmic polar transformation of coordinates [26]. For the comparison of cross-correlation dependences, we define the correlation functions for the SPO conventional recognition: $I_{\phi}(\alpha_j) = \left|\phi_i \otimes \phi_{i,\alpha_j}\right|_{max}$; by Fourier–Mellin rotation invariant recogni-

http://dx.doi.org/10.5772/65370

tion: $I_g(\alpha_j) = \left| g_i \otimes g_{i,\alpha_j} \right|_{max}$. For the SPO-method for the above-defined sets by the iteration scheme (**Figure 1**) at the initial $\varphi_0 = 0$ we calculate the SP-objects ϕ_i, $i = 1, 2, \ldots, 10$ for each reference object and for each comparison object $\chi_{i,\alpha_j}(x, y)$, $j = 1, 2, \ldots, 41$. All SP-objects were taken on the first iteration. Analogously, we define the correlation functions for the SPO conventional recognition: $I_\phi(\alpha_j) = \left| \phi_i \otimes \phi_{i,\alpha_j} \right|_{max}$; by SPO Fourier–Mellin rotation invariant recognition: $I_\phi(\alpha_j) = \left| \phi_i \otimes \chi_{i,\alpha_j} \right|_{max}$.

Below in **Figure 10**, we present an amplitude reference object of the binary type $f_1(x, y)$ (a), the object obtained for it after the logarithmic polar transformation of coordinates $g_1(exp(\rho), \theta)$ (b), and the SP-objects $\phi_{1,0}(x, y)$ (c) and $\chi_{1,0}(exp(\rho), \theta)$ (d) calculated for them.

To increase the peak values of correlation signal for recognition objects and the SNR, all amplitude objects f_i, g_i were transformed in phase ones by the Kallman method [20]. The results were obtained for ten objects with a dimension of 512 × 512 elements by the conventional and SPO methods. We analyzed the parameters of correlation signals and compared the correlation curves defined above. By the examples of **Figures 11–13**, we show the typical results of numerical experiments.

In **Figure 11a**, we show the dependence of the SNR of a recognition signal on the rotation angle of the object f_{1,α_j} at the subsequent calculation of the correlation of this object with the reference one f_1 (**Figure 10a**)— the curve formed by white squares.

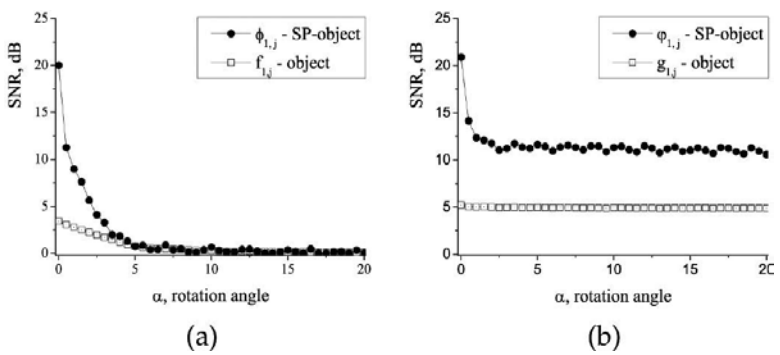

Figure 11. Dependence of the SNR for cross-correlation signals I_{corr} on the rotation angle α for: $\left| f_1 \otimes f_{1,\alpha_j} \right|$ (a), $\left| \phi_1 \otimes \phi_{1,\alpha_j} \right|$ (b) the conventional recognition; $\left| g_1 \otimes g_{1,\alpha_j} \right|$ (c), $\left| \chi_1 \otimes \chi_{1,\alpha_j} \right|$ (d) the recognition with the use of the Fourier-Mellin transformation.

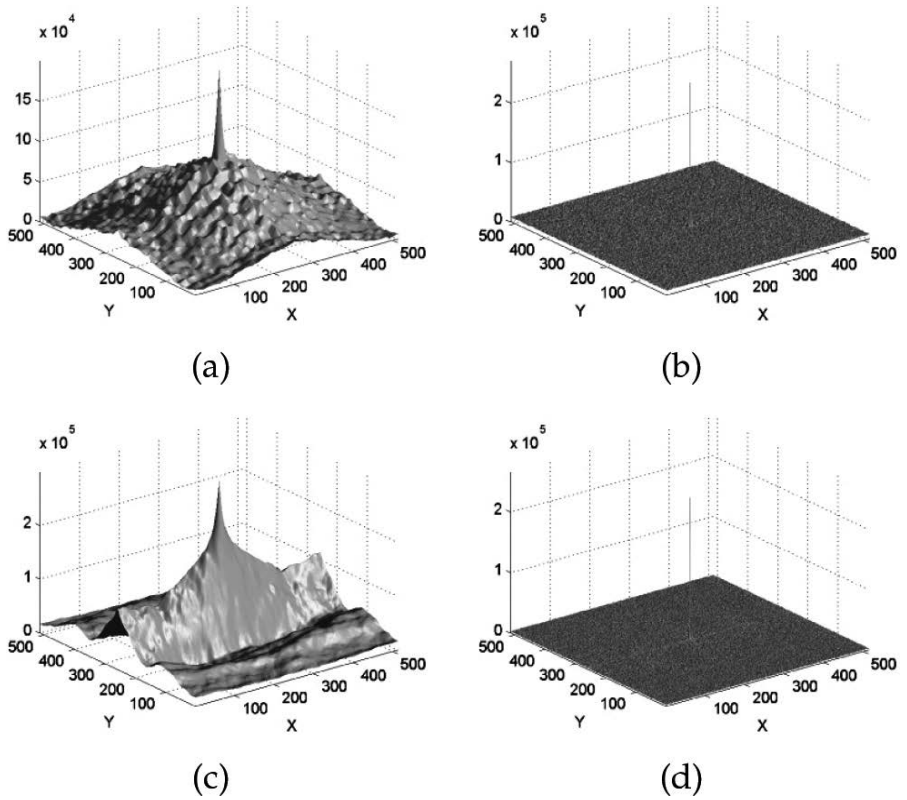

Figure 12. Autocorrelation signal: $|f_1 \otimes f_1|$ (a), $|\phi_1 \otimes \phi_1|$ (b) the conventional recognition; $|g_1 \otimes g_1|$ (c), $|\chi_1 \otimes \chi_1|$ (d) the recognition with the use of the Fourier-Mellin transformation; $\alpha = 0^0$.

The curve demonstrates the typical behavior [22, 23], namely the strong degradation of the correlation function under a rotation of the comparison object around the optical axis, while comparing it with the reference object. The correlation signal with *SNR* = 3.4 dB (**Figure 12a**) from the reference object under a rotation of the comparison object already at angles $\alpha > 5°$ is transformed into noise components of the cross-correlation signal, which change insignificantly their shapes at a subsequent rotation (**Figure 13a**). Curves (**Figure 11a**) demonstrate the above-written method for both conventional and SPO methods. As shown in [16], the SPO-method demonstrates a faster diminution of the curve with increase in distortions (in the given case, with increase in the rotation angle), δ-like shape of a recognition signal, and higher values of *SNR* about 20.2 dB for the autocorrelation (**Figure 12b**); for the angle $\alpha = 5°$, the signal is absent (**Figure 13b**). The curves in **Figure 11b** show variations in SNRs of the correlation functions with increase in the rotation angle for comparison objects for the conventional (light circles) and SPO (dark circles) methods at the Fourier-Mellin rotation invariant recognition. For *g*-objects, SNR of the signal is about 5 dB in the whole interval of change of the angles. For the SPO-method, we observe a change in SNR of the δ-like signal from 20 dB (**Figure 12d**) for autocorrelation to 11 dB; further, *SNR* of the cross-correlation signal is also independent of the angle of rotation of objects of the recognition (**Figure 12d**).

http://dx.doi.org/10.5772/65370

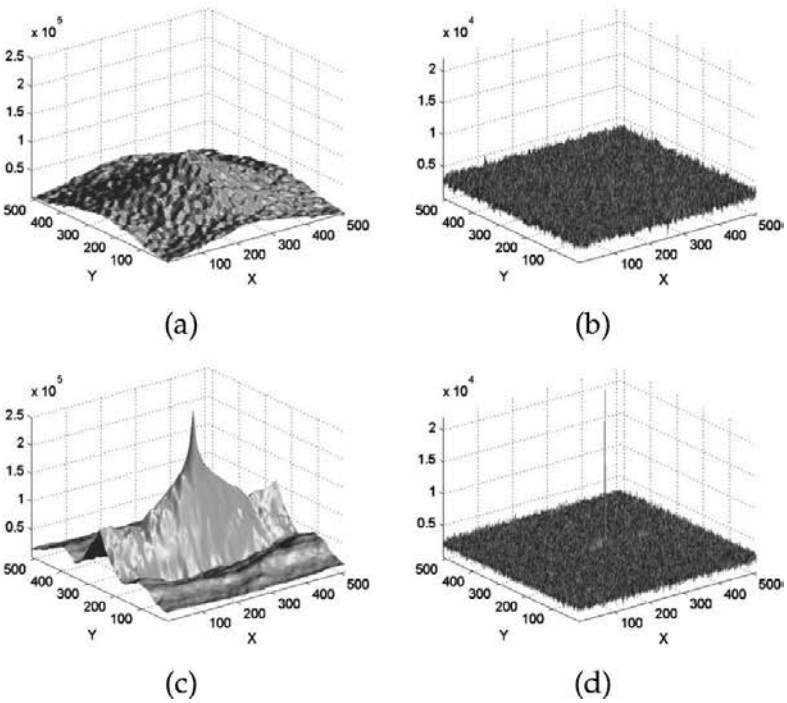

Figure 13. Cross-correlation signal: $|f_1 \otimes f_{1,\alpha}|$ (a), $|\phi_1 \otimes \phi_{1,\alpha}|$ (b) the conventional recognition; $|g_1 \otimes g_{1,\alpha}|$ (c), $|\chi_1 \otimes \chi_{1,\alpha}|$ (d) the recognition with the use of the Fourier-Mellin transformation; $\alpha = 20^0$.

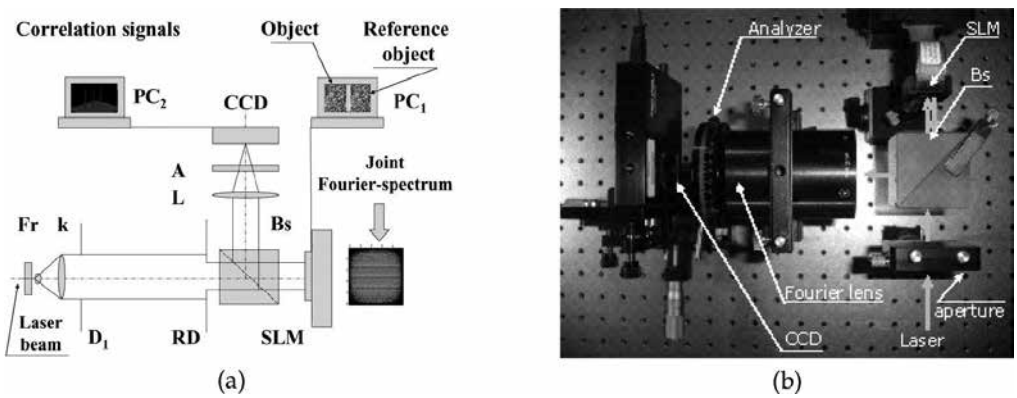

Figure 14. (a) Scheme and (b) photo of a digital-optical JT-correlator: Laser beam, P, D_1, RD, Bs, SLM, PC_1, L, A, CCD_1, CCD_2, PC_2—He-Ne (543 nm) laser beam, polarizer, circle and rectangle diaphragms, beam splitter, spatial light modulator HEO 1080 Pluto, Fourier lens, analyzer, a 12-bit SPU620 CCD with the BeamGage software and PC.

In view of the similar results obtained for the whole set of objects, we may say that the SPO-method is applicable for the rotation invariant recognition and conserves the same own advantages, as in the conventional recognition.

3.2. Optical experiment

For the corroboration of the results obtained in numerical experiments, we carried out experiments with an optical-digital system of recognition (see **Figure 14a** and **b**) on the basis of a JT-correlator. For this purpose, we got the autocorrelation signals for the objects $f_1(x, y)$, $g_{1,0}(exp(\rho), \theta)$, $\phi_1(x, y)$, and $\chi_{1,0}(x, y)$. The cross-correlation signals were obtained at the rotation of the indicated objects by $\alpha = 5°$.

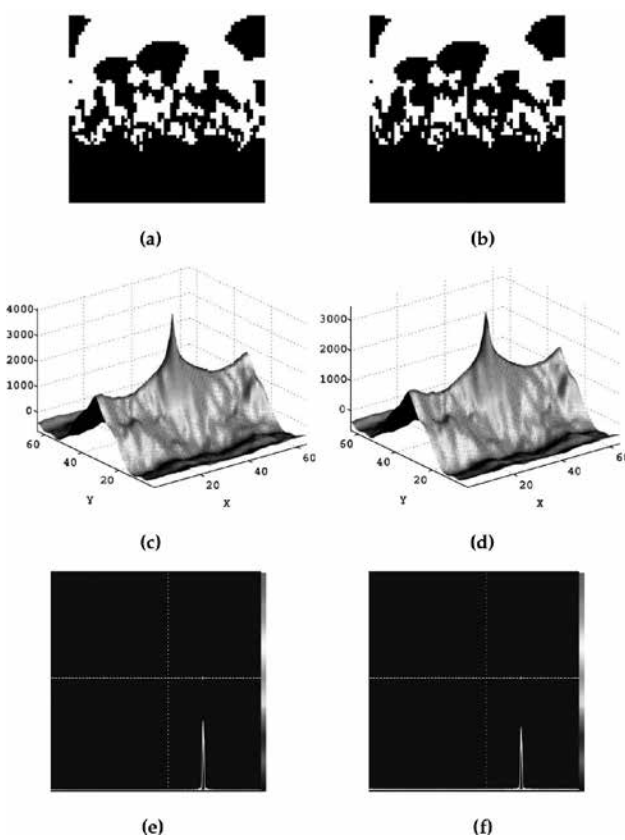

Figure 15. Pattern recognition results with Fourier-Mellin transformation: object's plane—reference g_1 (a) and recognition $g_{1,5°}$ (b) objects; calculation—autocorrelation (c) and cross-correlation (d) signals; experimental peaks—autocorrelation (e) and cross-correlation (f) in the correlation plane of the JT-correlator. The size of objects and JF-spectra is 64 × 64 and 512 × 512 elements, respectively.

The recognition in the JT-correlator includes two steps:

Formation of the joint Fourier spectrum (*JF*) *of compared objects*. With the help of a camera (is not shown in the scheme), the object of recognition is introduced in computer PC_1. We calculate the JT-spectrum moduli of a given object and the reference object. Then, JF-spectrum moduli is supplied to an SLM.

http://dx.doi.org/10.5772/65370

Production of a correlation signal. The collimated light beam of a He-Ne laser (543 nm) after masking by a working aperture is reflected from the SLM. In the correlation plane, a *CCD* camera registers the correlation signal obtained as a result of the inverse Fourier transform, which is performed by the lens *L*, of an optical signal reflected with the help of a splitting cube *Bs* from the SLM. The result is supplied to and is processed by computer PC_2.

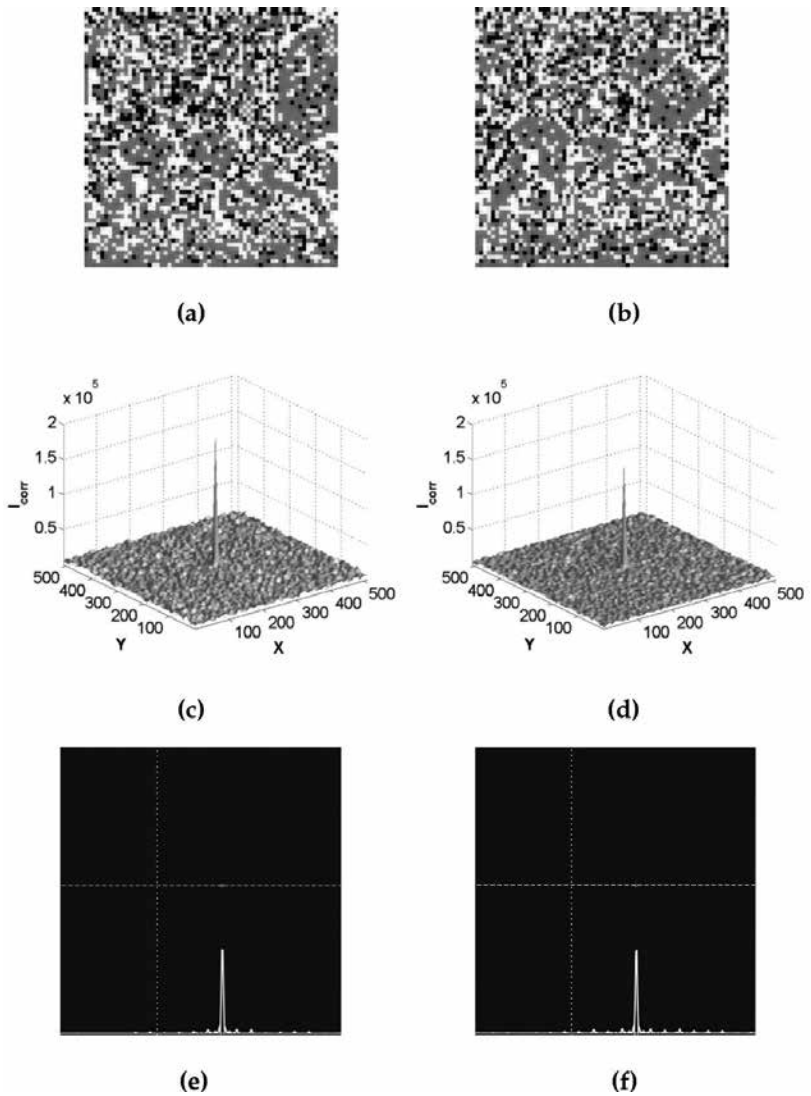

Figure 16. Pattern recognition results with the SPO-method and the Fourier-Mellin transformation: object's plane—reference χ_1 (a) and recognition $\chi_{1,5^\circ}$ (b) SP-objects; calculation results—autocorrelation (c) and cross-correlation (d) signals; experimental peaks—autocorrelation (e) and cross-correlation (f) in the correlation plane of the JT-correlator. The size of objects and JF-spectra is 64 × 64 and 512 × 512 elements, respectively.

3.3. Results and discussion

The results of optical experiments and their comparison with the results of numerical experiments (at least the qualitative one) allow us to evaluate a degree of applicability of the SPO-method for the rotation invariant recognition. **Figure 15** demonstrates objects **Figure 15a** and **b**, calculated autocorrelation **Figure 15c** and cross-correlation signals **Figure 15d**, and the autocorrelation **Figure 15e** and cross-correlation signals **Figure 15f** registered by a camera (**Figure 14a**).

The similar experimental result was obtained also within the SPO-method. The presence of cross-correlation signals is clearly seen for the conventional and studied methods (**Figures 15** (**e**, **f**) and **16** (**e**, **f**)) in the case of the rotation invariant recognition by Fourier-Mellin.

The SNR for recognition signals is in the limit 23–25 dB. Thus, the results (the presence of a recognition signal at a rotation of the recognition object) confirm qualitatively the applicability of the SPO-method to the rotation invariant correlation.

Thus, the numerical and optical experiments show the applicability of the SPO-method to the rotation Fourier-Mellin invariant recognition for amplitude and half-tone objects of the binary type. The estimate of correlation signals and the obtained dependences of $SNR(\alpha)$ indicate that the SPO-method gives signals of the δ-like shape irrespective of the type of objects that gives a constant value of SNR exceeding SNR for the conventional method in the whole interval of the angles of rotation of comparison objects by 6 dB higher on the average for the rotation invariant recognition. These results are typical of the whole set of reference objects.

4. Conclusion

The hypothesis about the possibility to solve the problem of optical recognition by means of the change of the recognized objects by the corresponding object-dependent SP-objects in model and optical experiments is verified. The advantages and the drawbacks of such approach are determined. The conditions of recording of matched filters on original photopolymeric compositions, which ensure the optimum parameters of correlation signals at the recognition of amplitude objects, are determined. Auto- and cross-correlation signals for amplitude objects of various classes and for the corresponding SP-objects are obtained by computer simulation experimentally and compared at the recognition with a hybrid optical-digital VL-correlator. The influence of controlled changes in the structure of objects on correlation signals in the conventional and proposed approaches is experimentally studied in the optical-digital systems of recognition on the basis of the VL and JT correlators. The development of the SPO-method for the rotation invariant pattern recognition with an optical-digital JT-correlator is presented.

http://dx.doi.org/10.5772/65370

Acknowledgements

This research was supported by the research fund from Chosun University, 2015, South Korea.

Author details

Pavel V. Yezhov[1*], Alexander P. Ostroukh[2], Jin-Tae Kim[3*] and Alexander V. Kuzmenko[2]

*Address all correspondence to: yezhov@iop.kiev.ua and kimjt@chosun.ac.kr

1 Institute of Physics of the NAS of Ukraine, Kyiv, Ukraine

2 IC "Institute of Applied Optics" of the NAS of Ukraine, Kyiv, Ukraine

3 Department of Photonic Engineering, College of Engineering, Chosun University, Gwangju, South Korea

References

[1] Talukder A, Casasent D. General methodology for simultaneous representation and discrimination of multiple object classes. Opt. Eng. (Special Issue on Advanced Recognition Techniques). 1998; 37(3):904–913. doi:10.1117/1.601925

[2] Kashi R, Turin W, Nelson W. On-line handwritten signature verification using stroke direction coding. Opt. Eng. 1996; 35(9):2526–2533. doi:10.1117/1.600857

[3] Roberge D, Soutar C, Vijaya Kumar B. Optimal trade-off filter for the correlation of fingerprints. Opt. Eng. 1999; 38(1):108–113. doi:10.1117/1.602075

[4] Fleisher M, Mahlab U, Shamir J. Entropy optimized filter for pattern recognition. Appl. Opt. 1991; 29(14):2091–2098. doi:10.1364/AO.29.002091

[5] Rajan P, Raghavan E. Design of synthetic estimation filters using correlation energy minimization. Opt. Eng. 1994; 33(6):1829–1837. doi:10.1117/12.171617

[6] Farn M, Goodman J. Optimal binary phase-only matched filters. Appl. Opt. 1988; 27(21): 4431–4436. doi:10.1364/AO.27.004431

[7] Casasent D. Unified synthetic discriminant function computational formulation. Appl. Opt. 1984; 23(10):1620–1627. doi:10.1364/AO.23.001620

[8] Wang Z, Liu H, Guan J, Mu G. Phase shift joint transform correlator with synthetic discriminant function. Optik. 2000; 111(2):71–74

[9] Refregier Ph. Application of the stabilizing functional approach to pattern recognition filter. J. Opt. Soc. Am. A. 1994; 11(4):1243–1252. doi:10.1364/JOSAA.11.001243

[10] Rosen J, Shamir J. Application of the projection-onto-constraint-sets algorithm for optical pattern recognition. Opt. Lett. 1991; 16(10):752–754. doi:10.1364/OL.16.000752

[11] Vanderlugt A. Practical considerations for the use of spatial carrier-frequency filters. Appl. Opt. 1966; 5(11):1760–1765

[12] Weaver C, Goodman J. Technique for optically convolving two functions. Appl. Opt. 1966; 5:1248–1249. doi:10.1364/AO.5.001248

[13] Gerchberg R, Saxton W. A practical algorithm for the determination of phase from image and diffraction plane pictures. Optik. 1972; 35:237–246

[14] Yezhov P, Kuzmenko A. Synthesized phase objects instead of real ones for optical-digital recognition systems. In: Proceedings of the SPIE Sixth International Conference on Correlation Optics (CorrOpt 2004); 16–19 September 2003; Ukraine. Chernivtsi: SPIE 5477; 2003. p. 412–421; doi:10.1117/12.559771

[15] Yezhov P, Kuzmenko A, Smirnova A, Ivanovskiy A. Synthesized phase objects used instead of real ones for optical-digital recognition systems: experiment. In: Proceedings of the SPIE Seventh International Conference on Correlation Optics 625419 (CorrOpt 2006); 14 June 2006; Ukraine. Chernivtsi: SPIE 6254; 2006. p. 349–361; doi: 10.1117/12.679944

[16] Yezhov P, Kuzmenko A, Kim J, Smirnova T. Method of synthesized phase objects for pattern recognition: matched filtering. Opt. Exp. 2012; 20(28):29854–29866. doi:10.1364/OE.20.029854

[17] Ostroukh A, Butok A, Shvets R, Yezhov P, Kim J and Kuzmenko A. Method of synthesized phase objects for pattern recognition with rotation invariance. In: Proceedings of the SPIE Twelfth International Conference on Correlation Optics 98090B (CorrOpt 2015);14 September 2015; Ukraine. Chernivtsi: SPIE 9809; 2006. p. 98090B; doi: 10.1117/12.2219848

[18] Gallaher N. Method for computing kinoform that reduces image reconstruction error. Appl. Opt. 1973; 12(10):2328–2335. doi:10.1364/AO.12.002328

[19] Fitio L, Muravsky V, Stefansky A. Using phase masks for image recognition in optical correlators. In: Proceedings of the SPIE Seventh International Conference on Holography and Correlation Optics, 224 (CorrOpt 1995); 10 November 1995; Ukraine. Chernivtsi: SPIE 2647; 1995. p. 224–234; doi:10.1117/12.226700

[20] Kallman R, Goldstein D. Phase-encoding input images for optical pattern recognition. Opt. Eng. 1994; 33:1806–1811. doi:10.1117/12.171322

[21] Kuzmenko A. Laplace transform in coherent optics and its application for the realization of the Mellin transform. Autometriya. 1975; 5:22–26.

[22] Casasent D, Psaltis D. Position, rotation, and invariant optical correlator. Appl. Opt. 1994; 15:1795–1799. doi:10.1364/AO.15.001795

[23] Casasent D, Psaltis D. Scale invariant optical correlation using Mellin transforms. Opt. Commun. 1976; 17:59–63. doi:10.1016/0030-4018(76)90179-6

[24] Sheng Y, Arsenault H. Experiments on pattern recognition using invariant Fourier–Mellin descriptors. J. Opt. Soc. Am. A. 1986; 3:771–776. doi:10.1364/JOSAA.3.000771

[25] Chen M, Defrise Q, Deconinc F. Symmetric phase-only matched filtering of Fourier–Mellin transforms for image registration and recognition. IEEE Trans. Pattern Recognit. Mach. Intell. 1994; 16(12):1156–1168. doi:10.1109/34.387491

[26] Ayyalasomayayajula S, Grassi P, Farine P. Low complexity RST invariant image recognition using Fourier–Mellin transform. In: Proceedings 19th European Signal Processing Conference (EUSIPCO 2011); 29 August–2 September 2011; Spain. Barcelona: IEEE. ISSN: 2076-1465; 2011. p. 769–773

[27] Flusser J, Suk T. Pattern recognition by affine moment invariants. Pattern Recognit. 1993; 26(1):167–174. doi:10.1016/0031-3203(93)90098-H

[28] Wang W, Chen Y. New approach for scale, rotation, and translation invariant pattern recognition. Opt. Eng. 1997; 36(4):1113–1122. doi:10.1117/1.601291

[29] Leclers L, Sheng Yu, Arsenault H. Rotation invariant phase-only and binary phase-only correlation. Appl. Opt. 1989; 28(6):1251–1256. doi:10.1364/AO.28.001251

[30] Leclers L, Sheng Yu, Arsenault H. Optical binary phase-only filters for circular harmonic correlations. Appl. Opt. 1991; 30(32):4643–4649. doi:10.1364/AO.30.004643

[31] Rosen J, Shamir J. Circular harmonic phase filters for efficient rotation invariant pattern recognition. Appl. Opt. 1988; 27:2895–2899. doi:10.1364/AO.27.002895

[32] Wang Z, Guan J, Liang B. et al. Rotation invariant binary joint transform correlator. Optik. 2000; 111(9):413–417

[33] Sweeney D, Ochoa E, Schils G. Experimental use of iteratively designed rotation invariant correlation filters. Appl. Opt. 1987; 26(16):3458–3465. doi:10.1364/AO.26.003458

[34] Silvera E, Kotzer T, Shamir J. Adaptive pattern recognition with rotation, scale, and shift invariance. Appl. Opt. 1995; 34(11):1891–1900. doi:10.1364/AO.34.001891

[35] Alam M, Awwal A, Grenwal B. Scale invariant amplitude modulated phase-only filtering. Opt. Laser Tech. 2000; 32:231–234. doi:10.1016/S0030-3992(00)00047-5

Section 2

Pattern Recognition: Applications

Chapter 4

Automated Face Recognition: Challenges and Solutions

Joanna Isabelle Olszewska

Additional information is available at the end of the chapter

http://dx.doi.org/10.5772/66013

Abstract

Automated face recognition (AFR) aims to identify people in images or videos using pattern recognition techniques. Automated face recognition is widely used in applications ranging from social media to advanced authentication systems. Whilst techniques for face recognition are well established, the automatic recognition of faces captured by digital cameras in unconstrained, real-world environment is still very challenging, since it involves important variations in both acquisition conditions as well as in facial expressions and in pose changes. Thus, this chapter introduces the topic of computer automated face recognition in light of the main challenges in that research field and the developed solutions and applications based on image processing and artificial intelligence methods.

Keywords: face recognition, face identification, face verification, face authentication, face labelling in the wild, computational face

1. Introduction

Automated face recognition (AFR) has received a lot of attention from both research and industry communities since three decades [1] due to its fascinating range of scientific challenges as well as rich possibilities of commercial applications [2], particularly in the context of biometrics/forensics/security [3] and, more recently, in the areas of multimedia and social media [4, 5].

Face recognition is the field trying to bring an answer to the question: *'Whose face it is?'* For this purpose, people have natural abilities through their human perceptive and cognitive systems [6], whereas machines need complex systems involving multiple, advanced algorithms and/or large, adequate face databases. Studying, designing and developing such methods and technologies are the domain of automated face recognition (AFR).

AFR could be distinguished further into the computer automated face identification and the computer automated face verification. Hence, on the one hand, automated face identification consists in a one-to-many (1:N) search of a face image among a database containing many different face images in order to answer questions such as '*Is it a known face?*' [7]. On the other hand, automated face verification is a one-to-one (1:1) search to solve the matter of '*Is it the face of …?*' search [8].

Moreover, AFR could be the basis to the solution of the '*Who is in the picture?*' problem, leading to the computer automated face labelling/face naming [9].

The general AFR process is illustrated in **Figure 1**. Usually, it first applies techniques addressing questions such as '*Is there a face in the image?*' (face detection) and '*Where is the face in the image?*' (face location) and next, it handles the computer-automated recognition mechanism itself [10].

Figure 1. Overview of the face detection and recognition processes.

In particular, this chapter is dedicated to the 'why' and 'how' of the computer-automated face recognition in constrained and unconstrained environments. The remaining parts of this chapter are structured as follows: in Section 2, we describe AFR's today challenges, while corresponding scientific solutions and industrial applications are presented in Sections 3 and 4, respectively. Section 5 draws up new trends and future directions for automated face recognition performance improvements and evolution.

2. Challenges

The study and analysis of faces captured by digital cameras address a wide range of challenges, as detailed in Sections 2.1–2.7, which all have a direct impact on the computer automated face detection and recognition.

2.1. Pose variations

Head's movements, which can be described by the egocentric rotation angles, i.e. pitch, roll and yaw [11], or camera changing point of views [12] could lead to substantial changes in face

http://dx.doi.org/10.5772/66013

appearance and/or shape and generate intra-subject face's variations as illustrated in **Figure 2**, making automated face recognition across pose a difficult task [13].

Figure 2. Illustration of pose variations around egocentric rotation angles, namely (a) pitch, (b) roll and (c) yaw.

Since AFR is highly sensitive to pose variations, pose correction is essential and could be achieved by means of efficient techniques aiming to rotate the face and/or to align it to the image's axis as detailed in reference [13].

2.2. Presence/absence of structuring elements/occlusions

The diversity in the intra-subject face's images could also be due to the absence of structuring elements (see **Figure 3a**) or the presence of components such as beard and/or moustache (see **Figure 3b**), cap (see **Figure 3c**), sunglasses (see **Figure 3d**), etc. or occlusions of the face (see **Figure 3e**) by background or foreground objects [14].

Figure 3. Illustration of (a) absence or (b-d) presence of structuring elements, i.e. (b) beard and moustache, (c) cap, (d) sunglasses or (e) partial occlusion.

Thus, face's images taken in an unconstrained environment often require effective recognition of faces with disguise or faces altered by accessories and/or by occlusions, as dealt by appropriate approaches such as texture-based algorithms [15].

2.3. Facial expression changes

Some more variability in face appearance could be caused by changes of facial expressions induced by varying person's emotional states [16] which are displayed in **Figure 4**.

Hence, efficiently and automatically recognizing the different facial expressions is important for both the evaluation of emotional states and the automated face recognition. In particular, human expressions are composed of macro-expressions, which could express, e.g., anger, disgust, fear, happiness, sadness or surprise, and other involuntary, rapid facial patterns, i.e. micro-expressions; all these expressions generating non-rigid motion of the face. Such facial dynamics can be computed, e.g., by means of the dense optical flow field [17].

Figure 4. Illustration of varying facial expressions that reflect emotions such as (a) anger, (b) disgust, (c) sadness or (d) happiness.

2.4. Ageing of the face

Another reason of face appearance's changes could be engendered by the ageing of the human face, and could impact on the entire AFR process if the time between each image capture is significant [18], as illustrated in **Figure 5**.

Figure 5. Illustration of the human ageing process, where the same person has been photographed (a) at a younger age and (b) at an older age, respectively.

To overcome face ageing issue in AFR, methods need to take properly into account facial ageing patterns [18]. Indeed, over time, not only face characteristics such as its shape or lines are modified [19], but other aspects are changing as well, e.g. hairstyle [20].

2.5. Varying illumination conditions

Large variations of illuminations could degrade the performance of AFR systems. Indeed, for low levels of lighting of the background or foreground, face detection and recognition are much harder to perform [21], since shadows could appear on the face and/or facial patterns could be (partially) indiscernible. On the other hand, too high levels of lights could lead to over-exposure of the face and (partially) indiscernible facial patterns (see **Figure 6**).

Robust automated face detection and recognition in the case of (close-to-) extreme or largely varying levels of lighting apply to image-processing techniques such as illumination normalization, e.g. through histogram equalization [22]; or machine-learning methods involving the actual image global image intensity average value [21].

http://dx.doi.org/10.5772/66013

Figure 6. Illustration of camera lighting variations, leading to (a) over-exposure of the face, (b) deep shadows on the face or (c) partial backlight.

2.6. Image resolution and modality

Other usual factors influencing AFR performance are related to the quality and resolution of the face image and/or to the set-up and modalities of the digital equipment capturing the face [23]. For this purpose, ISO/IEC 19794-5 standard [24] has been developed to specify scene and photographic requirements as well as face image format for AFR, especially in the context of biometrics. However, real-world situations of face image acquisition imply the use of different photographic hardware, including one or several cameras which could be omnidirectional or pan-tilt-zoom [25], and which could include, e.g. wide-field sensors [25], photometric stereo [26], etc. Cameras could work in the range of the visible light or use infra-red sensors, leading to multiple modalities for AFR [6]. Hence, faces acquired in real-world conditions lead to further AFR challenges.

Figure 7. Illustration of variations of the image scale and resolution, with (a) a large-scale picture, (b) a small-scale picture and (c) a low-resolution picture.

For example, as shown in **Figure 7**, in some situations, a face could be captured at distance resulting in a smaller face region image compared to the one in a large-scale picture. On the other hand, some digital camera could have a low resolution [27] or even very low resolution [28], if the resolution is below 10 × 10, leading to poor quality face images, from which AFR is very difficult to perform. To deal with this limitation, solutions have been proposed to reconstruct a high-resolution image based on the low-resolution one [28] using the super-resolution method [29, 30].

2.7. Availability and quality of face datasets

Each AFR technology requires an available, reliable and realistic face database in order to perform the 1:N or 1:1 face search within it (see **Figure 1**). Hence, the quality such as com-

pleteness (e.g. including variations in facial expressions, in facial details, in illuminations, etc.) as well as accuracy (e.g. containing ageing patterns, etc.) and the characteristics (e.g. varying image file format and colour/grey level, face resolution, constrained/unconstrained environment, etc.) of a face dataset are crucial to the AFR process [31]. Moreover, when dealing with face data, people's consent and privacy should be respected as AFR systems should comply with the Data Protection Act 2010 [32].

For research purpose, several face databases have been developed and are publicly available. Well-established, online face databases are as follows:

- ORL [33] is a 400-picture dataset of 40 distinct subjects, in portable grey map (*pgm*) format and with a 92 × 112 pixel resolution, 8-bit grey level. Men and women's faces are taken against a dark homogeneous background, under varying illumination conditions. The subjects are in up-right, frontal position, with variations in face expressions, facial details and poses within ±20% in yaw and roll.
- Caltech Faces [34] dataset consists of 450 *jpeg* images with a resolution of 896 × 592 pixels. Each image shows the frontal view of a face (single pose) of one out of 27 unique persons, under different lighting, expressions and backgrounds.
- The Face Recognition Technology (FERET) [35] database has been built with 14,126 face images from 1199 individuals, defining sets of 5–11 greyscale images per person. Each set contains mugshots with different facial expressions and facial details, acquired using various cameras and varying lighting.
- BioID Face database [36] has 1521 frontal face images of 23 people. Images of 384 × 286 pixel resolution are in *pgm* format and have been captured in real-world conditions, i.e. with a large variety of illumination, background and face size.
- Yale face database [37] has 165 greyscale, *gif* images of 15 individuals. There are 11 images per subject, one per different facial expression or configuration, i.e. left/centre/right-light, with or without glasses and with different expressions.
- Caltech 10,000 web faces [38] have collected 10,524 human faces of various resolutions and in different settings (e.g. portrait images, group of people, etc.) from *Google Image*. Coordinates of eyes, nose and the centre of the mouth for each frontal face are provided in order to be used as ground truth for face detection algorithms, or to align and/or crop the human faces for AFR.

Some databases contain both 2D and 3D face data, e.g. Face Recognition Grand Challenge (FRGC) dataset [39] recorded such 50,000 un-/controlled images from 4003 subject sessions.

Other datasets have multiple modalities such as XM2VTSDB multi-modal face database [40] which is the Extended M2VTS database. It is a large, multi-modal database captured onto high-quality, digital video. It contains four recordings, each with a speaking head shot and a rotating head shot, of 295 subjects taken over a period of 4 months. This database includes high-quality colour images, 32 kHz 16-bit sound files, video sequences and also a 3D model.

Another multi-modal database is the Surveillance Cameras Face (SCFace) [41] dataset. It has recorded 4160 static human faces of 130 subjects, in the visible and infrared spectrum, in an unconstrained indoor environment, using a multi-camera set-up consisting of five video-surveillance cameras which various qualities mimic real-world conditions.

Recent developments of face databases focus on capturing faces in the wild, i.e. in unconstrained environments. For example, Face Detection Data Set and Benchmark (FDDB) [42] is a dataset of 2845 images, both greyscale and colour ones, with 5171 faces in the wild, which could include occlusions, poses variations, low resolution and out-of-focus faces.

Labelled Faces in the Wild (LFW) [43] database is a popular dataset for studying multi-view faces in an unconstrained environment. It has recorded 13,233 foreground face images; other faces in the images being assimilated to the background. It has targeted 5749 different individuals, which could have one or more images in the database, and presents variations in pose, lighting, expression, background, race, ethnicity, age, gender, clothing, hairstyles, camera quality, colour saturation, focus, etc. Images have a 250 × 250 pixels resolution and are in *jpeg* format; they are mostly in colour, although few are greyscale only.

Some other available face datasets have been designed for specific purposes. Hence, Spontaneous MICro-expression database (SMIC) [44] is used for facial micro-expressions recognition, while the Acted Facial Expression in the Wild (AFEW) database [45], which has semi-automatically collected face images with acted emotions from movies, is dedicated to macro-expression recognition in close-to-real conditions. On the other hand, FG-NET Ageing database (FG-NET) [46] could be applied for age estimation, age-invariant face recognition and age progression.

3. Solutions

Major pattern recognition techniques as well as main machine-learning methods used for AFR systems are presented in Section 3.1, while classic approaches for AFR in still images or video databases/live video streams are mentioned in Section 3.2.

3.1. Face recognition systems

Most of the AFR systems consist in a two-step process (see **Figure 8**) based firstly on facial feature extraction, as explained in Section 3.1.1, and second, on facial feature classification/matching against an available face database, as mentioned in Section 3.1.2.

3.1.1. Feature extraction

Facial features are representing the face in a codified way which is computationally efficient for further processes such as matching, classification or other machine-learning techniques, in order to perform AFR. On the other hand, computing facial features in an image could serve to detect a face and to locate it within the image, as illustrated in **Figure 9**.

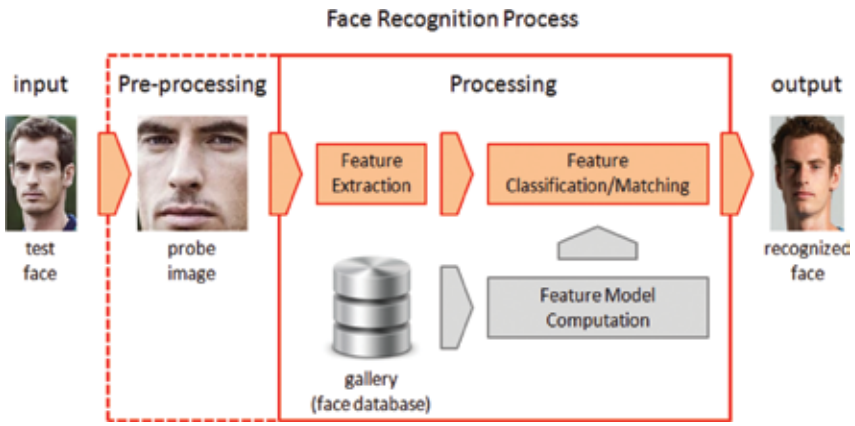

Figure 8. Schematic representation of the automated face recognition system.

Figure 9. Face location via (a) a bounding box and (b) an ellipse.

Facial feature representations could be of different nature from sparse to dense ones, and could be focused on face appearance, face texture or face geometry [15].

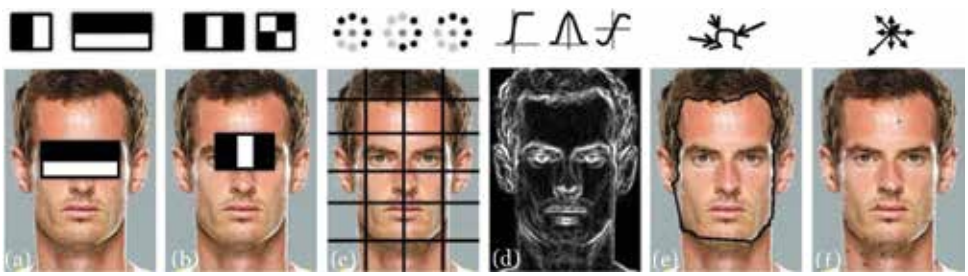

Figure 10. Results of facial feature modelling using different approaches, e.g. (a-b) Haar-like features; (c) Linear Binary Patterns (LBP); (d) Edge map; (e) Active shape; (f) SIFT points.

Commonly computed facial features are Haar-like features [47] (**Figure 10(a, b)**); linear binary patterns (LBP) [48] (**Figure 10(c)**), which have been extended to local directional pattern (LDP) [49] for micro-expressions recognition in particular; edge maps (**Figure 10(d)**) and their

extension to line edge maps (LEM) [50]; active shape or active contours [51] (**Figure 10(e)**); SIFT points [52] (**Figure 10(f)**), etc.

The detected facial features, e.g. with SIFT points usually correspond to some or all elements of the set of facial anthropometric landmarks, i.e., facial fiducial points (FPs) (see **Figure 11**), which are defined as follows: FP1—top of the head, FP2—right eyebrow right corner, FP3—right eyebrow left corner, FP4—left eyebrow right corner, FP5—left eyebrow left corner, FP6—right eye right corner, FP7—right eye centre of pupil, FP8—right eye left corner, FP9—left eye right corner, FP10—left eye centre of pupil, FP11—left eye left corner, FP12—nose right corner, FP13—nose centre bottom, FP14—nose left corner, FP15—mouth right corner, FP16—mouth left corner, FP17—chin corner, FP18—right ear top corner, FP19—right ear bottom corner, FP20—left ear top corner and FP21—left ear bottom corner [53].

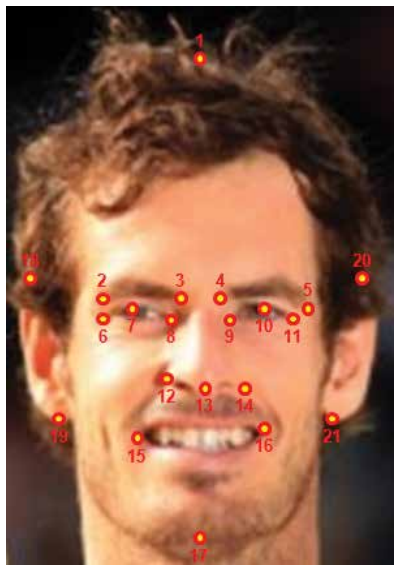

Figure 11. Illustration of the 21 facial landmarks.

Computer automated face recognition relies on facial features, in the same way forensic examiners focus their attention not only on the overall similarity of two faces regarding their shape, size, etc. [54], but also on morphological comparisons region by region, e.g. nose, mouth, eyebrows, etc. [53]. Some AFR methods evaluate also discriminative characteristics such as the distance from people's mouth to the nose, nose to eyes, mouth to eyes, etc. [55]. This adds robustness into AFR systems in the case of modification of some facial patterns over the course of time or occlusions.

Once the face is detected/located and the facial features are extracted, actions to crop the face, to correct its alignment by rotating it, etc., could be performed to address the challenges mentioned in Section 2, before passing the facial features into the next stage described in Section 3.1.2.

3.1.2. Feature classification/matching

For the recognition stage itself of the face recognition process, classification is often used as shown in **Figure 12**. Indeed, it is a machine-learning technique [56] that has the task of first learning and then applying a function that maps the facial features of an individual to one of the predefined class labels, i.e. class 1 (face of the individual) or class 2 (not the face of the individual), leading in this case to a binary classifier. Classifiers could be applied to the entire set of the extracted facial features or to some specific face attributes, e.g. gender, age, race, etc. [57]. More recently, methods like neural networks are used as classifiers [58].

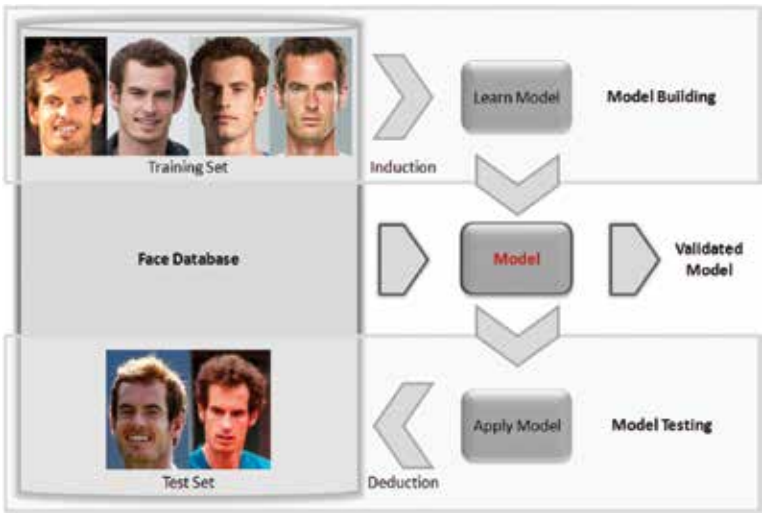

Figure 12. Overview of the model computation.

On the other hand, some AFR systems use the matching technique that could be applied on facial geometric features or templates [59]. This approach is also useful for multimodal face data [60].

3.2. Examples of methods

Among hundreds of techniques developed in this field [1–10], Sections 3.2.1–3.2.4 explain briefly some well-established methods for automated face recognition.

3.2.1. Eigenfaces

The eigenface approach [61] is a very successful AFR method. It involves pixel intensity features and uses the principal component analysis (PCA) of the distribution of faces, or *eigenvectors*, which are a kind of set of features characterizing faces' variations where each face image contributes more or less to each eigenvector. Thus, an eigenvector can be seen as a ghostly face, or *eigenface*. Recognition of a test face is determined by applying the nearest-

http://dx.doi.org/10.5772/66013

neighbour technique to the probe face projection in the face space [13]. Fisherfaces extend the eigenface approach by using linear discriminant analysis (LDA) instead of PCA [62, 63].

3.2.2. Active appearance models

The active appearance model (AAM) [64] combines shape and texture features; thus it is slower but more robust for AFR than active shape models (ASM). AAM is built as a multi-resolution model based on a Gaussian-image pyramid. For each level of the pyramid, a separate texture model is computed using 400 face images. Each face is labelled with 68 points around the main features, and the facial region is sampled by c. 10,000 intensity values. AFR is performed by matching the test face with the AAM, following a multi-resolution approach that improves speed and robustness of this method [64].

3.2.3. Local binary patterns

In reference [48], local binary patterns (LBP), which are texture features, have been introduced for AFR. In particular, the face image is divided into independent regions where the LBP operator is applied to codify every pixel of each region by thresholding the 3 × 3-neighbourhood of each pixel with the centre pixel value and by binarizing it, and then, creating a local texture descriptor with the histogram of the codes for each face region. A global description of the face is formed by concatenating the local descriptors. Next, the nearest-neighbour classifier is used [48]. LBP approach has been widely adopted for AFR, and several enhancements have been proposed, e.g. the local directional patterns (LDP) [49].

3.2.4. SIFT

The discriminative deep metric-learning (DDML) [52] approach for AFR in unconstrained environment uses facial features such as SIFT descriptors and trains a deep neural network as a classifier to learn a Mahalanobis distance metric in order to maximize face's inter-class variations and minimize face's intra-class variations, simultaneously [52].

4. Applications

Nowadays, industry integrates cutting-edge, face recognition research into the development of the latest technologies for commercial applications such as mentioned in Sections 4.1–4.2.

4.1. Security

Face recognition is one of the most powerful processes in biometric systems [8] and is extensively used for security purpose in tracking and surveillance [65, 66], attendance monitoring, passenger management at airports, passport de-duplication, border control and high security access control as developed by companies like *Aurora* [67].

AFR is applied in forensics for face identification [68], face retrieval in still image databases or CCTV sequences [69], or for facial sketch recognition [70]. It could also help law enforcement

through behaviour and facial expression observation [71], lie detection [72], lip tracking and reading [73].

Moreover, AFR is now used in the context of 'Biometrics as a Service' [74], within cloud-based, online technologies requiring face authentication for trustworthy transactions. For example, *MasterCard* developed an app which uses selfies to secure payments via mobile phones [75]. In this *MasterCard*'s app, AFR is enhanced by facial expression recognition as the application requires the consumer blinks to prove that s/he is human.

4.2. Multimedia

In our today's life, AFR engines are embedded in a number of multi-modal applications such as aids for buying glasses or for digital make-up and other face sculpting or skin smoothing technologies, e.g. designed by *Anthropics* [76].

In social media, many collaborative applications within *Facebook* [77], *Google* [78] or *Yahoo!* [79] are calling upon AFR. Applications such as *Snapchat* require AFR on mobile [80]. With 200 million users of which half of those engage on daily basis [81], *Snapchat* is a popular image messaging and multimedia mobile application, where 'snaps', i.e. a photo or a short video, can be edited to include filters and effects, text caption and drawings. *Snapchat* has features such as the 'Lens', which allows users to add real-time effects into their snaps by using AFR technologies, and 'Memories' which searches content by date or using local recognition systems [82].

Other multimedia applications are using AFR, e.g. in face naming to generate automated headlines in *Video Google* [83], in face expression tracking for animations and human-computer interfaces (HCI) [84], or in face animation for socially aware robotics [85]. Companies such as *Double Negative Visual Effects* [86] or *Disney Research* [87] propose also AFR solutions for face synthesis and face morphing for films and games visual effects.

5. Conclusions

Since constraints shape the path for innovative solutions, we focused this chapter on scientific and technical challenges brought by computer automated face recognition, and we explained current solutions as well as potential applications. Moreover, there are a number of challenges ahead and plenty of room for innovations in this field of automated face recognition. In particular, three emerging directions are discussed in Sections 5.1–5.3.

5.1. Deep face

On the one hand, the proliferation of mobile devices such as smartphones and tablets, which are world-widely available for consumers and which allow users to easily record digital pictures, and on the other hand, the outbreak of mobile and web applications, which manipulate and store thousands of pictures, have paved the way to the Big Data, and, among others, to the necessity to analysis large-scale, face databases. This phenomenon has given rise to

http://dx.doi.org/10.5772/66013

questions such as AFR technology scalability and computational power, and it has led to the development of a new AFR approach called deep face recognition [88], which involves deep-learning techniques using convolutional neural networks [89], well fitted for big datasets [90]. Indeed, deep face methods are using large databases for training their models, as by biomimetics, they rely on the familiarity concept [91], which is based on the fact that more people are familiar with a person's face, more easily they recognized his/her face, even in complex situations like occlusions or low resolution. Moreover, the recent development of the deep face approach has benefited from progress in parallel computing tools for acceleration and enhancement of distributed computing techniques for scalability. In particular, for deep face recognition, graphics processing units (GPUs), which are specialized processors for real-time, high-resolution 3D graphics, are used as highly parallel multi-core systems for big data [92], together with the Compute Unified Device Architecture (CUDA), which provides a simple and powerful platform [93], making easier for specialists in parallel programming to utilize GPU resources without advanced skills in graphics programming. Since the above-mentioned, iterative computation consists of local parallel processing, CUDA implementation is employed for reducing the computation time of the AFR system [93]. However, deep face-based methods generate themselves further challenges, e.g. face frontalization [94] that is the process of synthesizing frontal facing views of faces appearing in single unconstrained photos, in order to boost AFR performance within intelligent systems.

5.2. Wild face

Another challenge that has appeared with the generation of a large amount of visual data captured 'in the wild', i.e. in an unconstrained environment, by commercial cameras is the automated recognition of faces in the wild. It involves the enhancement of AFR methods [95] in order they efficiently deal with complex, real-world backgrounds [96], multiple-face scenes [51], skin-colour variations [97], gender variety [98] and with inherent challenges such as image quality, resolution, illumination or facial pose correction [23, 27, 99].

5.3. Dynamic face

In the recent years, handling facial dynamics efficiently is crucial for AFR systems, because people have recorded a large amount of faces as still digital images, e.g. selfies or as video streams, e.g. CCTV sequences or online movies. Indeed, on the one hand, the different variations in facial micro/macro expressions [100], which generate fast, facial dynamics and the different processes such as ageing, which is an extremely slow, dynamic problem since the face evolves over large periods of time [18], have all an impact on AFR techniques. On the other hand, face acquisition in videos intrinsically creates facial dynamics due to camera motion, change of point of view, as well as head's movements or pose variations. Such situations require AFR engines perform in real time [84], apply image/frames pre-processing such as face alignment [101], cope with intra-class variations/inter-class similarities [102] and are able to process single/multiple camera views [41] or synthesize a 3D face model from a single camera [103], leading to the wider study of the computational face.

Author details

Joanna Isabelle Olszewska

Address all correspondence to: joanna.olszewska@ieee.org

School of Computing and Technology, University of Gloucestershire, Cheltenham, UK

References

[1] Sirovich L., Kirby M. Low-dimensional procedure for the characterization of human faces. *Journal of the Optical Society of America A - Optics, Image Science and Vision.* 1987. 4(3):519–524.

[2] Zhao W., Chellappa R., Rosenfeld A., Phillips P.J. Face recognition: A literature survey. *ACM Computing Surveys.* 2003. 35(4):399–458.

[3] Kisku D. R., Gupta P., Sing J. K., editors. *Advances in Biometrics for Secure Human Authentication and Recognition*. CRC Press, Taylor and Francis. 2013. 450 p.

[4] Face Detection & Recognition Online Resources. Maintained by Dr. R. Frischholz [Internet]. 2016. Available from: https://facedetection.com/ [Accessed: 2016-07-07]

[5] Face Recognition Online Resources. Information Pool for the Face Recognition Community. Maintained by Dr. M. Grgic [Internet]. 2016. Available from: http://www.face-rec.org/ [Accessed: 2016-07-07]

[6] Chellappa R., Wilson C.L., Sirohey S. Human and machine recognition of faces: A survey. *Proceedings of the IEEE.* 1995. 83(5):705–740.

[7] Iosifidis, A., Gabbouj, M. Scaling-up class-specific kernel discriminant analysis for large-scale face verification. *IEEE Transactions on Information Forensics and Security*. 2016.11(11):2453–2465

[8] Almudhahka N., Nixon M., Hare J. Human face identification via comparative soft biometrics. In: *Proceedings of the IEEE International Conference on Identity, Security and Behavior Analysis (ISBA).*Sendai, JP, 29 Feb–02 Mar 2016. pp. 1–6.

[9] Berg T.I., Berg A.C., Edwards J., Forsyth D.A. Who's in the Picture?. In: *Proceedings of the Neural Information Processing Systems Conference (NIPS).* Springer. 2004. pp. 137–144.

[10] Torres L. Is there any hope for face recognition? In: *Proceedings of the IEEE International Workshop on Image Analysis for Multimedia Interactive Services (WIAMIS)*. 2004.

[11] Murphy-Chutorian E., Trivedi M.M. Head pose estimation in computer vision: A survey. *IEEE Transactions on Pattern Analysis and Machine Intelligence*. 2009. 31(4):607–626.

[12] Zhang X., Gao, Y. Face recognition across pose: A review. *Pattern Recognition*. 2009. 42(11):2876–2896.

[13] Nash S., Rhodes M., Olszewska J. I. iFR: Interactively-pose-corrected face recognition. In: *Proceedings of the INSTICC International Conference on Bio-Inspired Systems and Signal Processing (BIOSIGNALS).* 2016. pp. 106–112.

[14] Du S., Ward R. Face recognition under pose variations. *Journal of the Franklin Institute.* 2006. 343(6):596–613.

[15] Singh R., Vatsa M., Noore A. Recognizing face images with disguise variations. In: Delac K., Grgic M., Bartlett M. S.; editors. *Recent Advances in Face Recognition*. Vienna: InTech; 2008. pp. 149–160.

[16] Prikler F. Evaluation of emotional state of a person based on facial expression. In: *Proceedings of the IEEE International Conference on Perspective Technologies and Methods in MEMS Design (MEMSTECH).* 2016. pp. 161–163.

[17] Shreve M., Godavarthy S., Goldgof D., Sarkar, S. Macro- and micro-expression spotting in long videos using spatio-temporal strain. In: *Proceedings of the IEEE International Conference on Automatic Face and Gesture Recognition Workshops* (AFGR). 2011. pp. 51–56.

[18] Liu L., Xiong C., Zhang H., Niu Z., Wang M., Yan S. Deep aging face verification with large gaps. *IEEE Transactions on Multimedia*. 2016. 18 (1):64–75.

[19] Iqbal M.T.B., Ryu B., Song G., Chae O. Positional Ternary Pattern (PTP): An edge based image descriptor for human age recognition. In: *Proceedings of the IEEE International Conference on Consumer Electronics (ICCE).* 2016. pp. 289–292.

[20] Julian P., Dehais C., Lauze F., Charvillat V., Bartoli A., Choukroum A. Automatic hair detection in the wild. In: *Proceedings of the IEEE International Conference on Pattern Recognition (ICPR).* 2010. pp. 4617–4620.

[21] Wood R., Olszewska J. I. Lighting-variable AdaBoost based-on system for robust face detection. In: *Proceedings of the INSTICC International Conference on Bio-Inspired Systems and Signal Processing (BIOSIGNALS).* 2012. pp. 494–497.

[22] Shan S., Gao W., Cao B., Zhao D. Illumination normalization for robust face recognition against varying lighting conditions. In: *Proceedings of the IEEE International Conference on Automatic Face and Gesture Recognition* (AFGR). 2003. pp. 157–164.

[23] Abaza A., Harrison M.A., Bourlai T., Ross A. Design and evaluation of photometric image quality measures for effective face recognition. *IET Biometrics.* 2014. 3(4):314–324.

[24] ISO/IEC 19794-5:2011. The Face Image Format Standards. In: Information Technology —Biometric data interchange formats: Part 5: Face image data. 2nd Ed. 2011.

[25] Prince S.J.D., Elder J., Hou Y., Sizinstev M., Olevskiy E. Towards face recognition at a distance. In: *Proceedings of the IET Conference on Crime and Security.* 2006. pp. 570–575.

[26] Kautkar S.N., Atkinson G.A., Smith M.L. Face recognition in 2D and 2.5 D using ridgelets and photometric stereo. *Pattern Recognition.* 2012. 45(9):3317–3327.

[27] Mudunuri S.P., Biswas S. Low resolution face recognition across variations in pose and illumination. *IEEE Transactions on Pattern Analysis and Machine Intelligence.* 2016. 38(5): 1034–1040.

[28] Zou W.W.W., Yuen P.C. Very low resolution face recognition problem. *IEEE Transaction on Image Processing*. 2012. 21(1):327–340.

[29] Huang H., He H. Super-resolution method for face recognition using non-linear mappings on coherent features. *IEEE Transaction on Neural Networks*. 2011. 22(1):121–130.

[30] Li H., Lam K.M. Guided iterative back-projection scheme for single image super-resolution. In: *Proceedings of the IEEE Global High Tech Congress on Electronics (GHTCE).* 2013. pp. 175–180.

[31] Gross R. Face databases. In: Li S.Z., Jain A.K., editors. *Handbook of Face Recognition.* Springer-Verlag. 2005. pp. 301–327.

[32] Senior A.W, Pankanti S. Privacy protection and face recognition. In: Li S.Z., Jain A.K., editors. *Handbook of Face Recognition*. 2nd ed. Springer. 2011. pp. II.5–II.21.

[33] ORL. Face Database. AT&T Laboratories Cambridge [Internet]. 1994. Available from: www.cl.cam.ac.uk/research/dtg/attarchive/facedatabase.html [Accessed: 2016-07-07]

[34] Caltech Faces. A Public Dataset for Face Recognition. CalTech University. USA [Internet]. 1999. Available from: http://www.vision.caltech.edu/html-files/archive.html [Accessed: 2016-07-07]

[35] Phillips P.J., Moon H., Rizvi S.A., Rauss P.J. The FERET evaluation methodology for face-recognition algorithms. *IEEE Transactions on Pattern Analysis and Machine Intelligence*. 2000. 22(10):1090–1104.

[36] Jesorsky O., Kirchberg K., Frischholz R. Face detection using the Hausdorff distance. In Bigun J., Smeraldi F., editors. *Audio and Video based Person Authentication*. LNCS Springer. 2001. pp. 90–95.

[37] Yale Face Database. Yale University. Connecticut, USA [Internet]. 2001. Available from: http://vision.ucsd.edu/yale_face_dataset_original/yalefaces.zip [Accessed: 2016-07-07]

[38] Caltech 10000 Web Faces. Human Faces Collected from Google Image Search. CalTech University. Pasadena, California, USA [Internet]. 2005. Available from: www.vision.caltech.edu/Image_Datasets/Caltect_10K_WebFaces [Accessed: 2016-07-07]

[39] Phillips P.J., Flynn P.J., Scruggs T., Bowyer K.W., Chang J., Hoffman K., Marques J., Min J., Worek W. Overview of the face recognition grand challenge. In: *Proceedings of the IEEE Conference on Computer Vision and Pattern Recognition (CVPR).* 2005. pp. I.947–I.954.

[40] Matas J., Hamouz M., Jonsson K., Kittler J., Li Y., Kotroupolous C., Tefas A., Pitas I., Tan T., Yan H., Smeraldi F., Bigun J., Capdevielle N., Gerstner W., Ben-Yacoub S., Abdul-

jaoued Y., Mayoraz E. Comparison of face verification results on the XM2VTS database. In: *Proceedings of the IEEE International Conference on Pattern Recognition (ICPR).* 2000. pp. 858–863.

[41] Grgic M., Delac K., Grgic S., Klimpak B. SCface - Surveillance cameras face database. *Multimedia Tools Applications.* 2011. 51:863–879.

[42] FDDB. A Benchmark for Face Detection in Unconstrained Settings. Jain V., Learned-Miller E. Technical Report. UM-CS-2010-009. University of Massachusetts, Amherst. USA [Internet]. 2010. Available from: http://vis-www.cs.umass.edu/fddb/ [Accessed: 2016-07-07]

[43] Learned-Miller E., Huang G.B., Roy-Chowdhury A., Li H., Hua G. Labeled Faces in the Wild: A Survey. In: Kawulok M., Emre Celebi M., Smolka B., editors. *Advances in Face Detection and Facial Image Analysis*. Springer. 2016. pp. 189–248.

[44] Li X., Pfister T., Huang X., Zhao G., Pietikainen M. A spontaneous micro-expression database: Inducement, collection and baseline. In: *Proceedings of the IEEE International Conference on Automatic Face and Gesture Recognition* (AFGR). 2013. pp. 1–6.

[45] Dhall A., Goecke R., Joshi J., Wagner M., Gedeon T. Emotion recognition in the wild challenge 2013. In: *Proceedings of the ACM International Conference on Multimodal Interaction (ICMI).* 2013. pp. 509–516.

[46] Panis G., Lanitis A., Tsapatsoulis N., Cootes T.F. Overview of research on facial ageing using the FG-NET ageing database. *IET Biometrics*. 2016. 5(2):37–46.

[47] Viola, P., Jones, M.J. Robust real-time face detection. *International Journal of Computer Vision*. 2004. 57(2):137–154.

[48] Ahonen T., Hadid A., Pietikainen M. Face description with local binary patterns: Application to face recognition. *IEEE Transactions on Pattern Analysis and Machine Intelligence*. 2006. 28(12):2037–2041.

[49] Jabid T., Kabir M. H., Chae O. Local Directional Pattern (LDP) for Face Recognition. In: *Proceedings of the IEEE International Conference on Consumer Electronics (ICCE)*. 2010. pp. 329–330.

[50] Gao Y., Leung M.K.H. Face recognition using line edge map. *IEEE Transactions on Pattern Analysis and Machine Intelligence*. 2002. 24(6):764–779.

[51] Olszewska J. I. Multi-scale, multi-feature vector flow active contours for automatic multiple-face detection. In: *Proceedings of the INSTICC International Conference on Bio-Inspired Systems and Signal Processing (BIOSIGNALS)*. 2013. pp. 429–435.

[52] Hu J., Lu J., Tan Y.P. Discriminative deep metric learning for face verification in the wild. In: *Proceedings of the IEEE Conference on Computer Vision and Pattern Recognition (CVPR).* 2014. pp. 1875–1882.

[53] Tome P., Fierrez J., Vera-Rodriguez R., Ramos D. Identification using face regions: Application and assessment in forensic scenarios. *Forensic Science International.* 2013. 233:75–83.

[54] Tanaka J.W., Farah M.J. Parts and wholes in face recognition. *Quarterly Journal of Experimental Psychology, Section A: Human Experimental Psychology.* 1993. 46(2):225–245.

[55] Guo J.M., Tseng S.H., Wong K.S. Accurate facial landmark extraction. *IEEE Signal Processing Letters*. 2016. 23(5):605–609.

[56] Mitchell T. *Machine Learning.* McGraw Hill. 1997.

[57] Kumar N., Berg A., Belhumeur P.N., Nayar S.K. Attribute and smile classifiers for face verification. In: *Proceedings of the IEEE International Conference on Computer Vision (ICCV)*. 2009. pp. 365–372.

[58] Gallego-Jutgla E., de Ipin K. L., Marti-Puig P., Sole- Casals J. Empirical mode decomposition-based face recognition system. In: *Proceedings of the International Conference on Bio-Inspired Systems and Signal Processing*. 2013. pp. 445–450.

[59] Brunelli R., Poggio T. Face recognition: Features versus Templates. *IEEE Transactions on Pattern Analysis and Machine Intelligence*. 1993. 15(10):1042–1052.

[60] Sun Y., Nasrollahi K., Sun Z., Tan T. Complementary cohort strategy for multimodal face pair matching. *IEEE Transactions on Information Forensics and Security*. 2016. 11(5): 937–950.

[61] Turk J., Pentland A. Face recognition using eigenfaces. In: *Proceedings of the IEEE Conference on Computer Vision and Pattern Recognition (CVPR)*. 1991. pp. 586–591.

[62] Ruiz-del-Solar J., Navarrete P. Eigenspace-based face recognition: A comparative study of different approaches. *IEEE Transactions on Systems, Man and Cybernetics, Part C*. 2005. 35(3):315–325.

[63] Belhumeur P.N., Hespanha J.P., Kriegman D.J. Eigenfaces vs. Fisherfaces: Recognition using class specific linear projection. *IEEE Transactions on Pattern Analysis and Machine Intelligence*. 1997. 19(7):711–720

[64] Cootes T.F., Edwards G.J., Taylor C.J. Active appearance model. *IEEE Transactions on Pattern Analysis and Machine Intelligence*. 2001. 23(6):681–685.

[65] Olszewska J. I., De Vleeschouwer C., Macq B. Multi-Feature Vector Flow for Active Contour Tracking. In: *Proceedings of the IEEE International Conference on Acoustics, Speech and Signal Processing (ICASSP)*. 2008. pp. 721–724.

[66] Uiboupin T., Rasti P., Anbarjafari G., Demirel H. Facial image super resolution using sparse representation for improving face recognition in surveillance monitoring. In: *Proceedings of the IEEE Signal Processing and Communication Application Conference (SIU).* 2016. pp. 437–440.

[67] Aurora Computer Services. Provider of Biometric Solutions [Internet]. 2016. Available from: http://auroracs.co.uk/ [Accessed: 2016-07-07]

[68] Balasubramanian Y., Sivasankaran K., Krishraj S.P. Forensic video solution using facial feature-based synoptic Video Footage Record. *IET Computer Vision*. 2016. 10(4):315–320.

[69] Jain A.K., Klare B., Park U. Face matching and retrieval in Forensics applications. *IEEE MultiMedia*. 2012. 19(1):20–28.

[70] Jain A.K., Klare B., Park U. Face recognition: Some challenges. In: *Proceedings of the IEEE Conference on Automatic Face and Gesture Recognition* (AFGR). 2011. pp. 726–733.

[71] Baltrusaitis T., Robinson P., Morency L.P. OpenFace: An open source facial behavior analysis toolkit. In: *Proceedings of the IEEE Winter Conference on Applications of Computer Vision (WACV).* 2016. pp. 1–10.

[72] Owayjan M., Kashour A., Al Haddad N., Fadel M., Al Souki G. The design and development of a lie detection system using facial micro-expressions. In: *Proceedings of the IEEE International Conference on Advances in Computational Tools for Engineering Applications (ACTEA)*. 2012. pp. 33–38.

[73] Jang M., Gan Z.H., Gao W.Y. Combining particle filter and active shape models for lip tracking. In: *Proceedings of the IEEE World Congress on Intelligent Control and Automation (WCICA).* 2006. pp. 9897–9901.

[74] BioID Web Service (BWS). Biometrics as a Service [Internet]. 2016. Available from: https://playground.bioid.com/ [Accessed: 2016-07-07]

[75] Mastercard App Using Selfies as a Payment Method [Internet]. 2016. Available from: http://newsroom.mastercard.com/videos/mastercard-identity-check-facial-recognition-biometrics/ [Accessed: 2016-07-07]

[76] Anthropics Technology. Provider of Face Control Solutions [Internet]. 2016. Available from: http://www.anthropics.com [Accessed: 2016-07-07]

[77] Taigman Y., Yang M., Ranzato M.A., Wolf L. DeepFace: Closing the gap to human-level performance in face verification. In: *Proceedings of the IEEE Conference on Computer Vision and Pattern Recognition (CVPR).* 2014. pp. 1701–1708.

[78] Schroff F., Kalenichenko D., Philbin J. FaceNet: A unified embedding for face recognition and clustering. In: *Proceedings of the IEEE Conference on Computer Vision and Pattern Recognition (CVPR).* 2015. pp. 815–823.

[79] Farfade S.S., Saberian M.J., Li L.J. Multi-view face detection using deep convolutional neural networks. In: *Proceedings of the ACM International Conference on Multimedia Retrieval (ICMR).* 2015. pp. 643–650.

[80] Sarkar S., Patel V. M., Chellappa R. Deep feature-based face detection on mobile devices. In: *Proceedings of the IEEE International Conference on Identity, Security and Behavior Analysis (ISBA).* 2016. pp. 1–8.

[81] Temelkov I. Why Facial Recognition will Change Marketing Forever [Internet]. 2016. Available from: http://curatti.com/facial-recognition/ [Accessed: 2016-07-07]

[82] Snapchat. Image Messaging & Multimedia Mobile Application [Internet]. 2016. Available from: https://www.snapchat.com [Accessed: 2016-07-07]

[83] Everingham M., Sivic J., Zisserman A. "Hello! My name is … Buffy - Automatic naming of characters in TV video". In: *Proceedings of the British Machine Vision Conference (BMVC).* 2006. pp. 898–908.

[84] Tasli H.E., den Uyl T.M., Boujut H., Zaharia T. Real-time facial character animation. In: *Proceedings of the IEEE International Conference on Automatic Face and Gesture Recognition* (AFGR). 2015.

[85] Han M.J., Lin C.H., Song K.T. Robotic emotional expression generation based on mood transition and personality model. *IEEE Transactions on Cybernetics.* 2013. 43(4):1290–1303.

[86] Double Negative Visual Effects. Provider of Visual Effects for Films [Internet]. 2016. Available from: http://www.dneg.com/ [Accessed: 2016-07-07]

[87] Disney Research. Provider of Advanced Visual Technologies [Internet]. 2016. Available from: https://www.disneyresearch.com/ [Accessed: 2016-07-07]

[88] Parkhi O.M., Vedaldi A., Zisserman A. Deep Face recognition. In: *Proceedings of the British Machine Vision Conference (BMVC).* 2015. pp. 41.1–41.12.

[89] Hu G., Yang Y., Yi D., Kittler J., Christmas W., Li S.Z., Hospedales T. When face recognition meets with deep learning: An evaluation of convolutional networks for face recognition. In: *Proceedings of the IEEE International Conference on Computer Vision Workshops (ICCV).* 2015.

[90] Sun Y., Wang X., Tang X. Deep learning face representation from predicting 10,000 classes. In: *Proceedings of the IEEE Conference on Computer Vision and Pattern Recognition (CVPR).* 2014. pp. 1891–1898.

[91] Sinha P., Balas B., Ostrovsky Y., Russell R. Face recognition by humans: 19 results all computer vision researchers should know about. *Proceedings of the IEEE*. 2006. 94(11): 1948–1962.

[92] Fung J., Mann S. Using graphics devices in reverse: GPU-based image processing and compute revision. In: *Proceedings of the IEEE International Conference on Multimedia & Expo (ICME)*. 2008. pp. 9–12.

[93] Owens J. D., Luebke D., Govindaraju N., Harris M., Kruger J., Lefohn A. E., Purcell T. J. A survey of general-purpose computation on graphics hardware. *Computer Graphics Forum*. 2007. 26(1): 80–113.

[94] Sagonas C., Panagakis Y., Zafeiriou S., Pantic M. Robust statistical face frontalization. In: *Proceedings of the IEEE International Conference on Computer Vision (ICCV).* 2015. pp. 3871–3879.

[95] Simonyan K., Parkhi O.M., Vedaldi A., Zisserman A. Fisher vector faces in the wild. In: *Proceedings of the British Machine Vision Conference (BMVC).* 2013. pp. 8.1–8.12.

[96] Wolf L., Hassner T., Taigman Y. Effective unconstrained face recognition by combining multiple descriptors and learned background statistics. *IEEE Transactions on Pattern Analysis and Machine Intelligence*. 2011. 33(10):1978–1990.

[97] Rouge C., Shaikh S., Olszewska J. I. HD: Efficient hand detection and tracking. In: *Proceedings of the IEEE International Conference on Computer Science and Information Science Workshop (FedCSIS)*. 2016.

[98] Prince S. J. D., Aghajanian J. Gender classification in uncontrolled settings using additive logistic models. In: *Proceedings of the IEEE International Conference on Image Processing (ICIP).* 2009. pp. 2557–2560.

[99] Zhu X., Lei Z., Yan J., Yi D., Li S.Z. High-fidelity pose and expression normalization for face recognition in the wild. In: *Proceedings of the IEEE Conference on Computer Vision and Pattern Recognition (CVPR).* 2015. pp. 787–796.

[100] Khorsheed J.A., Yurtkan K. Analysis of Local Binary Patterns for face recognition under varying facial expressions. In: *Proceedings of the IEEE Signal Processing and Communication Application Conference (SIU).* 2016. pp. 2085–2088.

[101] Travieso-Gonzalez C.M., del Pozo-Banos M., Alonso, J.B. Facial identification based on transform domains for images and videos. In: Riaz Z., editor. *Biometric Systems, Design and Applications*. InTech. 2011. pp. 293–316.

[102] Du M., Chellappa R. Video-based face recognition using the intra/extra-personal difference dictionary. In: *Proceedings of the British Machine Vision Conference (BMVC).* 2014.

[103] Hu X., Wang Y., Zhu F., Pan C. Learning-based fully 3D face reconstruction from a single image. In: *Proceedings of the IEEE International Conference on Acoustics, Speech and Signal Processing (ICASSP).* 2016. pp. 1651–1655.

Chapter 5

Histogram-Based Texture Characterization and Classification of Brain Tissues in Non-Contrast CT Images of Stroke Patients

Kenneth K. Agwu and Christopher C. Ohagwu

Additional information is available at the end of the chapter

http://dx.doi.org/10.5772/65349

Abstract

This chapter describes histogram-based texture characterization and classification of brain tissue in CT images of stroke patients using a case study. It explored texture analysis in medical imaging. In the case study, two radiologists independently inspected non-contrast CT images of 164 stroke to identify and categorize brain tissue into normal, ischaemic and haemorrhagic strokes. Four regions of interest (ROIs) in each CT slice with lesion were selected for analysis; two each represented the lesion and normal tissue. Histogram texture parameters were calculated for them. Raw data analysis identified parameters that discriminated between normal brain tissue, ischaemic and haemorrhagic stroke lesions. The artificial neural network (ANN) and k-nearest neighbour (k-NN) algorithms were used to classify the ROIs into normal tissue, ischaemic and haemorrhagic lesions using the radiologists' categorization as the gold standard, and further analysed using the ROC curve. Three parameters namely mean, 90 and 99 percentiles discriminated between normal brain tissue, ischaemic and haemorrhagic stroke lesions. With ANN and k-NN, the weighted sensitivity and specificity were above 0.9 while the false positive and false negative rates were negligible. The characterization and classification of brain tissue using histogram parameters were satisfactory and may be suitable for automated diagnosis of stroke.

Keywords: histogram texture parameters, texture analysis, characterization, classification, brain tissues, stroke, computed tomography

1. Introduction

Medical imaging is a rapidly developing branch of modern medicine. It has in the past few decades evolved into a highly sophisticated diagnostic tool. It has improved the study of human internal anatomy and to an extent physiology and detection of pathologies which were previously impossible. At this stage of its development, detection of lesions and their interpretation is becoming an automated computer-aided process. It can safely be said now that machine vision has become an emerging part of radiology and imaging in medicine. This is as a result of advances in medical imaging technology and computer science [1] which have greatly enhanced the interpretation of medical images and contributed to early diagnosis. The bases for computer-aided diagnosis (CAD) in radiology are medical image processing and artificial intelligence.

Stroke accounts for a significant proportion of neurological disorders seen in Nigerian hospitals [2]. It carries a high morbidity and mortality statistics in industrialized countries [3–6], and in Africa, it is reported to be the leading neurological cause of death [7]. The World Health Organization (WHO) defined stroke a rapidly developing clinical syndrome of focal or global disturbance of cerebral function presumably of vascular origin, lasting longer than 24 hours unless interrupted by surgery or death [8]. A stroke occurs when the blood supply to the brain is disturbed which results in brain cells being starved of oxygen and consequently, some cells die while others are left damaged. Brain cells being permanent in nature achieve only very limited recovery, and thus, the patient may be left with a permanent disability. Clinical diagnosis of stroke and its subtyping is sometimes inaccurate [9–12]. Neuroimaging is, therefore, essential for accurate diagnosis. Stroke remains one of the most important clinical diagnoses for which patients are referred to the radiology department for emergency imaging because a timely and accurate diagnosis would help in the management of the patients [13]. Previous studies have highlighted the time-critical nature of ischaemic stroke diagnosis. Ischaemic stroke has a narrow therapeutic window in the first few hours following stroke ictus and a dramatic rise in haemorrhage complications thereafter [14–20].

Non-contrast head computed tomography (NCCT) has been suggested as the mainstay for early stroke diagnosis because computed tomography (CT) scanners are more widely available in the communities and may be accessed much more easily [13]. Computed tomography examinations are not only cheaper than magnetic resonance imaging (MRI) but also faster to perform. Thus, taking the time-critical nature of early stroke diagnosis into consideration, NCCT is the preferred first-line imaging tool. Computed tomography and other neuroimaging procedures will, however, not benefit the patient until the images have been accurately interpreted. For visual analysis and interpretation of stroke CT images, the radiologist seeks to identify affected areas of the brain by examining the dissimilarity between the left and right cerebral hemispheres. The challenges associated with the visual interpretation of stroke CT images are dearth of neuroradiologists [21] and the human errors of interpretation and diagnosis. Errors in visual interpretation result from poor technique, failures of perception, lack of knowledge and misjudgements [22]. Visual interpretation can be improved upon by texture analysis which will make it possible for automated computer-aided approach to be

http://dx.doi.org/10.5772/65349

used as a second opinion for clinicians, especially in equivocal cases. Automatic method of stroke detection follows the same pattern as visual analysis and interpretation used by radiologists [23].

Computer-aided diagnosis (CAD) in medical imaging is an application of artificial intelligence in medicine. Artificial intelligence (IA) simulates the human brain or recreates it electronically. It is defined as the study and design of intelligent agents [24], where an intelligent agent is a system that perceives its environment and takes actions that maximize its chances of success [24–26]. The simplest intelligent agents are programs written to solve specific problems. More complicated intelligent agents include human beings and organization of human beings such as a firm or a team. Artificial intelligence is based on the central characteristic of human beings: intelligence—the sapience of ***Homo sapiens***. This can be so precisely described that it can be simulated by a machine.

One very important stage in medical image processing leading to CAD is image texture analysis. Texture analysis of a medical image is the measurement of the quantitative parameters that constitute the image of a supposed lesion or normal tissue. This has the advantages of helping clinicians make accurate diagnosis and monitor disease processes under treatment. The analysis of texture parameters is a useful way of increasing the information obtainable from medical images [27].

2. The concept of texture and analysis of texture

Texture is a very difficult term to give a precise definition. This is because there is no unified definition of texture and every definition that has been used has rather aimed at relating it to the area of its application. The non-existence of a universally agreed-upon definition of texture is an acknowledged fact [28, 29]. In general, texture can be defined as a descriptor that provides measures of properties such as smoothness, coarseness and regularity [28]. For medical images, image texture is defined as the appearance, structure and arrangement of the parts of an object within the image [27]. The concept of texture as a quantitative measure is applied only to digital images which are made up of numerous rectangular picture elements (pixels) as illustrated in **Figure 1**.

In consideration of this technicality, the texture concept in a digital image is regarded as the distribution of grey-level values among the pixels of a given region of interest in the image [27]. This definition is in agreement with a recent one which referred to texture as the spatial variation of pixel intensities in an image [29]. In order to understand texture better, it is important to draw an analogy from the way the human visual system perceives scenes. The human eye perceives scenes as sets of objects that are related to each other over various surfaces despite varying ambient illumination [30]. Texture has components called texels, which are notional uniform micro-objects placed in an appropriate way to form any particular texture. The placing may be random, regular, directional and so on, and there may be a degree of overlap in some cases [30]. From the foregoing, texture in very simple physical concept is

composed of the randomness, periodicity, directionality and orientation of the composite elements making up an object's structure.

Texture analysis is an aspect of imaging science which analyses pixel intensity variations or its spatial distribution on a pixel-by-pixel scale to unravel patterns which may not be perceptible to the human visual system. The technique evaluates the location and signal intensity of the image represented by the pixel and contrast index for digital images [27]. Texture features represent the mathematical parameters obtained from the distribution of pixels which characterize the texture type and hence the structural components of an object [27]. Texture analysis is employed in image classification, segmentation and synthesis. It also plays a very vital role in computer-aided detection or diagnosis or more broadly machine vision.

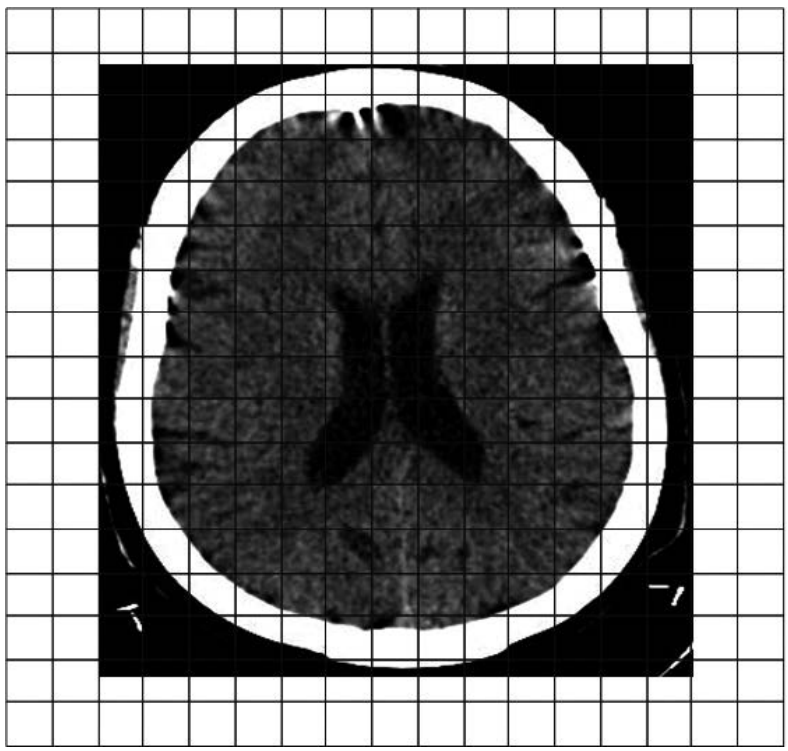

Figure 1. An illustration of the pixel concept of digital medical images using a cranial CT.

3. Methods of texture analysis

There are four major issues in texture analysis, namely feature extraction, texture discrimination, texture classification and shapes from texture [31]. The purpose of feature extraction is to compute a characteristic of a digital image able to numerically describe its texture properties, while texture discrimination partitions a textured image into regions, each corresponding to

http://dx.doi.org/10.5772/65349

a perceptually homogeneous texture (leads to image segmentation). In texture classification, the goal is to determine to which of a finite number of physically defined classes, such as normal or abnormal tissue, a homogeneous texture region belongs, while shape from texture reconstructs the three-dimensional surface geometry from texture information.

The first stage in texture analysis is the extraction of texture parameters, and the results obtained during this process are used for the remaining stages in texture analysis. The approaches to texture analysis are categorized into structural, statistical, model-based and transform methods [31]. These approaches are herewith described briefly.

3.1. Structural methods

In this method, texture is represented by well-defined primitives. In other words, a square object is represented in terms of the straight lines or the primitives that form its border [27]. To describe texture using the structural approach, one must first define the primitives (micro-texture) and then the placement rules. Primitives are the parts from which texture is composed. Note well that primitives may be tonal, that is, grey levels. Tonal primitives are regions of an image with tonal properties [32]. The advantage of structural methods is that they provide a good symbolic description of the image [31], but the disadvantage is that it is not a very powerful way describing texture.

3.2. Statistical methods

The statistical approach to texture analysis uses grey-level distribution within an image to describe texture. This approach provides better discrimination between classes than structural or transforms methods. It is the most widely used method in medical applications. Statistical methods can be used to analyse the spatial distribution of pixel grey values in an image. This is done by computing local features at each point in the image and then deriving a set of statistics from the distributions of the local features [33]. Statistical methods are classified as first-order, second-order and higher-order statistics based on the number of pixels that define the local feature. In the first-order statistics, only one pixel is involved; in second-order statistics, a pair of pixels; and higher-order statistics, three or more pixels [33]. There are differences between the different statistical methods. In the first-order statistics, properties such as average and variance of individual pixel values are estimated, but the spatial interaction between the image pixels is not taken into consideration. More specifically, first-order statistics measure the frequency of a particular grey level at a random image position without taking into account the correlations or co-occurrences between the pixels. Thus, information on texture is derived from the histogram of image pixel grey values [29]. The second-order and higher-order statistics estimate properties of two or more pixel values occurring at specific locations relative to each other, and thus, pixel-pixel interaction is a feature of these two methods [33]. Specifically, information on the texture of an image based on second-order statistical texture analysis is based on the probability of finding a pair pixels with the same grey level at random distances and orientations over an entire image, while higher-order statistics means the number of variables studied is increased [29].

3.2.1. The co-occurrence matrix (COM)

The co-occurrence matrix is a second-order histogram that analyses the grey-level distribution of pairs of pixels [27]. In grey-level co-occurrence matrix method, the probability of finding a pixel with a defined grey level (i) at a defined distance (d) and a defined angle (α) from another pixel with defined grey level (j) is calculated. So, the co-occurrences of pixel pairs are calculated in vertical, horizontal and two diagonal directions, as well as distances up to five pixels. An essential feature of this arrangement is that each pixel has eight nearest neighbours connected to it except when the pixel is located at the periphery. A very simple illustration of grey-level co-occurrence matrix as relative positions of pixels of the same grey-level intensities is shown in **Figure 2**. In this illustration, the reference pixel (X) is of the same grey-level value with the pixels X_1 in horizontal direction for inter-pixel distance of 1, X_2 in vertical direction for inter-pixel distance of 2, X_3 in 45° diagonal direction for inter-pixel distance of 3 and X_4 in 135° diagonal direction for inter-pixel distance of 3.

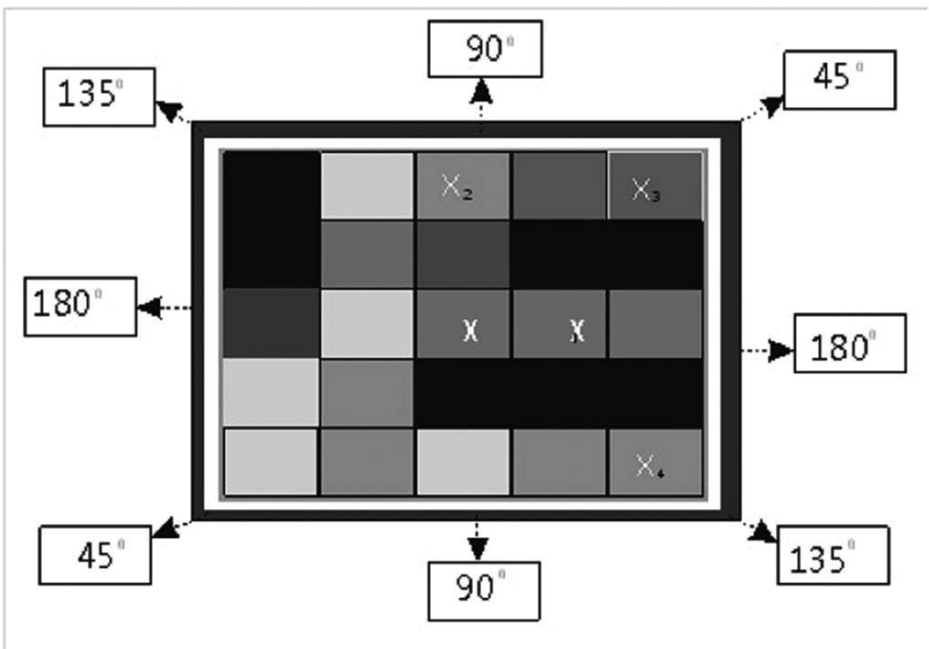

Figure 2. An illustration of the grey-level co-occurrence matrix concept of texture computation.

A co-occurrence matrix is produced in each direction (α), for each inter-pixel distance (d), with the matrix dimension being equal to the number of intensity levels. It, therefore, means that the process becomes computationally intense and the number of grey levels in an image would undergo a rescaling and re-binning procedure to reduce the range of pixel values contained within an image [34]. The implication of rescaling and re-binning of the grey levels in the image is loss of texture information.

http://dx.doi.org/10.5772/65349

The co-occurrence matrix parameters include the angular second moment, contrast, correlation, sum of squares, inverse difference moment, sum average, sum variance, sum entropy, entropy, difference variance and difference entropy. The construction of the co-occurrence matrix and mathematical derivation of the formulae for calculating the parameters are both tedious processes and further reading is necessary for better understanding [28, 31].

3.2.2. The run-length matrix (RLM)

The grey-level run-length matrix is a higher-order statistical method of texture feature extraction. The run-length matrix aims to calculate the number of consecutive pixels in a given direction that has the same grey-level intensity. It is a number of pixels in a particular direction with the same grey-level intensity value [29]. A coarse texture will, therefore, be dominated by relatively long runs, whereas a fine texture will be populated by much shorter runs [29]. The parameters derivable from the run-length matrix are usually computed in four different directions: horizontal, vertical and two diagonals. The grey-level run-length matrix is illustrated in **Figure 3** which shows a run-length of 4 pixels in a 45° diagonal direction [34].

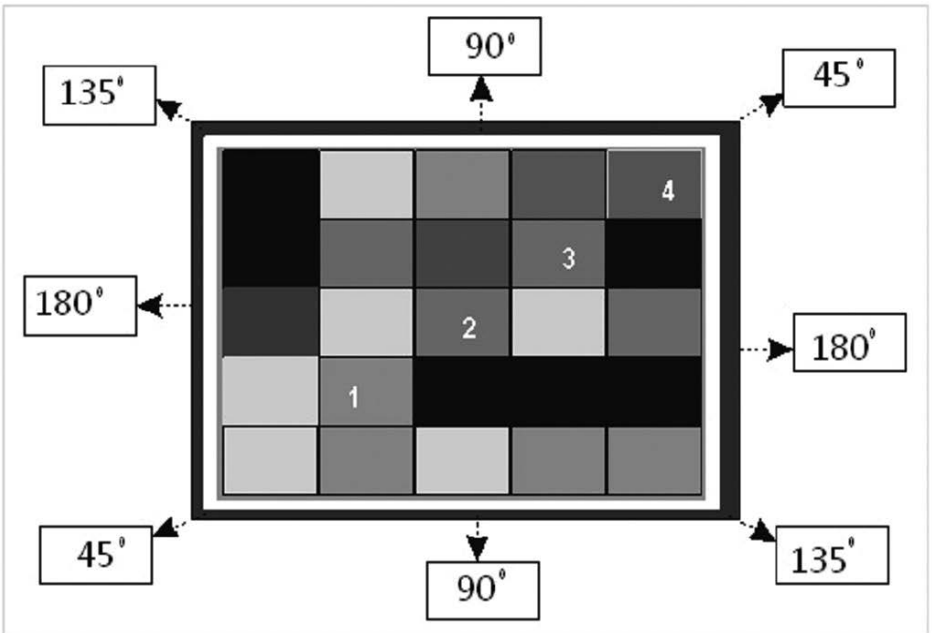

Figure 3. An illustration of the grey-level run-length matrix concept of texture computation.

The run-length emphasis describes a number of consecutive pixels with the same grey-level value. It could be suitably termed long- or short-run emphasis depending on the number of consecutive pixels in the chosen direction with the same grey-level value [35]. The run-length and grey-level non-uniformity describe the disorderliness in pixel and pixel grey-level runs. The fraction of the image in runs simply refers to run percentages. That is, the ratio of the total

number of runs in the image to the total number of pixels in the image expressed as a percentage [35].

The run-length method of texture analysis was first introduced by Galloway [36], but it has not gained the desired general acceptance as an efficient way of calculating texture [35]. It is therefore not popular among researchers working to develop diagnostic tools for medical applications.

The calculation of the run-length matrix parameters using MaZda® can be illustrated as follows. If $p(i, j)$ is the frequency of the run of a length j with a grey-level intensity i, N_g is the number of grey-level intensities and N_r is the number of runs. Then, the parameters for the run-length matrix $p(i, j)$ can be calculated using the following equations:

$$Short\ Run\ Emphasis = \left(\sum_{i=1}^{Ng} \sum_{j=1}^{Nr} \frac{p(i.j)}{j^2} \right) \Big/ C \tag{1}$$

$$Long\ Run\ Emphasis = \left(\sum_{i=1}^{Ng} \sum_{j=1}^{Nr} j^2\, p(i,j) \right) \Big/ C \tag{2}$$

$$Grey\ Level\ Nonuniformity = \left(\sum_{i=1}^{Ng} \sum_{j=1}^{Nr} p(i,j)^2 \right) \Big/ C \tag{3}$$

$$Run\ Length\ Nonuniformity = \left(\sum_{j=1}^{Nr} \sum_{i=1}^{Ng} p(i,j)^2 \right) \Big/ C \tag{4}$$

$$Fraction\ of\ Image\ in\ Runs = \sum_{i=1}^{Ng} \sum_{j=1}^{Nr} p(i,j) \Big/ \sum_{i=1}^{Ng} \sum_{j=1}^{Nr} jp(i,j) \tag{5}$$

The coefficient C in Eqs. (1)–(4) above is defined as:

$$C = \sum_{i=1}^{Ng} \sum_{j=1}^{Nr} p(i,j) \tag{6}$$

3.2.3. The absolute gradient (Gr)

The gradient of an image measures the spatial variation in grey-level values across the image [27]. This method evaluates the relationship of variations in grey-level intensity values across neighbouring pixels as shown in **Figure 4** according to the illustration by Waugh [34]. A high gradient is produced when there is abrupt change, from extreme pixel grey-level intensity

http://dx.doi.org/10.5772/65349

value to another extreme grey-level intensity value. Conversely, a low gradient is produced in gradually changing pixel grey-level values. The five parameters derived from absolute gradient are the gradient mean, gradient variance, gradient skewness, gradient kurtosis and gradient non-zeros. Conventionally, only the magnitude of the gradient is taken into consideration [27]. The direction of variation, whether it is positive or negative, is irrelevant and hence the term "absolute gradient".

Figure 4. An illustration of the gradient concept of texture computation.

The gradient non-zero is the number of pixels in an image with a grey-level value greater than zero, and gradient variance is the deviation of absolute pixel grey-level value from the mean, while gradient mean is the average variation in pixel grey-level value across the image [31]. The absolute gradient as a method of texture analysis find application in accentuating the boundaries of an image [27] and therefore is useful in edge enhancement.

3.2.4. The histogram

This is a first-order statistical analysis and uses pixel occurrence probability to calculate texture. To illustrate the histogram approach to texture analysis, assume in an image the grey levels are in the range $0 \leq i \leq Ng - 1$, where Ng is the total number of particular grey levels. If N(i) is the total number of pixels with intensity i and M is the total number of pixels in the image, then the pixel occurrence probability P(i) is given by [29]

$$P(i) = N(i) \div M \tag{7}$$

The probability of occurrence of a pixel of particular grey level (intensity) is called the histogram. It does not consider the spatial relationships, and correlations, between pixels [29]. The main advantage of the histogram is its simplicity by the use of standard descriptors such as mean and variance to characterize texture data. The features derivable from the histogram are mean, variance, skewness, kurtosis, percentile 01, percentile 10, percentile 50, percentile 90 and percentile 99. Some of the features from the histogram used to characterize texture are represented by the equations below:

$$Mean(\mu) = \sum_{i=0}^{N-1} ip(i) \tag{8}$$

$$Variance\left(\sigma^2\right) = \sum_{i=0}^{N-1} (i-\mu)^2 \, p(i) \tag{9}$$

$$Skewness\left(\mu_3\right) = \sigma^{-3} \sum_{i=0}^{N-1} (i-\mu)^3 \, p(i) \tag{10}$$

$$Kurtosis(\mu_4) = \sigma^{-4} \sum_{i=0}^{N-1} (i-\mu)^4 \, p(i) - 3 \tag{11}$$

3.3. The model-based methods

In model-based texture analysis, there is an attempt to fit an image texture to a computational (mathematical) model. For MaZda® texture analysis software, the model used is referred to as the auto-regressive model (ARM). In this model, an assumption that knowing the grey-level intensity value of one pixel, the grey-level intensity values of other neighbouring pixels can be deduced holds. In a more formal way, the ARM assumes a local interaction between image pixels in that pixel grey-level value is a weighted sum of the grey-level values of the neighbouring pixels [27]. The main disadvantage of the model-based approach to texture analysis is the complexity involved in the computations to estimate the model parameters. Other models of texture aside ARM are Markov random field (MRF) and fractal models [31].

3.4. The transform methods

In the transform methods, the texture of an image can be analysed in the frequency or scale space. These methods can employ the Fourier [37], Gabor [38] or wavelet transform [39]. However, the wavelet transform is the most popular because it can easily be adjusted to suit the problem at hand as desired by the user [27]. Wavelet is a technique that analyses the frequency content of an image with different scales of that image. The wavelet analysis yields a set of numbers called the wavelet coefficients which correspond to different scales and frequency directions [27]. Each pixel of an image analysed by wavelet transform is associated with a set of wavelet coefficients which describe the frequency content of the image at that point over a set of scales.

4. Texture analysis of medical images

Texture analysis of medical images remained without much clinical interest until 1998 when it took a giant leap. This was when MaZda®, a computer program for calculating texture parameters (features) in digitized images, was developed. The software has been under development since 1998, to satisfy the needs of the participant of COST B11 European Project "Quantitative Analysis of Magnetic Resonance Image Texture" and the subsequent COST B21 "Physiological Modelling of Magnetic Resonance Image Formation" [31]. MaZda® is a very

http://dx.doi.org/10.5772/65349

versatile software package that is capable of 2D and 3D image texture analysis. It can be used for quantitative analysis of image texture, computation of texture features, feature selection and extraction. The software also has algorithms for data classification, data visualization and image segmentation tools [40]. The software was originally developed in 1996 at the Institute of Electronics, Technical University of Lodz (TUL), Poland, for texture analysis of mammograms [41]. The software has been further developed and made more versatile to be used in the analysis of other textured image. It has been found to be efficient and reliable for quantitative image analysis even in more accurate and objective medical diagnosis. There has also been a non-medical application in the food industry to assess food product quality [40]. Other computer softwares that are used for texture analysis of digital images are MATLAB® and Scilab® [42, 43]. Scilab® is available to users free, while MATLAB® is commercially available.

The medical importance of texture analysis cannot be over-emphasized. Analysis of medical image texture helps to increase the information obtained from medical images [27], which may improve diagnosis. It is an emerging aspect of medical imaging and finds applications in segmentation of specific anatomical structures and detection of lesions. The detection of lesions implies differentiating between unhealthy and healthy tissues in the different organs of the body. The differentiation between unhealthy and healthy tissues implies that texture parameters obtained from medical images form the basis for computer-aided diagnosis. Just recently, it was demonstrated that texture analysis can be used in patients undergoing neoadjuvant chemotherapy treatment of breast cancer to indicate whether the patient will respond well or not. The results of that study appeared to correlate well with the final pathological outcome [34].

5. Role of texture analysis in computer-aided diagnosis

Many researchers have shown interest in texture analysis of medical images. The researches in texture analysis of medical images have been targeted at developing computer-aided diagnosis systems. Computer-aided diagnosis systems are gaining popularity in one way or another because of their ability to improve the precision and accuracy of characterization of lesions beyond what radiologists do by visual inspection [44]. The main objectives of a CAD system in the diagnostic process are to accurately detect and precisely characterize potential abnormalities [45]. This a very important step towards the effective treatment of diagnosed abnormalities. The radiologist detects and characterizes abnormalities by visual interpretation. To do this, the radiologists must successfully integrate of two distinct processes, namely image perception to recognize unique image patterns and the process of reasoning to identify the relationships between perceived patterns and possible diagnosis. The two processes are heavily dependent on the empirical knowledge, memory, intuition and diligence of the radiologist. The approach of the radiologist is not always error-free as there are well-documented errors and variations in the human interpretation of clinical images [46]. In summary of the foregoing, CAD aims to provide a computer output as a second opinion in order to assist physicians in the detection of abnormalities, quantification of disease progress and differential diagnosis of lesions [1]. One important step in the generic architecture of CAD system is feature

extraction (texture analysis), and thus, texture analysis is the fundamental basis of CAD at its present stage of development [1].

The human visual system can discriminate between different morphologic information such as shape and size, but there is evidence that the human visual system has difficulty in the discrimination of textural information that is related to higher-order statistics or spectral properties of an image [47, 48]. The human visual system if unaided has a limited number of grey levels it can tell apart. Thus, texture analysis can potentially augment the visual skills of the radiologist by extracting image features that may be relevant to the diagnostic problem but that are not necessary visually extractable [45]. In the use of image texture analysis as a preprocessing step in CAD schemes, the input generation process is automated and, therefore, is reproducible and robust. Although useful to the diagnostic process, texture analysis is not a panacea for the diagnostic interpretation of radiologic images [45]. The pursuit of texture analysis is based on the hypothesis that the texture signature of an image is relevant to the diagnostic problem at hand. A major drawback is that the effectiveness of texture analysis is bound by the type of algorithm that is used to extract meaningful textural features.

6. Decision making in computer-aided diagnosis

Texture analysis is the fundamental basis of computer-aided diagnosis in radiology and is, therefore, indispensable to the process. The main problem with calculated texture is that it produces an avalanched of outputs, especially co-occurrence matrix. The outputs need to be reduced to a manageable level so that useful information which could be used for decision making can be obtained from the further analysis. Using the MaZda® software, feature reduction is achieved by using the Fisher coefficient, classification error combined with the correlation coefficient, mutual information [41, 49] and a selection of optimal feature subsets with minimal classification error of 1-nearest neighbour (1-NN) classifier [50, 51]. The Fisher coefficient selects features by reducing intra-group variance and maximizing inter-group difference [52]. If the above methods do not reduce the features sufficiently initially, further reduction is carried out by transforming the original features into a new feature space with lower dimensionality [40]. This method is called feature extraction or projection [53] and can be achieved in MaZda® using principal component analysis (PCA), linear discriminant analysis (LDA), nonlinear discriminant analysis (NDA) [50, 54–57] and raw data analysis (RDA). Artificial intelligence tools are used for automated decision making in computer-aided diagnosis. Such tools include different algorithms which are provided by different computer softwares. The Waikato Environment for Knowledge Analysis (WEKA) version 3.6.11 data mining software is useful software equipped with many classification algorithms. It is a landmark system in data mining and machine learning [58]. The software came about through the perceived need for a unified workbench that would allow researchers easy access to the state-of-art techniques in machine learning [59].

The two tools for decision making or classification in computer-aided diagnosis popular with researchers are the artificial neural networks (ANN) and k-nearest neighbour (k-NN). The

http://dx.doi.org/10.5772/65349

ANN and k-NN algorithms are part of the resources provided in the WEKA software. Both algorithms perform supervised classifications implying that the classification is under the guidance of a human being. In supervised classification, the user selects sample pixels in an image that he considers representative of specific classes and then initiates the software to use these training sites as references for the classification of other pixels in the image.

6.1. The artificial neural network

Artificial neural networks are regarded as relatively crude electronic networks of "neurons" which simulate the neural structure of the human brain. They literally imitate the decision-making process of the human brain. The networks are the electronic equivalent of the human brain and are therefore trainable for improved performance. They process records one at a time as the records are fed into them and "learn" from "experience" by comparing their classification of each record with a known actual classification of the record. The subsequent classifications are therefore made more accurate by using the errors from the classification of previous records which are fed back into the network to modify the networks' algorithm.

A multilayer feed-forward neural network is the one that has one or more hidden layers. The neurons in the hidden layer arbitrate between the input and the output of the network. The source nodes in the input layer of the neural network receive the input feature vector. The input signals which are applied to the neurons in the hidden layer are made up of the neurons in the input layer. The output signals of the hidden layer can be used as inputs to the next hidden or output layer, and this process continues but terminates when the output layer produces the final output result [60].

6.2. The k-nearest neighbour

The k-nearest neighbour is a non-parametric method used for classification and regression [61]. In the algorithm, the training data set is stored, so that classifying a previously unclassified (new) record is by comparing it to the most similar records in the training data set. Simply put, in the k-nearest neighbour classification algorithm, a database in which data points are separated into several separate classes is used to predict the classification of a new data point. The data set is assumed to be in space and classification is achieved by assigning the new data point to its closest neighbour. It is a rather simple and versatile concept.

7. The case study

7.1. Research design and location

A prospective cross-sectional design that targeted patients clinically diagnosed with stroke and who underwent non-contrast CT (NCCT) investigation of the brain was adopted for the study. The research design and protocol were approved by the Research Ethics Committee of Nnamdi Azikiwe University Teaching Hospital, Nnewi, Anambra State, Nigeria. The study was carried in two locations, namely Onitsha, Anambra State in south-eastern Nigeria, and

Ibadan, Oyo State in south-western Nigeria. Two privately owned radiodiagnostic centres were selected. The choice of the centres was to have an adequate number of patients because the centres have a high number of stroke patients referred to them for brain CT examination.

7.2. Sample size determination

The minimum sample size required for this study was determined using the Taro Yamane's formula for finite population [62]:

$$n = N \div 1 + Ne^2 \tag{12}$$

where n = sample size; N = number of patients clinically diagnosed with a stroke who underwent NCCT study of the brain in the two radiodiagnostic centres in previous one year: May 2012 to April 2013; e = the level of precision or confidence level required.

So,

$$n = 208 \div 1 + 208(0.05)^2 = 137 \tag{13}$$

Within the period: May 2012 and April 2013, a total 208 patients with clinically diagnosed stroke underwent non-contrast CT of the brain in the two centres, and thus, a minimum sample of approximately 137 was calculated as shown above.

7.3. Patient selection

A total of 164 clinically diagnosed stroke patients who were referred to the two radiodiagnostic centres for CT scan and who met the inclusion criteria for the study were enlisted in the study to improve its precision. The inclusion criteria were:

1. Patients clinically diagnosed with stroke at the Nnamdi Azikiwe University Teaching Hospital (NAUTH), Nnewi, Anambra State, and University College Hospital (UCH) Ibadan, Oyo State, and peripheral private and public hospitals in these two states.
2. Patients clinically diagnosed with stroke who underwent non-contrast CT of the brain at the two selected private radiodiagnostic centres.
3. Patients in whose CT images stroke lesions were identified by the radiologist.
4. Patients who met criteria 1–3 and consented to participate in the study.

All the participating patients directly or indirectly, through their relatives, expressed willingness to participate in the study by signing an informed consent form before enlistment in the study.

7.4. Equipment and softwares used

The equipment and computer softwares used include the following:

http://dx.doi.org/10.5772/65349

1. A four-slice helical ***Toshiba Asteion***™ CT scanner with 512×512 reconstruction matrix manufactured by Toshiba Medical Systems Corporation and a two-slice ***Philips MX8000 Dual***™ CT scanner also with 512×512 reconstruction matrix manufactured by Philips Medical Systems. The CT scanners were used to carry out non-contrast studies of the patients' brains.
2. ***Datamax***™ digital video discs (DVDs) to copy the CT images from the scanners.
3. An ***HP C2000***™ laptop with 64-bit Windows 7 operating system used to view the images and perform texture analysis.
4. ***Medisynapse***™ and ***Microdom***™ DICOM viewers.
5. ***MaZda***® texture analysis software version 4.7 for performing texture analysis on the images. The software was developed at the Institute of Electronics, Technical University of Lodz (TUL), Poland.
6. The ***Waikato Environment for Knowledge (WEKA)*** version 3.6.11 data mining software (Hamilton, New Zealand) used for image classification.

7.5. Patient data and image acquisition

The enlistment of patients in the study, collection data and acquisition CT images commenced in May 2013 and ended in April 2014. The patients after being clinically diagnosed with stroke in the hospitals were referred to undergo NCCT of the head to confirm or rule out the disease as the cause of their signs and symptoms. On arriving the radiodiagnostic centre, the patient or his/her relatives were approached and the study explained to them. The researcher through the request form identified the provisional diagnosis necessitating the scan. If it was a stroke, an appeal was made to the patient or his/her relatives to enlist in the study. If the response is affirmative, an informed consent form is signed by the patient or his/her relatives. There was no financial reward for participating in the study. Demographic data of the patient such as age and gender were thereafter obtained and documented. The approximate time interval between the onset of symptoms and head CT examination was ascertained and documented. Non-contrast CT images of the brain were obtained using the CT machine, ***Toshiba Asteion***™ in one centre. In the second centre, a ***Philips MX8000 Dual***™ CT scanner was used for the same purpose. Scans were obtained at 0.5–1 mm contiguous sections from the base of the skull to the vertex. The scan parameters used were exclusively chosen by the attending radiographer in each centre. The images were transferred from the CT archive to a DVD and then loaded into an ***HP 2000***™ laptop for viewing using either ***Medysynapse***™ or ***Microdom***™, both DICOM viewing softwares.

7.6. Radiological reporting of the images

The CT images obtained were visually inspected and reported by a team of two radiologists with experiences in CT diagnosis of stroke. The first radiologist had five-year post-qualification experience as a consultant radiologist, while the second had seven-year post-qualification experience. Both radiologists reported on the images independently and were blind to each

other. The reports included in the study were those in which the two radiologists were in agreement for the presence of stroke, the subtype and anatomical location of the lesions. The reports that indicated there were no radiological signs of abnormality and those that indicated neurological abnormalities mimicking stroke were excluded from the study.

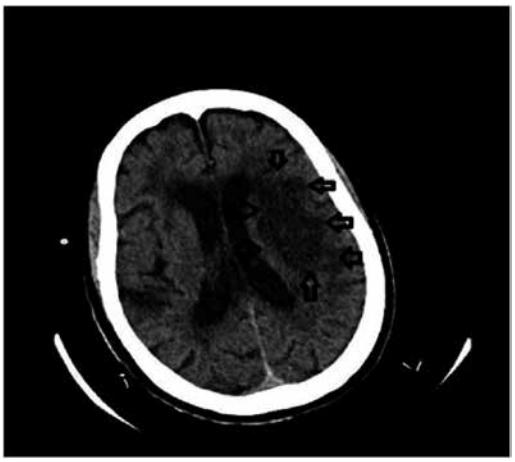

Figure 5. A non-contrast CT image showing left cerebral ischaemia (arrows). Note there is a small area of ischaemia on the right parietal lobe.

Figure 6. A non-contrast CT image showing left cerebral haemorrhage (arrows). Note the marked compression of the right and left ventricles.

The anatomical locations of the lesions were identified and the lesions categorized as ischaemic or haemorrhagic lesion by the two radiologists as shown in **Figures 5** and **6**. The radiologist's reports contained the patient's name, identification number, age, sex, provisional diagnosis

http://dx.doi.org/10.5772/65349

and radiological diagnosis, which contained details such as the type of stroke lesions identified, their number, anatomical locations of the lesions and geographic extent in the brain.

7.7. Texture analysis of stroke CT images

Texture analyses of stroke CT images were done using the ***MaZda***® texture analysis software. The procedure for the texture analysis of the CT images is represented in the block diagram shown in **Figure 7** below.

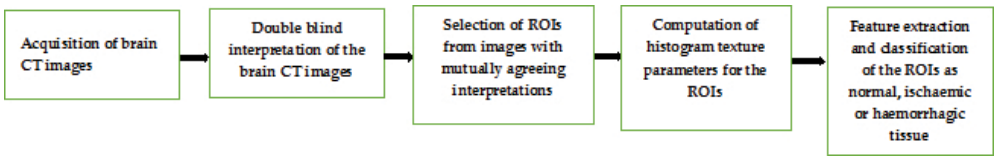

Figure 7. Block diagram illustrating the analytical procedure.

All the images in which lesion appeared were loaded into the computer program and analysed. Four regions of interest (ROIs) in each CT image that demonstrated the lesions were selected for analysis. Two ROIs each represented the lesion and normal brain tissue as shown in **Figure 8**. The lesioned brain tissue contained ROI 1 and RO1 2, while the adjacent normal brain tissue contained ROI 3 and ROI 4 as shown in **Figure 8**.

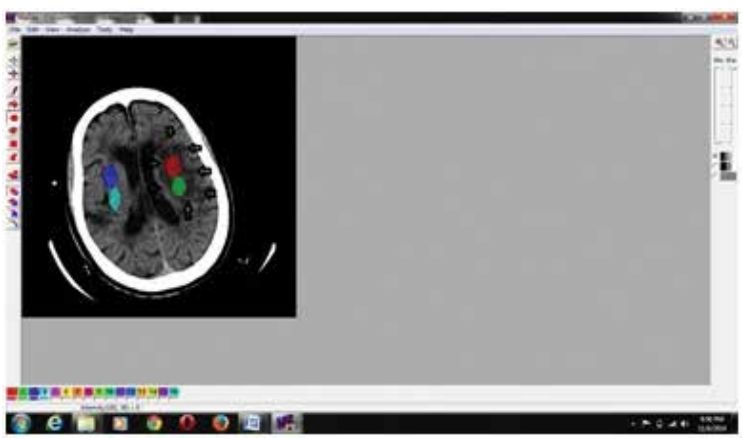

Figure 8. Illustration of the method of selection of the regions of interest (ROIs). Note that ROI 1 (red) and ROI 2 (green) are on ischaemic tissues on the left cerebral hemisphere, while ROIs 3 and 4 (blue and sky blue) are on normal tissues on the right cerebral hemisphere.

Precaution was taken to ensure that machine settings which differed between cases did not affect the image during texture analysis. This was achieved by normalizing the image. Normalization process literally changes the range of pixel grey-level values of different images so that they appear to have been obtained with the same machine settings. This is called image

consistency. The method of normalization prior to texture analysis was the ±3 sigma method selected from the program functions. Histogram texture parameters for the four ROIs were computed using the ***MaZda***® version 4.7 program. The output of the parameters computed for each CT image was saved as a comma separated value (CSV) file in ***Microsoft Excel*** for further analysis.

7.8. Statistical analyses

Statistical analyses were carried out in two stages. In the first stage, the lesioned brain tissues for which texture parameters were calculated were divided according to lesion types. The discriminating histogram texture parameters were obtained by raw data analysis (RDA). In the second stage, the normal brain tissues and lesions from which the histogram texture parameters were computed were then classified by the artificial neural network and k-nearest neighbour algorithms as normal tissue, haemorrhagic or ischaemic tissues. The classifications were then cross-validated with the radiologist's report as gold standard using the receiver operating characteristic (ROC) curve analysis. Raw data analysis of computed histogram texture parameters was performed with ***MaZda***® and classification of brain tissues with ***WEKA*** 3.6.11.

7.8.1. Feature reduction

In order to reduce the computed histogram texture parameters to only the ones useful for further analyses and eliminate redundant data, the Fisher coefficient was used. The Fisher coefficient reduced the intra-group variance and maximized the inter-group difference. It is a feature of the ***MaZda***® texture analysis software.

7.8.2. Feature extraction

The histogram texture parameters computation reports on the selected ROIs saved in ***Microsoft Excel*** files were loaded into ***MaZda***®, first according to lesion type and in combined lesion form, and raw data analysis was performed on them. The best discriminating texture parameters were extracted through the raw data analysis and displayed in a three-dimensional (3D) feature space. The process also classified the ROIs as that of normal tissue, ischaemic or haemorrhagic lesions using the best discriminating texture parameters. In this process, the ROIs in space were picked one at a time and assigned a class to which it belonged with the radiologist's interpretation taken as the expected ideal outcome.

7.8.2.1. Artificial neural network and k-nearest neighbour classifications

A multilayer feed-forward neural network and k-nearest neighbour algorithm were used to classify brain tissues as lesions, according to lesion type or normal tissues. For the purpose of classifying ROIs into normal brain tissue, ischaemic and haemorrhagic lesions using the k-nearest neighbour algorithm, a value of 1 was chosen for ***k***. The ***Waikato Environment for Knowledge Analysis (WEKA)*** version 3.6.11 data mining software was used to perform these

http://dx.doi.org/10.5772/65349

classifications. Both algorithms were trained by creating a model on retrospective data before applying them to a test data.

The performance of the neural network and k-nearest neighbour algorithms in classifying the ROIs as normal brain tissue or lesioned and according to lesion type was cross-validated with the radiologist's report using the ROC curve analysis. The accuracy, sensitivity, specificity, positive predictive value and negative predictive value were determined from the ROC curves plotted. The parameters from ROC analysis were calculated.

8. Results

The raw data analysis was used to analyse the data from histogram texture parameters. The raw data analysis was discriminated between the various ROIs as normal brain tissue, ischaemic stroke lesion or haemorrhagic stroke lesions. The classifications of the ROIs obtained in the discrimination are shown in the 3D feature space diagram (**Figure 8**). In the figure, the ischaemic lesion is represented by 1, haemorrhage by 2 and normal brain tissues by 3. The discriminating histogram parameters were the mean, 90 percentile and 99 percentile as shown in **Figure 8**. The result of the raw data analysis shows that histogram texture parameters were very accurate in discriminating between normal brain tissues, ischaemic lesion and haemorrhagic lesions as shown in **Table 1** and illustrated in **Figure 9**.

Total number of ROIs	Number of correctly classified ROIs	Number of misclassified ROIs	Accuracy (%)
1260	1161	99	92.14

Table 1. Classification accuracy of the ROIs by raw data analysis.

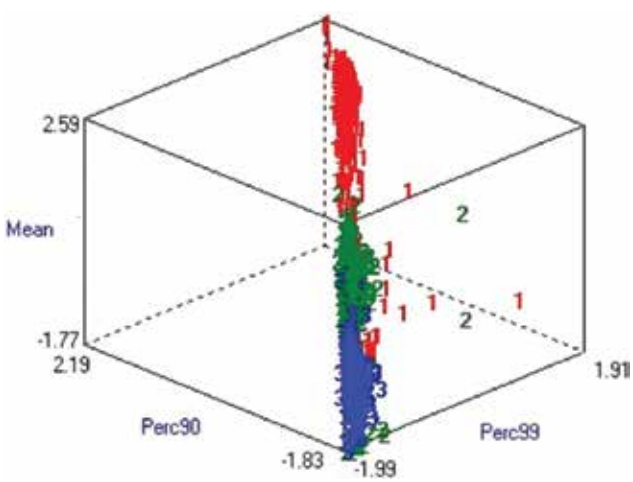

Figure 9. The distribution of ROIs in 3D feature space using data obtained from the histogram.

Evaluation parameters	Tissue/lesion type			
	Normal	Haemorrhage	Ischaemia	Weighted average
Sensitivity or true positive rate (TPR)	0.971	0.949	0.888	0.947
True negative rate or (TNR) Specificity	0.937	0.989	0.983	0.962
False positive rate (FPR)	0.063	0.011	0.017	0.038
False negative rate (FNR)	0.029	0.051	0.112	0.053
Positive predictive value (PPV)	0.938	0.971	0.936	0.947
Negative predictive value (NPV)	0.953	0.857	0.050	0.693
Area under ROC curve	0.979	0.986	0.977	0.980

Table 2. Receiver operating characteristic analysis of artificial neural network classification of brain tissues.

Evaluation parameters	Tissue/lesion type			
	Normal	Haemorrhage	Ischaemia	Weighted average
Sensitivity or true positive rate (TPR)	0.954	0.944	0.853	0.929
True negative rate (TNR) or Specificity	0.934	0.983	0.966	0.955
False positive rate (FPR)	0.066	0.017	0.034	0.045
False negative rate (FNR)	0.046	0.056	0.147	0.071
Positive predictive value (PPV)	0.934	0.957	0.878	0.928
Negative predictive value (NPV)	0.949	0.273	0.029	0.693
Area under ROC curve	0.944	0.963	0.909	0.942

Table 3. Receiver operating characteristic analysis of k-nearest neighbour classification of brain tissues.

Classification algorithm	Sensitivity	Specificity	FPR	AUROCC
ANN	0.947	0.962	0.038	0.980
k-NN	0.929	0.955	0.045	0.942
Remark	$p = 0.061$	$p = 0.378$	$p = 0.378$	$p = 0.373$

Table 4. Comparison of artificial neural network and k-nearest neighbour in classification of brain tissues.

The statistics in **Tables 2** and **3** show the performance of histogram-based texture parameters in the classification of brains tissues as normal, ischaemic or haemorrhagic using the artificial neural network and k-nearest neighbor algorithms. There was no difference in sensitivity, specificity, false positive rate and area under ROC curve between the artificial neural network and k-nearest neighbour classifications ($p > 0.05$) as shown in **Table 4**.

http://dx.doi.org/10.5772/65349

9. Discussion

Medical image analysis techniques play very important roles in several radiological interpretations. In general, the applications involve the automatic extraction of texture features from images which are then used for a variety of classification tasks, such as distinguishing normal tissue from abnormal tissue [33].

In this study, histogram parameters were computed for the selected ROIs chosen from stroke lesions and adjacent normal brain tissues using ***MaZda***®. The whole process involved computation of histogram texture parameters, feature selection or reduction and raw data analysis to extract discriminating parameters namely the mean, percentile 90 and percentile 99, were the best discriminators. They achieved very high accuracy in discriminating between normal brain tissues, ischaemic and haemorrhagic stroke lesions. According to the result of a previous study, histogram features when used with Radial Basis Function of Nerve Network (RBFNN) achieved accuracies of over 80% in classification brain of tissues [63]. The histogram measures the frequency of occurrence of the different grey-scale patterns throughout the image by moving in steps of one pixel across the image. This approach is attractive for its conceptual simplicity and most people are at ease with it. The result of this study shows that histogram is highly accurate in discriminating between normal brain tissues and lesions, and between ischaemic stroke and haemorrhagic stroke lesions. In another similar study, grey-level co-occurrence matrix features were used in automatic detection of ischaemic stroke [64]. Four different algorithms were used, namely decision tree, artificial neural network, k-nearest neighbour and support vector machine (SVM), and the results were quite similar to ours. The sensitivity was 93% for decision tree, 98% for artificial neural network, 96% for k-nearest neighbour and 98% for SVM, while specificity was 90% for decision tree and artificial neural network and 100% for k-nearest neighbour and SVM. The accuracy of detection was 92% for decision tree, 96% for artificial neural network, 97% for k-nearest neighbour and 98% for SVM [64].

The results of ROC curve analysis of the performance of the artificial neural network and k-nearest neighbour classifications of brain tissues based on data obtained from the histogram show that histogram-based texture parameters are highly accurate. A classification accuracy of over 90% was achieved, and the weighted average sensitivity, specificity and area under ROC curve of almost unity were recorded for both artificial neural network and k-nearest neighbour. Correspondingly, the false positive rate (referred to as fall-out in machine learning) and false negative rate in both methods were very low. Sensitivity and specificity are important measures of the diagnostic accuracy of a test [65]. A diagnostic test with high sensitivity is useful in ruling out a disease condition when the test result is negative. Correspondingly, a diagnostic test with high specificity is useful in ruling in a disease condition when the test result is positive. The foregoing explanation of the importance of sensitivity and specificity in diagnostic test performance can be applied to the present study which was aimed at being used for automatic detection of stroke lesions.

Studies similar to ours have been carried out in the past with quite good outcomes. In one such study, classification of stroke lesions into acute infarct, chronic infarct and haemorrhage on

non-contrast brain CT were done [23]. The researchers used histogram-based comparison and wavelet energy-based texture information to classify stroke lesions. In a study to propose a method for automatic diagnosis of abnormal tumour region present in CT images using wavelet-based statistical texture features and support vector machine (SVM) for classification of brain tissues, the researchers obtained a very high classification accuracy [66]. In another study, using extracted texture features from CT images with inductive learning techniques and Radial Basis Function Neural Network, brain tissues were classified as normal and abnormal with very high accuracy [63].

In this study, comparison of artificial neural network and k-nearest neighbour classifications of brain tissues showed that histogram-derived data achieved the same classification performance with both algorithms. This implies that either of the two algorithms can be used for classification and therefore may be used in real clinical situations. Histogram method of texture analysis is a rather simple concept and may be found attractive by many researchers with a view of developing computer-aided diagnostic softwares. The present database could be used in building a computer-aided diagnosis tool for stroke based on content-based image retrieval similar to that proposed by Yuan et al. [67].

The computer-aided diagnostic tool tries to emulate the radiologist's visual inspection and interpretation of brain CT images or any other image it has been presented with depending on the case under investigation. Classification is typically accomplished by using a decision or discriminant function [68]. In this study, supervised classification was carried using the artificial neural network [69, 70] and k-nearest neighbour [71], two algorithms popular with researchers in artificial intelligence in medicine. The performance of the artificial neural network and k-nearest neighbour algorithms in classifying brain tissues in non-contrast brain CT into normal, ischaemic and haemorrhagic lesions was evaluated using the ROC curves. In the ROC curve analysis, the classification of data points as belonging to normal brain tissue, ischaemic stroke or haemorrhagic stroke was cross-validated with the radiologist's identification of stroke lesions and normal brain tissues. Receiver operating characteristic curves are used to compare the diagnostic performance of two or more diagnostic tests [72–74] and also to discriminate between diseased and normal cases. With data from the histogram texture parameters obtained in this study, there was no difference in the results of ROC analysis of the classifications using the artificial neural network and k-nearest neighbour. This implies that both algorithms can be used with histogram-derived data to build automatic diagnostic tools for stroke.

The following factors may affect a generalization of the result of this study. So, its use should be with the following points in mind:

1. This study was not hospital-based. It was conducted in two radiodiagnostic centres, and the patients were carefully selected. The research conditions may therefore not reflect the actual clinical situation.

2. Sensitivity and specificity levels in this study were high but not 100% implying that a computer-aided scheme can make mistakes. This study recognizes this fact, but it did not consider how the mistaken cases may be identified. Sensitivity is rarely 100%

http://dx.doi.org/10.5772/65349

especially because of the wide variability in lesion and background appearance [75]. It may be the case that majority of the computer-aided detection schemes may never be trained with enough cases to "see" all possible variations in a given target lesion. Even for a scheme that uses artificial neural networks and continues to learn with each successive case they analyse, the sensitivity of 100% may not be achieved [75]. Thus, computer-aided detection systems should be used with caution and it ideally should not completely replace visual inspection and interpretation. Such systems are meant to complement visual inspection and interpretation. Heavy reliance on computer-aided detection system to detect and classify lesions may alter the normal search and decision-making processes [76].

3. Only stroke cases confirmed at CT were evaluated in this study. Clinical mimics of stroke were not included, and therefore, it is not possible to tell if this method can distinguish stroke from its clinical mimics.

4. The post-ictal intervals before CT imaging were not captured, and thus, the result of this study cannot be used to explain the changes in CT appearance of stroke lesions with time.

In view of the findings of this study, a larger-scale study in an actual clinical environment is recommended. This study will evaluate the performance of this proposed automatic method of detecting and classifying stroke lesions and compare it with radiologist's visual interpretation. This study will also include the changes in CT appearance of stroke lesions with the passage of time. The chronological sub-typing will be crucial to identifying hyperacute, acute and chronic stroke lesions on CT. This will help neurologist to estimate the post-stroke neurological deficit that should be expected in any individual case. In conclusion, this study has established that histogram-derived texture parameters are accurate in classifying brain tissues in NCCT images and therefore suitable for automatic detection and classification of stroke lesions using the artificial neural network and k-nearest neighbour classifiers. The results obtained in this study suggest that computer-aided diagnostic tool for stroke diagnosis utilizing histogram-derived texture parameters may be ideal.

Author details

Kenneth K. Agwu[1] and Christopher C. Ohagwu[2*]

*Address all correspondence to: cc.ohagwu@unizik.edu.ng

1 University of Nigeria, Nsukka, Nigeria

2 Nnamdi Azikiwe University, Awka, Nigeria

References

[1] Stoitsis J, Ioannis V, Stavroula GM, Spyretta G, Alexandra N, Konstantina SN. Computer aided diagnosis based on medical image processing and artificial intelligence methods. Nucl Instrum Methods Phys Res A 2006; 569 (2): 591–595. Doi: 10.1016.j.nima.2006.08.134

[2] Ojini FI, Danesi MA. The pattern of neurological admissions at the Lagos University Teaching Hospital. Niger J Clin Pract 2003; 5(1): 38–41.

[3] Warlow CP. Epidemiology of stroke. Lancet 1998; 352 (Suppl 3): S1111-S1114.

[4] Sudlow CLM, Warlow CP. Comparing stroke incidence worldwide: what makes studies comparable? Stroke 1996; 27(3): 550–558. Doi: 10.1161/01.STR.27.3.550

[5] Gorelick PB. Stroke prevention. Arch Neurol 1995; 52(4): 347–355. Doi: 10.1001.archneur.1995.00540280029015.

[6] Wolf PA, Kannel WB, Dawber TR. Prospective investigations: The Framingham study and the epidemiology of stroke. Adv Neurol. 1978; 19: 107–120.

[7] Howlett WP. Neurology in Africa: clinical skills and neurological disorders. Kilimanjaro Christian Medical Centre, Tanzania and Centre for International Health, University of Bergen, Norway. 2012. Pp. 101–115. Accessed on 12/09/2012 at https://bora.uib.no

[8] The WHO MONICA project principal investigators. The World Health Organization MONICA Project (monitoring trends and determinants in cardiovascular disease): a major international collaboration. J Clin Epidemiol 1988; 41(2): 105–114. Doi: 10.1016/0895-4356(88)90084–4.

[9] Chukwuonye II, Ohagwu KA, Uche EO, Chuku A, Nwanke RI, Ohagwu CC, Ezeani IU, Nwabuko CO, Nnoli MA, Oviasu E, Ogah SO. Validation of Siriraj stroke score in southeast Nigeria. Int J Gen Med. 2015; 8: 349–353. Doi: 10.2147/IJGM.S87293.

[10] Sheta YS, Al-Gohary AA, El-Mahdy M. Accuracy of clinical sub-typing of stroke in comparison to radiological evidence. Br J Sci 2012; 6(2): 1–7.

[11] Imarhiagbe FA, Ogbeide E. Clinical-imaging dissociation in strokes in a southern Nigerian tertiary hospital: review of 123 cases. Niger J Hosp Pract. 2011; 8(1–2): 3–7.

[12] Khan J, Rehman A. Comparison of clinical diagnosis with computed tomography in ascertaining type of stroke. J Ayub Med Coll Abbottabad 2005; 17(3): 65–67.

[13] Mullins ME. Modern emergent stroke imaging: pearls, protocols and pitfalls. Radiol Clin N Am 2006; 44(1): 41–62. Doi: http://dx.doi.org/10.1016/j.rcl.2005.08.002.

[14] Keris V, Rudnicka S, Vorona V, Enina G, Tilgale B, Fricbergs J. Combined intraarterial/intravenous thrombolysis for acute ischaemic stroke. Am J Neuroradiol 2001; 22(2): 352–358.

[15] Burnette WC, Nesbit GM. Intra-arterial thrombolysis for acute ischaemic stroke. Eur Radiol 2001; 11: 626–634.

[16] Jager HR. Diagnosis of stroke with advanced CT and MR imaging. Br Med Bull 2000; 56: 318–333.

[17] Tegos TJ, Kalodiki E, Sabetai MM, Nicolaides AN. Stroke: pathogenesis, investigations and prognosis - part II of III. Angiology 2000 51 (11): 885–894.

[18] Kidwell CS, Villablanca JP, Saver JL. Advances in neuroimaging of acute stroke. Curr Atherosc Rep 2000; 2 (2): 126–135.

[19] Lev MH, Nichols SJ. Computed tomographic angiography and computed tomographic perfusion imaging of hyperacute stroke. Top Magn Reson Imag 2000; 11:2 73–287.

[20] Burnette WC, Nesbit GM, Barnwell SL. Intra-arterial thrombolysis for acute stroke. Neuroimag Clin N A 1999; 99: 491–508.

[21] Atalabi OM, Adekanmi AJ, Bamgboye EA. The state of radiology subspecialty training in the West African sub region: the residents' perspective. W Afr J Radiol 2013; 20 (2): 69–73.

[22] Robinson PJA. Radiology's Achilles' heel: error and variation in the interpretation of the Roentgen image. Br J Radiol 1997; 70: 1085–1098.

[23] Chawla M, Sharma S, Swansiwamy J, Kishore LT. A method for automatic detection and classification of stroke from brain CT images. EMBC 2009 Report No: IIIT/TR/2009/188. Centre for Visual Information Technology, International Institute of Information Technology, Hyderabad 500 032, India. 2009.

[24] Poole D, Mackworth A, Goebel R. Computational intelligence: a logical approach. New York: Oxford University Press. 1998. ISBN 0-19-510270-3.

[25] Luger G, Stubblefield W. Artificial intelligence: structures and strategies for complex problem solving (5th edition). Benjamin Cummings. ISBN 0-8053-4780-1. 2004. Available at: http://www.cs.unm.edu

[26] Russel SJ, Norvig P. Artificial intelligence: a modern approach (2eedition). Upper Saddle River, New Jersey: Prentice Hall. ISBN 0-13-790395-2. 2003.

[27] Castellano G, Bonilha L, Li LM, Cendes F. Texture analysis of medical images. Clin Radiol 2004; 59 (12): 1061–1069.

[28] Gonzalez RC, Woods RE. Digital image processing (3rd edition). New Delhi: PHI Learning Private Limited. 2008. Pp. 827–860.

[29] Nailon WH. Texture analysis methods for medical image characterization. In: Mao Y (ed.). Biomedical imaging. Rijeka, Croatia: InTech. 2010. Pp. 75–100.

[30] Davies ER. Introduction to texture analysis. In: Mirmehdi M, Xie X, Suri J (eds.). Handbook of texture analysis. London: Imperial College Press. 2008. Pp. 1–31.

[31] Materka A, Strzelecki M. Texture analysis methods - a review. Technical University of Lodz, Institute of Electronics, COST B11 report, Brussels. 1998. Available online at: http://www.eletelop.lodz.pl/program/cost/pdf_1.pdf

[32] Haralick RM. Statistical and structural approaches to texture. Proc IEEE 1979; 67 (5): 786–804.

[33] Pham TA. Optimization of texture feature extraction algorithm. A Master of Science thesis submitted to Delft University of Technology, Netherlands. 2010. P. 8.

[34] Waugh SA (2014). The use of texture analysis in breast magnetic resonance imaging.Doctoral thesis submitted to University of Dundee, Scotland. Available online at: http://discovery.dundee.ac.uk/portal/en/theses/.

[35] Tang X. Texture information in run-length matrices. IEEE Trans Image Process. 1998; 7 (11): 1602–1609.

[36] Galloway MM. Texture analysis using grey level run lengths. Comput Graph Image Process 1975; 4: 172–179.

[37] Bracewell R. The Fourier transform and its applications (3rd edition). New York: McGraw-Hill. 1999.

[38] Qian S, Chen D. Discrete Gabor transform. IEEE Trans Signal Process 1993; 41: 2429–2438.

[39] Walnut DF. An introduction to wavelet analysis. Boston, Massachusetts: Birkhauser. 2001.

[40] Szcypiński PM, Strzelescki M, Materka A, Klepaczko A. MaZda – a software package for image texture analysis. Comput Methods Progr Biomed 2009; 94 (1): 66–76.

[41] Materka A, Strzelecki M, Szcypinski P. MaZda manual. 2006. Available at: http://www.eletel.p.lodz.pl/mazda/download/mazda_manual.pdf

[42] Gonzalez RC, Woods RE, Eddins SL. Digital image processing using MATLAB (2nd edition). USA: Gatesmark Publishing. 2009. Pp. 1–12.

[43] Galda HJ. Image processing with scilab and image processing design toolbox. 2011. Available at: www.d.umn.edu/˜snorr/ee5351s14/ImProcTut.pdf

[44] Jiang Y, Nishikawa RM, Schmidt RA, Metz CE, Giger ML, Doi K. Improving breast cancer diagnosis with computer-aided diagnosis. Acad Radiol 1999; 6: 22–33.

[45] Tourassi GD. Journey toward computer-aided diagnosis: role of image texture analysis. Radiology 1999; 213: 317–320.

[46] Robinson PJA. Radiology's Achilles' heel: error and variation in the interpretation of the Roentgen image. Br J Radiol 1997; 70: 1085–1098.

[47] Julesz B, Gilbert EN, Shepp LA, Frish HL. Inability of humans to discriminate between visual features that agree in second-order statistics-revisited. Perception 1973; 2: 391–405.

[48] Julesz B. Visual discrimination of textures with identical third-order statistics. Biol Cybernet 1978; 31: 137–140.

[49] Tourassi GD, Frederick ED, Markey MK, Floyd CE. Application of the mutualinformation criterion for feature selection in computer-aided diagnosis. Med Phys 2001; 28 (12): 2394–2402.

[50] Duda R, Hart PE, Stork DG. Pattern classification (2nd edition). New York: John Wiley and Sons. 2001.

[51] Dash M, Liu H. Feature selection for classification. Intell Data Anal 1997; 1 (3): 131–156.

[52] Plata S. A note on Fisher's correlation coefficient. Appl Math Lett 2006; 19: 499–502.

[53] Jian AK, Duin RPW, Mao J. Statistical pattern recognition: a review. IEEE Trans Pattern Anal Mach Intell 2000; 22 (1): 4–37.

[54] Krzanowski W. Principles of multivariable data analysis. Oxford: Oxford University Press. 1988.

[55] Hecht-Nielsen R. Neurocomputing (3rd edition). Boston: Addison-Wesley Longman Publishing Co., Inc. 1989.

[56] Fukunaga K. Introduction to statistical pattern recognition. New York: Academic Press. 1991.

[57] Mao J, Jian A. Artificial neural networks for feature extraction and multivariate data projection. IEEE Trans Neural Netwk 1995; 6: 296–316.

[58] Piatetsky-Shapiro G. KDnuggets news on SIGKDD service award. 2005. Available at: http://www.kdnuggets.com/news/2005/ni3/2i/html

[59] Hall M, Frank E, Holmes G, Pfahringer B, Reutmann P, Witten IH. The WEKA data mining software: an update. SIGKDD Explor 2009; 11 (1): 10–18.

[60] Chen DR, Chang RF, Huang YL. Computer-aided diagnosis applied to ultrasound of solid breast nodules by using neural networks. Radiology 1999; 213: 407–412.

[61] Altman NS. An introduction to kernel and nearest neighbour nonparametric regression. Am Statist 1992; 46 (3): 175–185.

[62] Uzoagulu AE. Practical guide to writing research project reports in tertiary institutions (New edition). Enugu: Cheston Nigeria Limited. 2011. Pp. 57–58.

[63] Zhang W, Wang X. Feature extraction and classification for human brain CT images. Proceedings of the Sixth International Conference on Machine Learning and Cybernetics, Hong Kong, 19–22 August, 2007.

[64] Rajini NH, Bhavani R. Computer aided detection of ischaemic stroke using segmentation and texture features. Measurement 2013; 46 (6): 1865–1874.

[65] Akobeng AK. Understanding diagnostic tests 1: sensitivity, specificity and predictive values. Acta Paediatr 2006; 96: 338–341.

[66] Padma A, Sukanesh R. Automatic diagnosis of abnormal tumor region from brain computed tomography images using wavelet based statistical texture features. Int J Comput Sci Eng Inform Technol 2011; 1 (3) 1–3. Doi: 10.5121/ijcseit.2011.1303.

[67] Yuan K, Tian Z, Zou J, Bai Y, You Q. Brain CT image database building for computer-aided diagnosis using content-based image retrieval. Inform Process Manage 2011; 47 (2): 176–185.

[68] Kassner A, Thronhill RE. Texture analysis: a review of neurologic MR imaging applications. Am J Neuroradiol 2010; 31: 809–816.

[69] Tzacheva AA, Najarian K, Brockway JP. Breast cancer detection in gadolinium-enhanced MR images by static region descriptors and neural networks. J Magn Resonan Imag 2003; 17: 337–342.

[70] Georgiadis P, Cavouras D, Kalatzis I, Daskalakis A, Kagadis GC, Sifaki K, Malamas M, Nikiforidis G, Solomou E. Improving brain tumor characterization on MRI by probabilistic neural networks and non-linear transformation of textural features. Comput Methods Progr Biomed 2008; 89: 24–32.

[71] Cover TM, Hart PE. Nearest neighbour pattern classification. IEEE Trans Inform Theor 1967; 13: 21–27.

[72] Griner PF, Mayewski RJ, Mushlin AI, Greenland P. Selection and interpretation of diagnostic tests and procedures. Ann Intern Med 1981; 94: 555–600.

[73] Zweig MH, Campbell G. Receiver-operating characteristic (ROC) plots: a fundamental evaluation tool in clinical medicine. Clin Med 1993; 39: 561–577.

[74] Metz CE. Basic principles of ROC analysis. Semin Nucl Med 1978; 8: 283–298.

[75] Krupinski EA. Computer-aided detection in clinical environment: benefits and challenges for radiologists. Radiology 2004; 231 (1): 7–9.

[76] Krupinski EA. An eye-movement study on the use of CAD information during mammographic search. Presented at the Seventh Far West Perception Conference, Tuscon, Arizona October 16–17, 1997.

Chapter 6

Data-Driven Methodologies for Structural Damage Detection Based on Machine Learning Applications

Jaime Vitola, Maribel Anaya Vejar,
Diego Alexander Tibaduiza Burgos and
Francesc Pozo

Additional information is available at the end of the chapter

http://dx.doi.org/10.5772/65867

Abstract

Structural health monitoring (SHM) is an important research area, which interest is the damage identification process. Different information about the state of the structure can be obtained in the process, among them, detection, localization and classification of damages are mainly studied in order to avoid unnecessary maintenance procedures in civilian and military structures in several applications. To carry out SHM in practice, two different approaches are used, the first is based on modelling which requires to build a very detailed model of the structure, while the second is by means of data-driven approaches which use information collected from the structure under different structural states and perform an analysis by means of data analysis . For the latter, statistical analysis and pattern recognition have demonstrated its effectiveness in the damage identification process because real information is obtained from the structure through sensors installed permanently to the observed object allowing a real-time monitoring. This chapter describes a damage detection and classification methodology, which makes use of a piezoelectric active system which works in several actuation phases and that is attached to the structure under evaluation, principal component analysis, and machine learning algorithms working as a pattern recognition methodology. In the chapter, the description of the developed approach and the results when it is tested in one aluminum plate are also included.

Keywords: SHM, PCA, machine learning, structural health monitoring

1. Introduction

Structural health monitoring (SHM) is a very interesting area, which main objective is the damage identification using permanently installed sensors to the structure. In general, one

of the aims is to monitor in real time a structure in order to know the current state starting from the damage detection, from this point of view, damage detection is extremely important: first, for safety, because it helps manage the downside risk resulting in a reduction cost by improving the visual inspection and maintenance processes [1, 2]. Currently, the new developments in several areas include the use of more complex structures. In many cases, the relation between the structure and the rest of the elements introduces interdependences which can be non-linear increasing the difficulty of the damage detection process. In these cases, a multicomponent and systemic approach can be incorporated to result in a safe and optimal maintenance model [3]. It is also important to note that there is infrastructure, which has been in use for several years, some examples can be found in historical buildings, bridges, aeronautical and aerospace structures, among others. This aging process brings new challenges [4] for SHM systems.

It is mandatory also to highlight the wide range of opportunities offered by the automation of the structural health monitoring process which can be used in conjunction with other automation systems such as an integrated transport system (ITS - Intelligent Transportation Systems), auto guided vehicles, among others. This symbiosis can offer benefits and give news perspectives about the use of the structures by providing additional information that the SHM systems can leverage to increase reliability, robustness and efficiency, reducing the probability of error, and providing tools for a better decision-making [5]. Structural health systems have a wide application in countless civilian infrastructures such as bridges [24] and buildings [6]. Similarly, SHM systems have been also applied to monitor mechanical components such as fuselages helicopters [7], wind turbines installed on land [8, 9] and sea (offshore) [10], aerospace equipment [11], aircraft [12], high-speed trains [13], aircraft turbines [14] and boats [15], in the same way SHM systems have been applied to marine renewable energy equipment [16]. It is noteworthy that the environmental conditions need to be considered to ensure a robust damage detection, in this sense, some works have been introduced to compensate the effects of the temperature changes [17, 18].

Regardless of the infrastructure design or the technology used in the development of the maintenance decision making, there are some factors to consider. Factors, such as information about the physical infrastructure, administrative information, use, and many others such as reliability, maintainability, operability, bearing capacity, and policy-adopted maintenance [19], need to be considered. Added to this it must be remembered drift probability [20]. The theories and the definition about the best inspection process are really complex, for instance in the machines which are working all time it is necessary to develop maintenance methodologies to avoid the failure or breakdown maintenance, in this sense, preventive maintenance and reliability-centered maintenance, among others need to be included [21]. This chapter includes a description of a methodology for damage detection and classification and the experimental validation with data from an aluminum plate instrumented with piezoelectric transducers permanently attached to its surface. In this sense, the chapter is organized as follows: Chapter 2 presents general concepts about the methods and concepts used in the methodology, Chapter 3 explains the methodology. Chapter 4 describes the experimental setup, after Chapter 5 presents the results, finally the conclusions are included.

http://dx.doi.org/10.5772/65867

2. General concepts

The methodology described in this work uses some well-known methods for data driven, however in this section some of this concepts will be introduced.

2.1. Principal components analysis

One of the greatest difficulties in data analysis occurs when the amount of data is very large and there is no apparent relationship between all the information or if it is very difficult to find. As solution, principal component analysis (PCA) was born as a very useful tool to reduce and analyze a big quantity of information. The principal component analysis technique was described by Pearson in 1901, as a Mechanism of Multivariate analysis and was also used by Hotelling in 1933 [22]. This method allows to find the principal components, which are a reduced version of the original dataset and include relevant information that identifies the reason for the variation between them. To find these variables, the analysis includes the transformation of the current coordinate space to a new space in order to re-express the original data trying to filter the noise and redundancies. These redundancies are measured by means of the correlation between the variables [23].

There are two mechanisms to implement the analysis of main components: first method is based on correlations and second is based on covariance. It is necessary to highlight that PCA is not invariant to scale, so the data under study must be normalized. Many methods can be used to do this as is shown in [23, 24]. In many applications, PCA is used as a tool to reduce the dimensionality of the data to be applied in a subsequent process to work with a reduced number of data. Currently, there are many useful toolboxes to apply PCA and analyze the reduced data provided by the technique [25], this is one of the reasons about PCA still being used. More information about PCA and the normalization process can be consulted in Refs. [24, 26–28].

2.2. Machine learning

Since Alan Turing showed interest in learning by machines, this area has remained at the forefront of the research by increasing his popularity and expanding its field of performance [29]. This has revolutionized the way in which complex problems has been tackled. In the relentless pursuit of best tools for data analysis, machine learning has been highlighted by finding a set of strategies for pattern recognition, which are able to find the relationship between data that at first glance have no correlation and are very difficult to define a deterministic mathematical model. Machine learning strategies and bio-inspired algorithms allow to avoid this difficulty through mechanisms designed to find the answer by themselves. In SHM or related areas, it is possible to find some applications about how machine learning has been used to detect problems, such as breaks, corrosion, cracks, impact damage, delamination, disunity, breaking fibers (some pertinent to metals and the others to composite materials [30]), in addition it has been used to provide information about the future behavior of a structure under extreme events such as earthquakes [31].

Depending on how the algorithms work, machine learning can be classified into two main approaches: unsupervised and supervised learning. First, the information is grouped and

interpreted only using the input data, however, the second, requires information about the output data to perform the learning task. **Figure 1** shows this classification and includes information about the works that each one of these learning can be used.

Since this work is aimed to classify damages, supervised learning is used. In practice, this task is performed through the classification learner toolbox of MATLAB®, and **Table 1** includes the methods used in the development of this work.

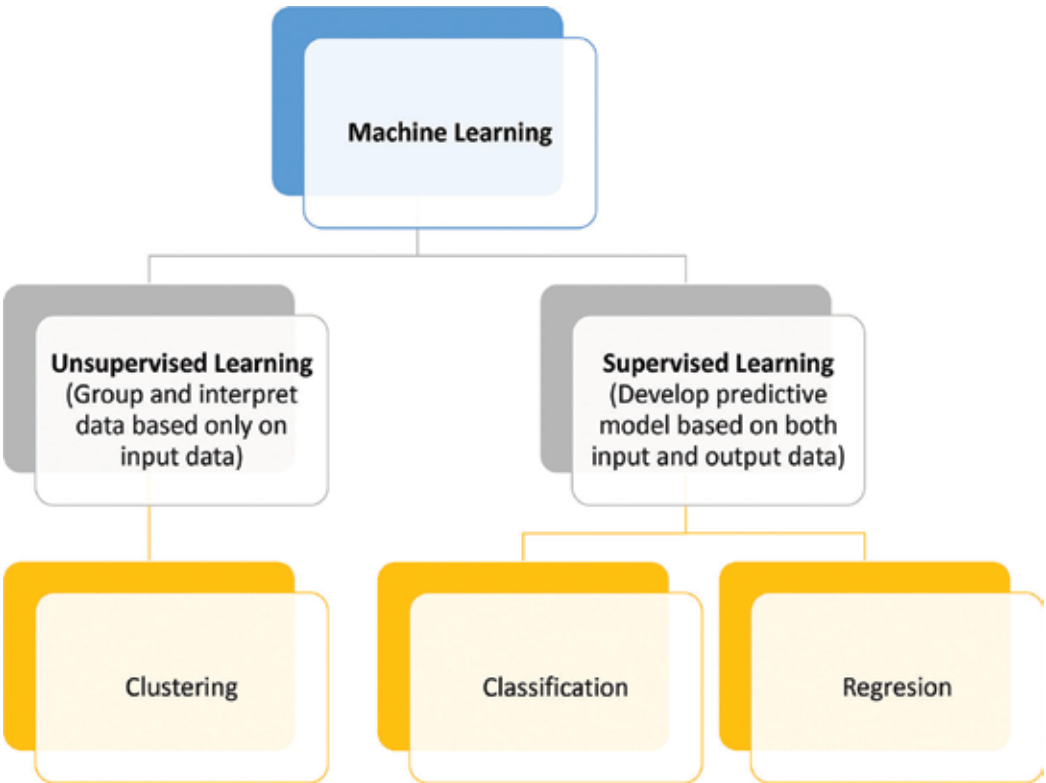

Figure 1. Machine learning approaches according to the learning.

Decision trees	Nearest neighbor classifiers	Support vector machines	Ensemble classifiers
Simple tree	Fine KNN	Linear SVM	Boosted trees
Medium tree	Cubic SVM	Fine Gaussian SVM	Bagged trees
Complex Tree	Medium KNN	Medium Gaussian SVM	Subspace KNN
	Coarse KNN	Coarse Gaussian SVM	Subspace discriminant
	Cosine KNN	Quadratic SVM	RUSBoosted
	Weighted KNN	Cubic SVM	Trees

Table 1. Methods included in the classification learner toolbox of MATLAB®.

http://dx.doi.org/10.5772/65867

3. Damage classification methodology

The methodology used in this work is aimed to the damage detection and classification. To perform this task, it is necessary to highlight that pattern recognition point of view is used, in this sense, the methodology works first with the definition of a healthy pattern which is obtained from different states of the structure. In this work, data from healthy and different damages are used as inputs to the machines. This stage is defined as training and is developed as in **Figure 2**.

In general terms, the process includes a pre-processing step, where all the experiments are organized in a matrix per each actuation phase as in **Figure 3**, and normalization is applied before to create PCA models.

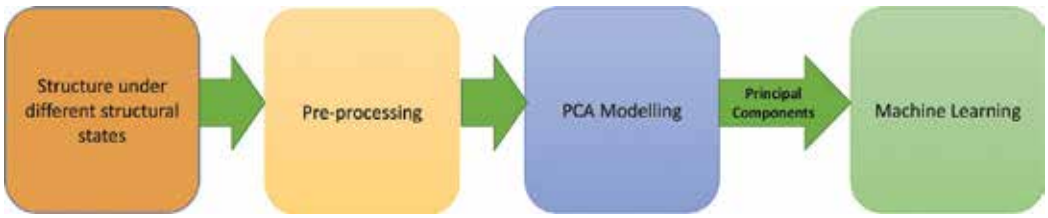

Figure 2. Training process.

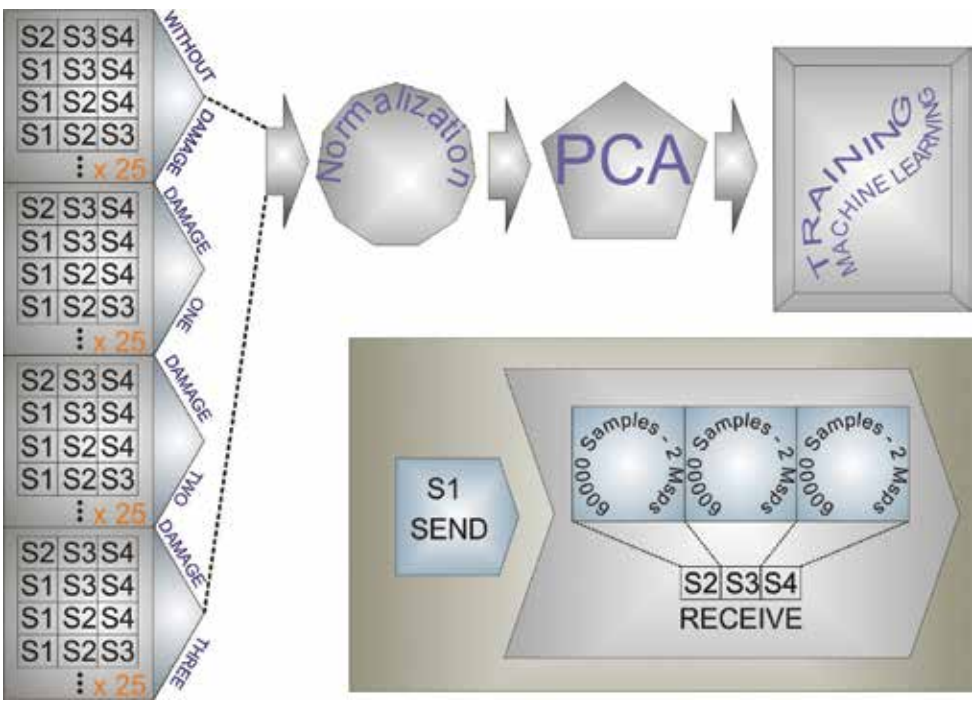

Figure 3. Organization and normalization data.

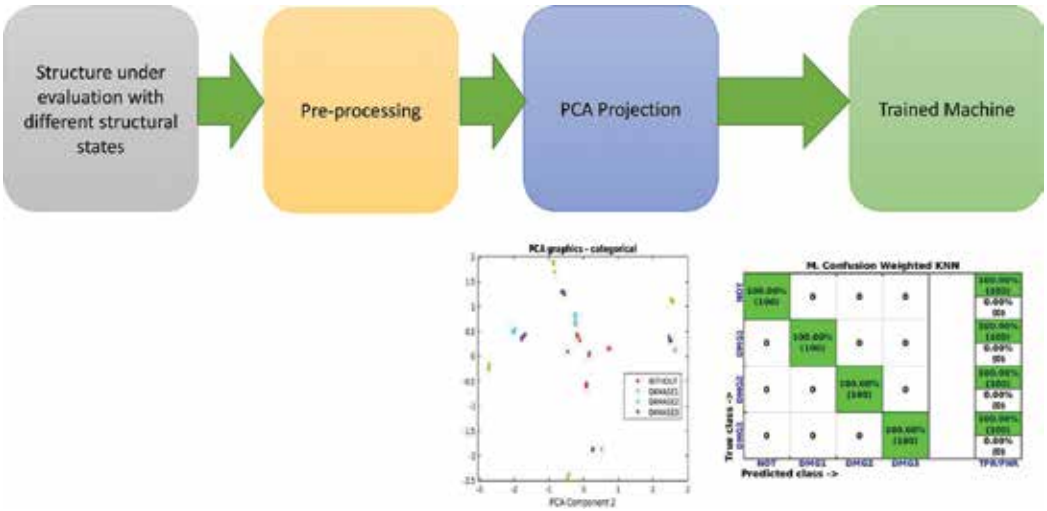

Figure 4. Test process.

After training step, same experiments with unknown scenarios are applied to the structure, and these data are pre-processed and projected in the principal components and included in the trained machine to determine to which state it correspond. **Figure 4** presents a description of the steps used on that process.

4. Experimental setup

Figure 5 shows a scheme of the SHM system, it is composed of one oscilloscope of four channels with an usb interface, one arbitrary generator, and a CPU as processing unit, additionally there is a switching device, which is implemented for automatizing the measurement as it is shown in **Figure 5**.

The inspection process can be summarized in the following steps:

- A burst signal is applied to one PZT and the rest of the transducers are used as sensors.
- A multiplexing system allows to change the actuator and collects the information from the rest of the sensors. This process is applied as many times as piezoelectric sensors are attached to the structure.
- A digitizer is finally used to capture the information collected by the sensors via an oscilloscope with usb interface.

The system collects the information in several files, in this case four since there are four transducers, and pre-processes, as was explained in the previous section. To validate the methodology, four structural states including the healthy state and three simulated damages were used as in **Figure 6**. These kinds of damages are used to produce changes in the wave propagation [27] and to provide different scenarios for validating the methodology.

http://dx.doi.org/10.5772/65867

Figure 5. Experimental setup.

Figure 6. Structural states used in the damage classification validation.

5. Experimental results

In order to validate the methodology with several machine learning methods, three experiments were implemented. The objective is to determine the behavior of the different methods of machine learning described in Section 2 and its performance under different scenarios which are obtained by changes in the input data and the pre-processing step. In most of the cases, these kinds of changes are the responsible for producing false alarms in the damage identification process. In this way, the acquisition process was made by looking the effect of the attenuation with long cables (2.5 m) and short cables (0.5 m), the addition of Gaussian noise to the acquired signals and the use of a Golay filter in the pre-processing step. These experiments are explained below.

First experiment: acquisition performed with a short cable (0.5 m) from the digitizer to the sensors, and the acquired signals filtered with a Golay filter algorithm in this experiment after adding white Gaussian noise.

Second experiment: acquisition performed with long cable to sensors (2.5 m), and signals filtered with the Golay algorithm.

Third experiment: acquisition performed with a short cable (0.5 m) from the digitizer to the sensors, and the signal filter without a Golay filter algorithm.

As it was previously introduced, in the first group of experiments, the influence of added noise to the data will be explored in order to determine how it affects the results in the principal components. For this, the Golay filter is applied to reduce the influence of aleatory signals and after the white Gaussian noise is added to the signals. Later, the methodology was applied to the signals with and without noise to determine the influence of the white noise in the detection process. An example of the signals used by the algorithms in the actuation phase 2 can be seen in **Figure 7**, similar results are obtained with all the signals.

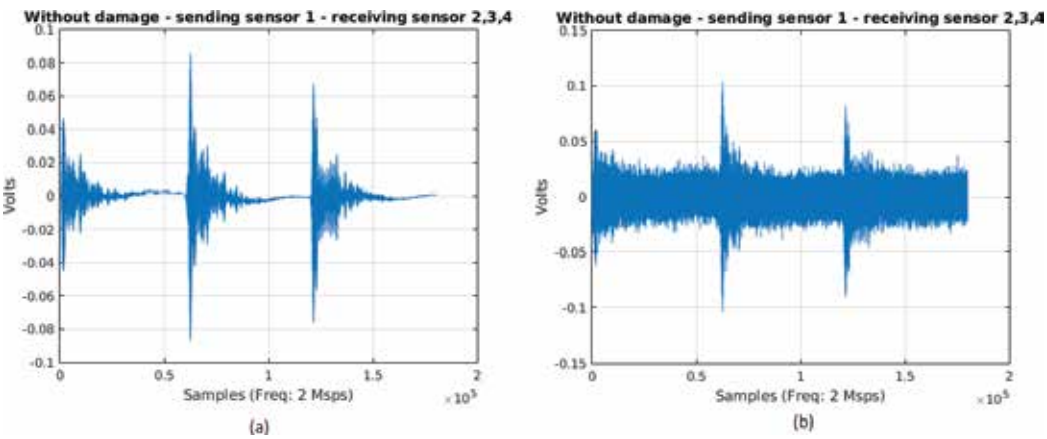

Figure 7. Signal received by sensors in the first experiment, without damage (a) with Golay filter applied without white Gaussian noise (b) with Golay filter applied with white Gaussian noise.

http://dx.doi.org/10.5772/65867

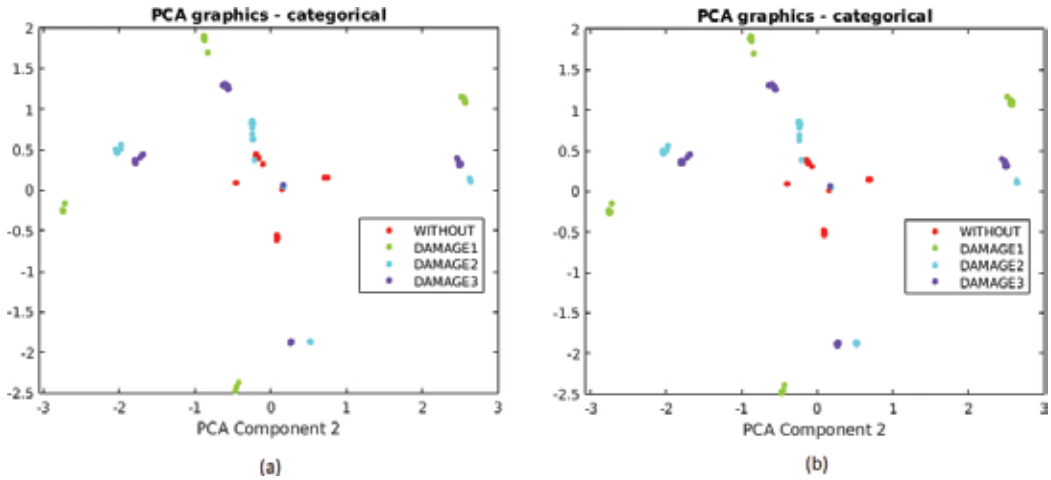

Figure 8. First two principal components for experiment 1: (a) without added noise (b) with 25dB of white Gaussian noise.

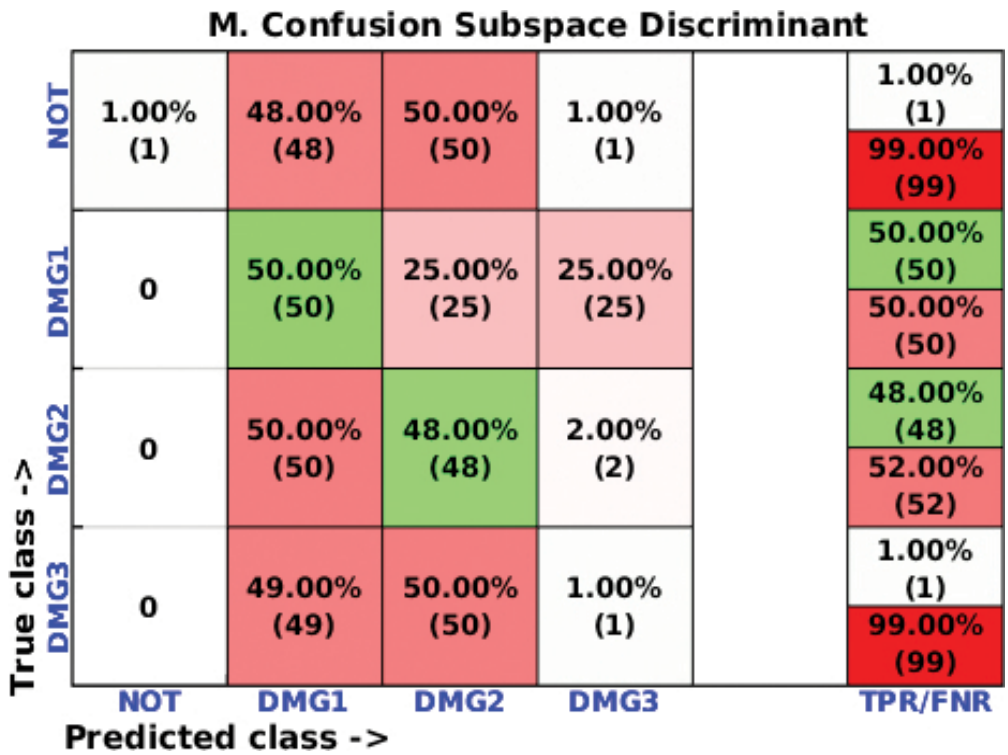

Figure 9. The bad case confusion matrix for experiment 1.

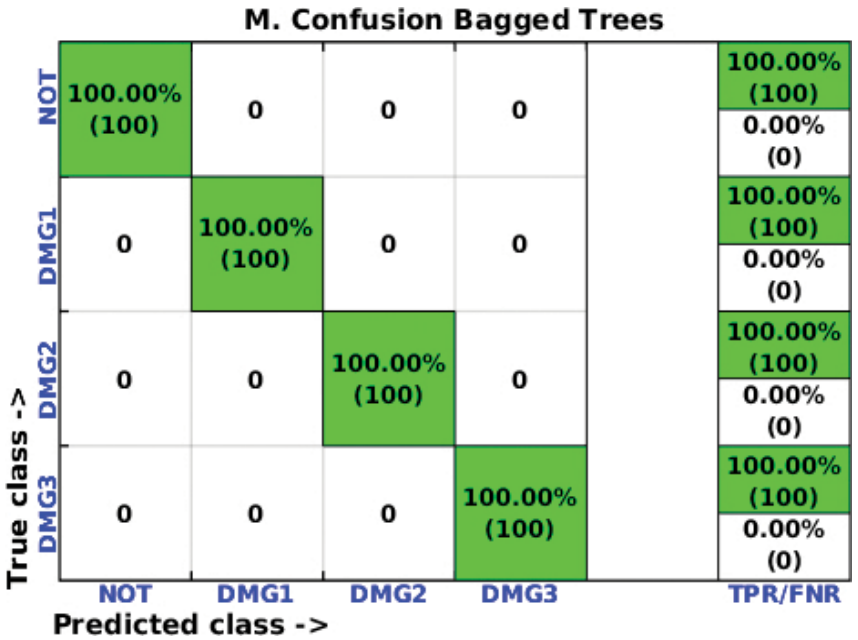

Figure 10. The good case confusion matrix for experiment 1.

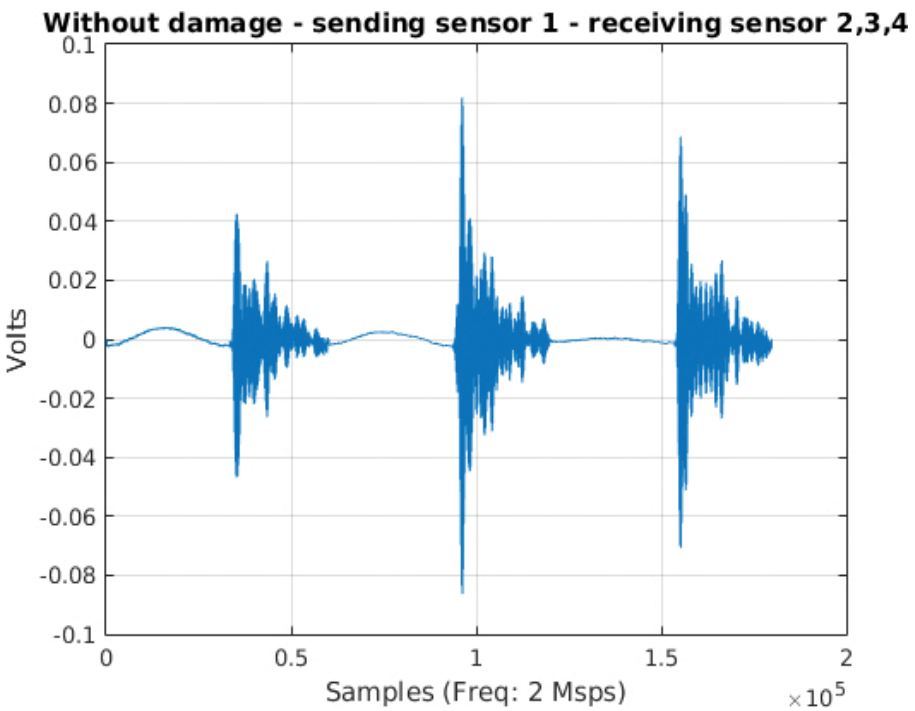

Figure 11. Signal received by sensors by experiment 2.

http://dx.doi.org/10.5772/65867

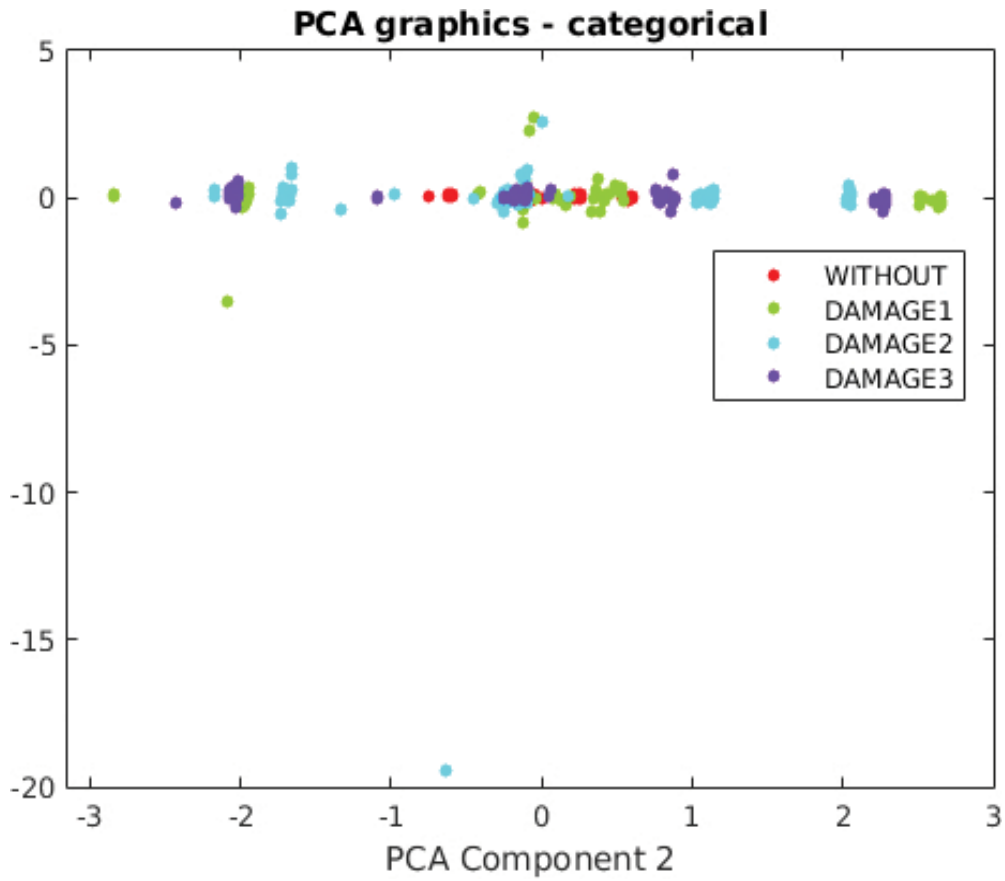

Figure 12. PCA components for experiment 2.

Figure 8a shows the first two principal components of the signal for the actuation phase 1, which are after used to train the machines, this train was made with methods included in the classification learner toolbox of MATLAB® shows in **Table 1**. This behavior is the same in all the actuation phases.

As seen in **Figure 8a** and **8b**, the first the principal components are able to eliminate the noise and prove that they are a good tool for defining the elements to include in the machine this is the experiment one.

After searching the principal components, the machines are trained with these data. Although all the machine learning methods were explored, following worst and best results are shown for a better understanding. **Figure 9** shows the confusion matrix with test Coarse KNN machine, and the result in all cases was very poor, with most machines having this behavior.

Figure 10 shows the confusion matrix with test Bagged Trees machine, the result in all cases was good, Fine KNN, Weighted KNN, Bagged Tree and subspace KNN, also the behavior was good, but only in some machines good response was obtained.

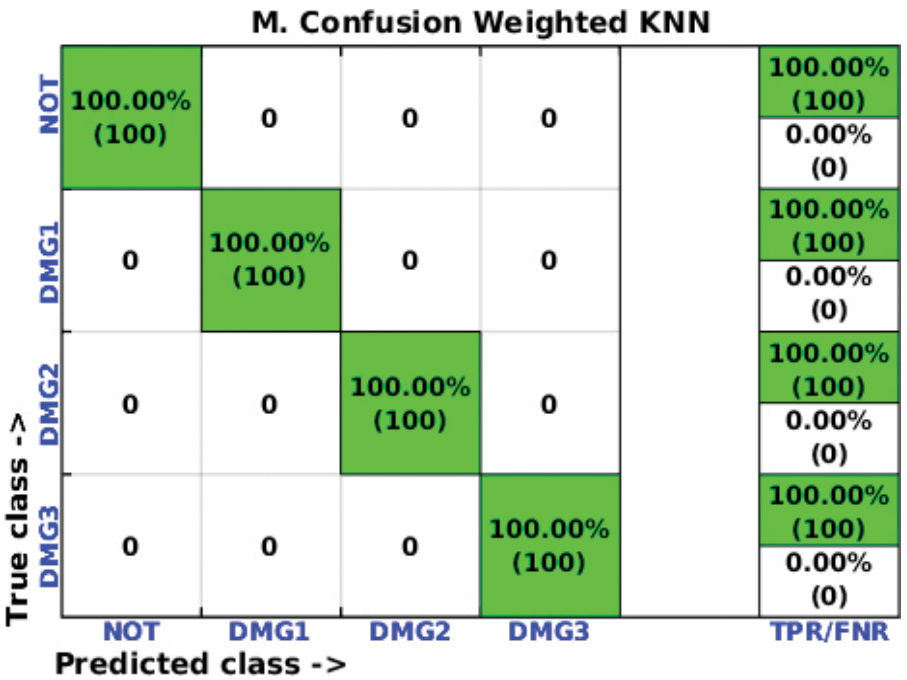

Figure 13. The best confusion matrix for experiment 2.

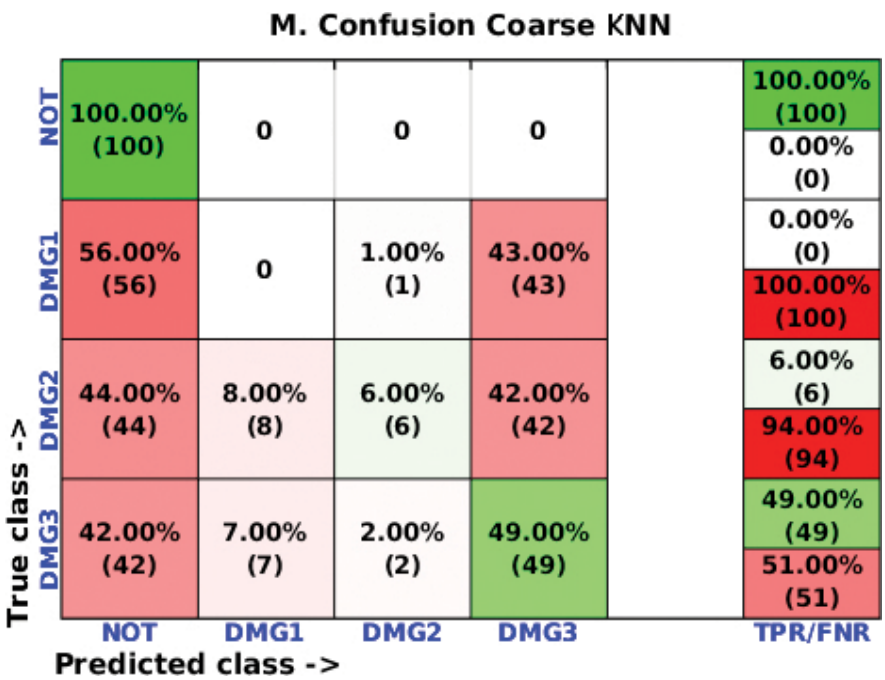

Figure 14. The bad case confusion matrix for experiment 2.

http://dx.doi.org/10.5772/65867

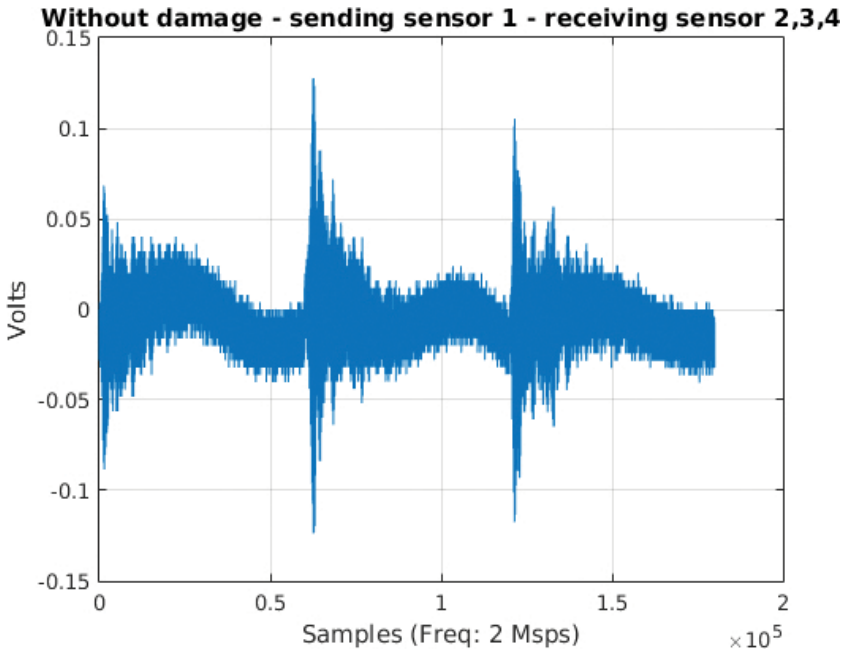

Figure 15. Signal received by sensors by experiment.

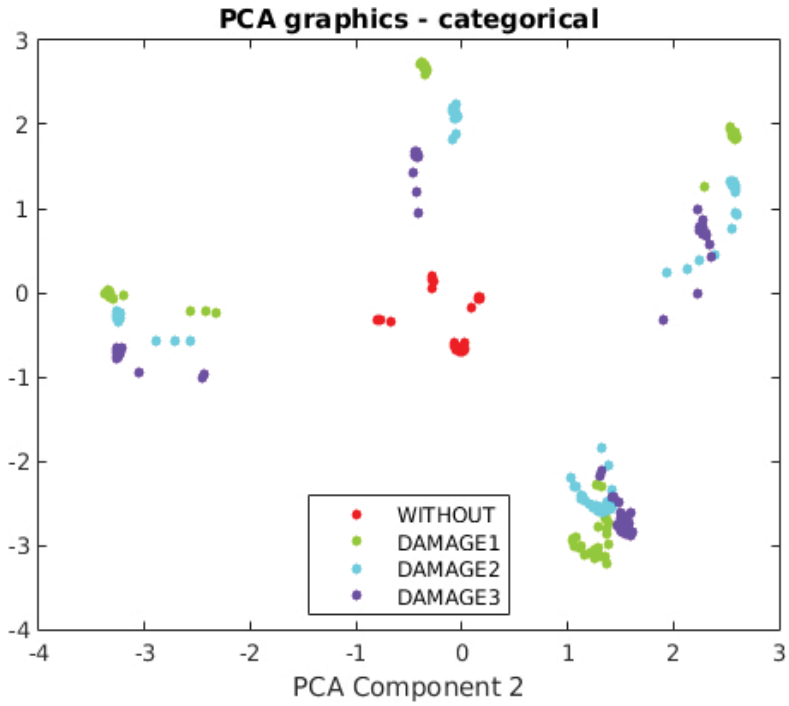

Figure 16. PCA components for experiment 3.

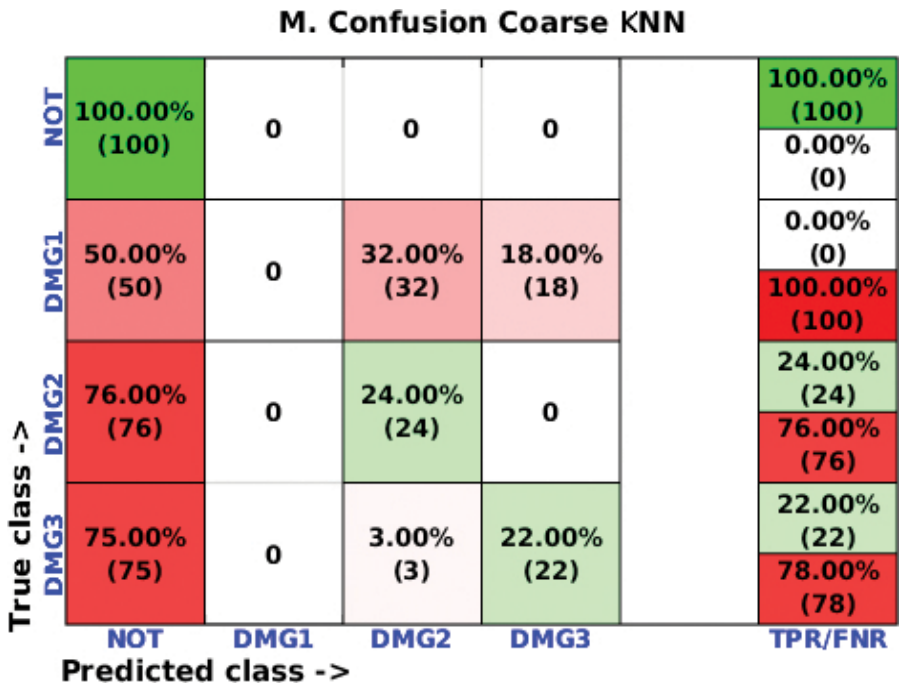

Figure 17. The worst case confusion matrix for processing with other training.

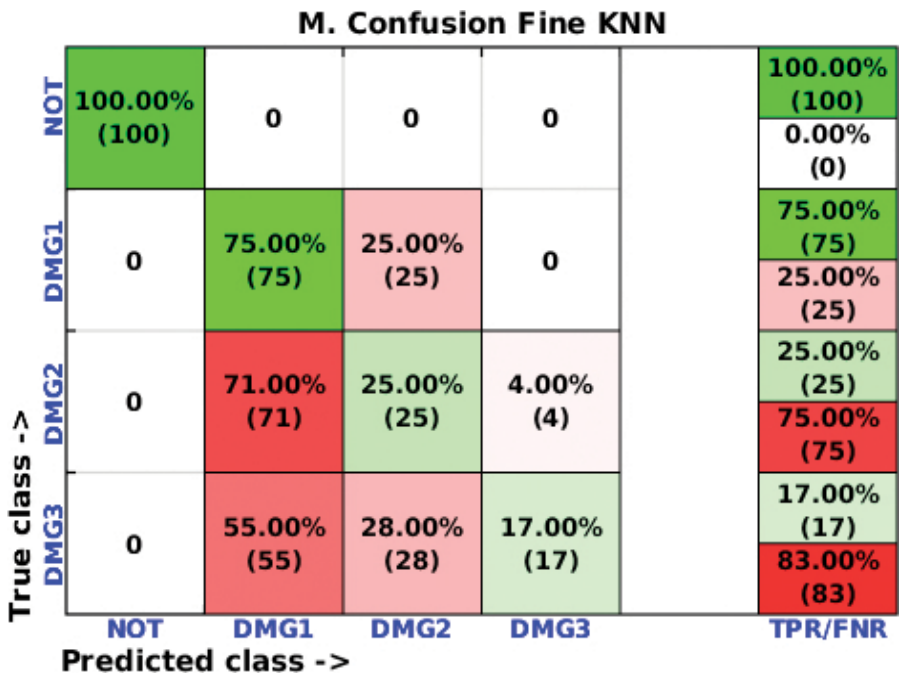

Figure 18. The bad case confusion matrix for processing with other training.

http://dx.doi.org/10.5772/65867

In general, the response of these machine learning algorithms was good with or without added noise because PCA has shown great ability to reject the noise.

The second case was considered when the acquisition system is connected with long cables, and Golay filter for pre-processing is used, in this case the signals in some cases were bad digitalized because of the impedance of cable, the noise, the low voltage of the stimulus, and other experimental features. An example of the captured signals is shown in **Figure 11**.

Figure 12 shows the first two principal components obtained from the signal, which were used to train the machines.

As in the previous experiment, all the methods were explored and best and worst results are included in this work. **Figure 13** shows the confusion matrix with Weighted KNN, and the behavior was similar to the first experiment. Similar results are obtained with adding Fine KNN, Weighted KNN, Bagged Tree, and subspace KNN.

Bad results were obtained with other methods for Coarse KNN. **Figure 14** shows this behavior, which is similar to the experiment 1.

Similar results were obtained with the third experiment; in this case, a short cable was used and unfiltered signals were used to calculate the scores. **Figure 15** shows the acquired signal in the actuation phase 1.

Figure 16 shows the first two principal components of the signal, however in this experiment these data were not used to train the machines, this means, principal components are projected into the machines trained in the first experiment to determine the influence of these changes in the results.

Figure 17 shows the response of the Coarse KNN machine, in this last case, the training is not success with this data series.

Figure 18 shows the response of the Fine KNN machine, similar results to the previous case are obtained, this means, a bad classification is provided by the machine.

6. Conclusions and future work

The piezoelectric transducers working as an active inspection system provide a good system to produce mechanical waves over materials under evaluation. In all the cases, the information obtained from the healthy state and the different damage scenarios applied to the methodology showed that algorithm is available to detect real and simulated damages in both structures in spite of shapes and differences in the element under inspection.

For all the experiments, the results showed that the behavior was very similar, only few machines architecture presented good results, these are: Fine KNN, Weighted KNN, Bagged Tree, and subspace KNN. Others types of machines did not work well for the experiments.

In all cases, it is necessary to train the machines with data pre-processed in the same way as in the definition of the healthy state, changes in the elements such as the cable length and the

use of the Golay filter are enough to change the results in the PCA model obtained which do that the machines do not work correctly.

PCA is a robust mechanism to characterize data since it was demonstrated to eliminate the noise, however, more experiments need to be considered by including environmental and operational noise to determine the effectiveness of the algorithm.

Acknowledgement

This work is supported by Universidad Santo Tomas through Grant FODEIN 2016, project code FODEIN 1608303-017.

Author details

Jaime Vitola[1,2], Maribel Anaya Vejar[2], Diego Alexander Tibaduiza Burgos[3,*] and Francesc Pozo[4]

*Address all correspondence to: dtibaduiza@gmail.com

1 Universitat Politecnica de Catalunya, CoDAlab, Department of Mathematics, Escola d'Enginyeria de Barcelona, Barcelona, Spain

2 Faculty of Electronics Engineering, Research Group MEM - Modeling, Electronics and Monitoring, Universidad Santo Tomas, Bogotá, Colombia

3 Faculty of Engineering, Fundación Universitaria Los Libertadores, Bogotá, Colombia

4 CoDAlab, Department of Mathematics, Escola d'Enginyeria de Barcelona Est (EEBE), Universitat Politècnica de Catalunya, Sant Adrià de Besòs (Barcelona), Spain

References

[1] N. Mrad, "SHM implementation," in *Fly by Wireless Workshop (FBW), 2011 4th Annual Caneus*, 2011, pp. 1–4.

[2] D. M. Laveuve, M. Lehmann, K. Erdmann, and A. Büter, "Shm - Reliability Demands on the Multidisciplinary Challenge of Structural Health Monitoring," in *NDT in Progress, 5th International Workshop of NDT Experts*, 2009, pp. 12–14.

[3] A. Van Horenbeek and L. Pintelon, "A prognostic maintenance policy - effect on component lifetimes," in *Reliability and Maintainability Symposium (RAMS), 2013 Proceedings - Annual*, 2013, pp. 1–6.

[4] W. J. Staszewski and K. Worden, "Signal processing for damage detection," *Encycl. Struct. Heal. Monit.*, Vol 1, 2009.

[5] S. M. Khan, S. Atamturktur, M. Chowdhury, and M. Rahman, "Integration of structural health monitoring and intelligent transportation systems for bridge condition assess-

ment: current status and future direction," *IEEE Trans. Intell. Transp. Syst.*, vol. PP, no. 99, pp. 1–16, 2016.

[6] K. S. Raju, Y. Pratap, Y. Sahni, and M. Naresh Babu, "Implementation of a WSN system towards SHM of civil building structures," in *Intelligent Systems and Control (ISCO), 2015 IEEE 9th International Conference on*, 2015, pp. 1–7.

[7] Güemes A. SHM Technologies and Applications in Aircraft Structures. 5th Int Symp NDT Aerosp. November 2013;13–5.

[8] M. A. Rumsey and J. A. Paquette, "Structural health monitoring of wind turbine blades," *Proc. SPIE 6933, Smart Sens. Phenomena Technol. Networks Syst.*, pp. 1–15, 2008.

[9] K. Smarsly, K. H. Law, and D. Hartmann, "Structural health monitoring of wind turbines observed by autonomous software components – 2nd level monitoring,". *ISCCBE (International Society for Computing in Civil and Building Engineering). 14th International Conference on Computing in Civil and Building Engineering*. 2012.

[10] R. Rolfes, S. Zerbst, G. Haake, J. Reetz, and J. P. Lynch, "Integral SHM-System for Offshore Wind Turbines Using Smart Wireless Sensors," *6th Int. Work. Struct. Heal. Monit.*, no. 734, pp. 1–8, 2007.

[11] W. Prosser, "Development of structural health management technology for aerospace vehicles," *NASA LaRC, JANNAF 39th CS/27th APS/21st PSHS/…*, 2003.

[12] M. S. Nisha, "Structural Health Monitoring of Aircraft Wing Using Wireless Network," *Int. J. Technol. Explor. Learn. www.ijtel.org Struct.*, vol. 3, no. 1, pp. 341–343, 2014.

[13] Q. Wang, Z. Su, and M. Hong, "Online damage monitoring for high-speed train bogie using guided waves: development and validation," *7th Eur. Work. Struct. Heal. Monit. July 8-11, 2014. La Cité, Nantes, Fr.*, 2014.

[14] M. Gruden, M. Jobs, and A. Rydberg, "Empirical tests of wireless sensor network in jet engine including characterization of radio wave propagation and fading," *Antennas Wirel. Propag. Lett. IEEE*, vol. 13, pp. 762–765, 2014.

[15] C. Vendittozzi, G. Sindoni, C. Paris, and P. P. del Marmo, "Application of an FBG sensors system for structural health monitoring and high performance trimming on racing yacht," in *Sensing Technology (ICST), 2011 Fifth International Conference on*, 2011, pp. 617–622.

[16] J. Walsh, I. Bashir, P. R. Thies, L. Johanning, and P. Blondel, "Acoustic emission health monitoring of marine renewables: Illustration with a wave energy converter in Falmouth Bay (UK)," in *OCEANS 2015 - Genova*, 2015, pp. 1–7.

[17] A. Deraemaeker, E. Reynders, G. De Roeck, and J. Kullaa, "Vibration-based structural health monitoring using output-only measurements under changing environment," *Mech. Syst. Signal Process.*, vol. 22, no. 1, pp. 34–56, 2008.

[18] M. H. Häckell and R. Rolfes, "a modular Shm- Scheme for engineering structures under changing conditions : application to an offshore wind," *EWSHM - 7th Eur. Work. Struct. Heal. Monit.*, pp. 796–803, 2014.

[19] T. Chitra, "Life based maintenance policy for minimum cost," in *Reliability and Maintainability Symposium, 2003. Annual*, 2003, pp. 470–474.

[20] H. Cherkaoui, K. T. Huynh, and A. Grall, "Towards an efficient and robust maintenance decision-making," in *2016 Second International Symposium on Stochastic Models in Reliability Engineering, Life Science and Operations Management (SMRLO)*, 2016, pp. 225–232.

[21] Z. Fu, G. Wang, F. Gao, X. Tian, Y. Li, and B. Lu, "Review of high-speed train maintenance," in *Quality, Reliability, Risk, Maintenance, and Safety Engineering (ICQR2MSE), 2012 International Conference on*, 2012, pp. 419–422.

[22] D. K. Stangl, "Encyclopedia of statistics in behavioral science," *J. Am. Stat. Assoc.*, vol. 103, no. 482, pp. 881–882, 2008.

[23] M. Anaya, D. A. Tibaduiza, and F. Pozo, "A bioinspired methodology based on an artificial immune system for damage detection in structural health monitoring," *Shock Vib.*, vol. 501, p. 648097, 2015.

[24] D. A. T. Burgos, "Design and validation of a structural health monitoring system for aeronautical structures," *PhD thesis*, vol. 1, 2013.

[25] D. H. Jeong, C. Ziemkiewicz, B. Fisher, W. Ribarsky, and R. Chang, "iPCA: an interactive system for pca based visual analytics," In computer Graphics Forum, vol. 28, no. 3, pp. 767–774, 2009.

[26] D. A. Tibaduiza, L. E. Mujica, J. Rodellar, and A. Güemes, "Structural damage detection using principal component analysis and damage indices," *J. Intell. Mater. Syst. Struct.*, p. 1045389X14566520, 2015.

[27] M. Anaya, "Design and validation of a structural health monitoring system based on bioinpired algorithms," PhD thesis, Universitat Politecnica de Catalunya, CoDAlab, Department of Mathematics, Escolad'Enginyeria de Barcelona, Barcelona, Spain, July 2016 .

[28] D. A. Tibaduiza Burgos, L. E. Mujica Delgado, A. Güemes Gordo, and J. Rodellar Benedé, "Active piezoelectric system using PCA," in *Fifth European Workshop on Structural Health Monitoring*, 2010, pp. 164–169.

[29] S. Muggleton, "Alan turing and the development of artificial intelligence," *AI Commun.*, vol. 27, no. 1, pp. 3–10, 2014.

[30] K. Worden and C. R. Farrar, Structural Health Monitoring: a machine learning perspective. Wiley, isbn 9781118443200, 2012.

[31] Singh S, Seah WKG, Ng B. Cluster-centric medium access control for WSNs in structural health monitoring. In: Modeling and Optimization in Mobile, Ad Hoc, and Wireless Networks (WiOpt), 2015 13th International Symposium on. 2015. p. 275–82.

Edited by S. Ramakrishnan

Pattern recognition continued to be one of the important research fields in computer science and electrical engineering. Lots of new applications are emerging, and hence pattern analysis and synthesis become significant subfields in pattern recognition. This book is an edited volume and has six chapters arranged into two sections, namely, pattern recognition analysis and pattern recognition applications. This book will be useful for graduate students, researchers, and practicing engineers working in the field of machine vision and computer science and engineering.

ISBN 978-953-51-5790-8

Photo by Samuel Zeller / unsplash

IntechOpen